REGULATION OF CARDIAC GENE EXPRESSION BY β-ADRENERGIC SIGNALING AND HEART FAILURE

SARA HASHEMI

A DISSERTATION SUBMITTED TO THE FACULTY OF GRADUATE STUDIES
IN PARTIAL FULFILLMENT OF THE REQUIREMENTS FOR THE DEGREE OF

DOCTOR OF PHILOSOPHY

GRADUATE PROGRAM IN BIOLOGY
YORK UNIVERSITY
TORONTO, ONTARIO

JANUARY 2017

© Sara Hashemi 2017

ABSTRACT

Cardiac diseases such as coronary artery disease, hypertension and heart failure are the major causes of death around the world. Regulation of beta-adrenergic receptors by catecholamines is an important facet of understanding cardiac function in health and disease. Acute sympathetic activation of βARs results in an increase in cardiac output; however, sustained stimulation of the βARs is cytotoxic, leading to myocyte death and cardiac remodeling. β-adrenergic blockers are a seminal class of drugs that play an important role in improving mortality and symptom control in various cardiac diseases.

An important transcriptional regulatory protein target of β-adrenergic signaling is MEF2, which plays a crucial role in cardiac gene expression during pathologic and physiological adaptation of the heart. In our experiments, we have observed a robust effect of β-blockers on MEF2 transcriptional activity. Myocardial MEF2 responses to β-blocker treatment indicates an important physiological linkage between β-adrenergic signaling and MEF2 activity in the heart, which underpins changes in cardiac gene expression in response to β-adrenergic blockade. In the first set of experiments, the link between MEF2 and cardiac survival pathways in the heart was examined. Initially, using flow cytometry we observed that levels of cell death are dramatically enhanced in cardiomyocytes when the expression of MEF2 is suppressed using siRNA technology. Also transcriptome analysis of siRNA-mediated gene silencing of MEF2 showed extensive apoptotic DEG define genes. Together these data indicate that MEF2 play a key role in cardiomyocyte survival. Furthermore, I demonstrated that β1AR mediated apoptosis was abrogated in cardiomyocytes expressing a PKA-resistant form of MEF2D (S121/190A). A β1-blocker, Atenolol, antagonizes isoproterenol-induced apoptosis while concomitantly enhancing MEF2 transcriptional activity. Kruppel-like factor 6, a MEF2 target gene in the heart; functions as a downstream pro-survival factor in cardiomyocytes. Collectively, these findings indicate a mechanism of the beneficial effects of acute β1AR blocker treatment through up-regulation of MEF2 activity, leading to cardiomyocyte survival. In the second set of experiments, I studied changes in MEF2 activity and global gene transcription

networks during heart failure and in response to chronic β1-blockade in an *in vivo* model. First, β1-blockade treatment resulted in an overall improvement in cardiac function in Transverse aortic constriction mice co-incident with repression of MEF2 activity. Dynamic changes in gene expression activated by TAC were reversed by β1-blockade treatment. Transcriptome profiling in MEF2A depleted cardiomyocyte identified a novel MEF2 target gene, *Rarres2*, which is upregulated with TAC and isoproterenol and is involved in cardiac apoptosis. Together these data demonstrate that chronic β1-blockade inhibits myocardial MEF2 activity while also minimizing dynamic changes in HF associated transcriptome dynamics. Collectively, these data indicate molecular events resulting from β1-adrenergic blockade that result in positive effects on heart pathology. These studies define novel molecules and pathways involved in heart pathology that may represent new genetic or pharmacologic targets for heart failure therapies.

ACKNOWLEDGEMENTS

My PhD has been a great experience and has taught me many things about science, life and myself. I have been fortunate to have extensive support from many individuals during graduate school.

I wish to express my sincere appreciation to my supervisor, Dr. John McDermott, It was an honour to be his PhD student. He has taught me much about science and research. I would like to sincerely thank him for being a great mentor and give me the opportunity to learn cardiovascular biology and has challenged me to be independent.

Very special thanks to my committee members Dr. Robert Tsushima and Dr. Logan Donaldson for their thoughtfulness and guidance. I would like to thank all the members of our lab for their kindness and friendship. First, special thanks to Dr. Tetsuaki Miyake and Dr. Mathew Dionyssiou for their feedback and continual support and many thanks to the most helpful lab manager, Catherine Chan, and my friend, Dr. Stephanie Wales, for her great and enthusiastic collaboration work. Most importantly, I would like to thank my family members, my parents, Soheila and Mahmoud, my brother, Pouria, and my sister, Elmira, for their endless love, support and for believing in me. Special thanks to my husband, Meysam, for his love and never complaining about long hours or scheduling our life around the rat litters. Without my family support, my degree would be meaningless and I couldn't have done it. Last but not least, special thanks to my beautiful dear daughter, Nila, for reminding me daily that being a mom is the best part of who I am.

TABLE OF CONTENTS

LIST OF FIGURES

Chapter I: Literature Review

CHAPTER 3: Pro-survival function of MEF2 in cardiomyocytes is enhance by β-blockers

CHAPTER 4: Heart failure and MEF2 transcriptome dynamics in response to β-blockers

Appendix

LIST OF ABBREVIATIONS

MEF2	Myocyte Enhancer Factor-2
TAD	Transcriptional activation domain
MCK	Muscle creatine kinase
α-MHC	α-Myosin heavy chain
MLC1/3	Myosin light chain 1/3
MLC2v	Ventricular myosin light chain 2
SERCA	Sarcoplasmic reticulum Ca^{2+}ATPase
GLUT4	Glucose transporter 4 (GLUT4)
BMK1	Big MAP kinase 1
ERK5	Extracellular regulated kinase 5
IGF-1	Insulin-like growth factor 1
CaMK	Calcium/calmodulin-dependent kinase
HDACs	Histone deacetylases
HATs	Histone acetylases
ANF	Atrial natriuretic factor
DCM	Dilated cardiomyopathy
MAPK	Mitogen-activated protein kinase
PKA	Protein kinase A
PKC	Protein kinase C
GPCRs	G-protein coupled receptors
AngII	Angiotensin II
ET-1	Endothelin I
PLC	Phospholipase C
βAR	β-adrenergic receptors
AC	Adenylate cyclase
NFAT	Nuclear factors of activated T
DISC	Death-inducing complex
AIF	Apoptosis inducing factor
Smac	Second mitochondria derived activator of caspase
Endo G	Endonuclease G

JNK	C-Jun N-terminal kinase
bFGF	Basic fibroblast growth factor
RSK	Ribosomal S6 kinase
cAMP	Cyclic adenosine monophosphate
CO	Cardiac output
LTCC	L-type Ca^{2+} channel
ICa	Calcium current
RyRs	Ryanodine receptors
PLB	Phopholamban
SERCA	The sarcoplasmic/endoplasmic reticulum Ca^{2+} ATPase
MI	Myocardial infarction
Ate	Atenolol

CHAPTER 1: Literature Review

1. General overview

Regulation of gene expression is important in cell growth, differentiation and disease. Signal dependent regulation of gene expression is controlled by transcription factors. Cardiac transcription factors control the complex process of heart development and are also involved in stress regulation of the adult heart, which may lead to cardiac disease. Knowledge of the network of cardiac transcription factors that link the upstream signaling pathways to direct or indirect target genes lead us to a better understanding of the cause of cardiac disease [1,2]. Cardiac disease activates pathological signaling pathways that target transcription factors and reprogram cardiac gene expression, [3] which, then translated into production of proteins involved in contraction, calcium handling, and metabolism, leads to cardiac dysfunction. Therefore, the regulation of a network of transcriptional regulatory proteins in the heart is a primary determinant of its gene expression signature and phenotype [4]. The clarification of these transcriptional networks is ongoing and has provided major steps in understanding the control of cardiac gene expression; however, the levels of control of transcriptional regulators by pharmacological manipulation is still not explained. Regulation of transcriptional regulatory protein by pharmaceutical manipulation can exert considerable control over the gene expression profile and consequently heart function. As mentioned above, regulation of transcription factors has indeed been a predominant theme in understanding the molecular control of physiology and pathology of the heart [4]. A number of transcriptional regulators such as nuclear factor of activated T-cell (NFAT) [5,6],

the GATA family [7,8] and the myocyte enhancer family (MEF2) [9] have been identified as playing important roles in the heart via control of cardiac gene expression [10].

Several studies reported the control of cardiac gene expression and the loss of function analysis in gene targeted mice have positioned MEF2 as a core transcription factor involved in cardiac physiological and pathological pathways [11].

2. MEF2 role and regulation

2.1. MEF2 overview

The Myocyte Enhancer Factor-2 (MEF2) family of transcription factors play a central role in regulating cardiac [12], skeletal [13,14], and smooth muscle differentiation [15], neuronal survival and plasticity, [16,17] and T cell activation [18]. MEF2 transcription factors belong to the evolutionarily ancient MADS (MCM1, Agamous, Deficiens, SRF) superfamily of DNA binding proteins. In vertebrates, there are four MEF2 genes (MEF2A, -B, -C, and –D) that are located on different chromosomes (Figure 1). By contrast, there is a single MEF2 gene in each of the genomes of *Drosophila*, *Caenorhabditis elegans* and *Saccharomyces cerevisiae* [19]. The requirement for MEF2 is evolutionarily conserved for cardiac and skeletal muscle development from flies to humans [19].

The N-terminus of MEF2 proteins is highly conserved among all family members and consists of a 57-amino acid MADS domain and an immediately adjacent 29-amino acid MEF2 domain. These two domains collectively mediate dimerization, co-factor interactions and DNA binding to the consensus DNA sequence (T/C) TA $(A/T)_4$TA(G/A) [20]. The MEF2 transcriptional activation domain (TAD), which is divergent among family members, is positioned in the C-terminus of the protein and is subject to complex patterns of alternative splicing and extensive posttranslational modifications [21].

MEF2 was originally identified in skeletal muscle cells as a DNA-binding factor that recognized a conserved A/T-rich sequence in the muscle creatine kinase (MCK) enhancer [22]. The MEF2 binding sequence was identified in a majority of muscle specific genes that have been confirmed to be essential for gene expression [22]. These MEF2-

dependent genes encode a wide array of proteins, including structural proteins like α-cardiac myosin heavy chain (α-MHC), myosin light chain 1/3 (MLC1/3), ventricular myosin light chain 2 (MLC2v), sarcoplasmic reticulum Ca^{2+}ATPase (SERCA), cardiac troponin (-T, -C and –I), desmin, dystrophin and insulin sensitive glucose transporter 4 (GLUT4) which regulates cardiac metabolism [23–27].

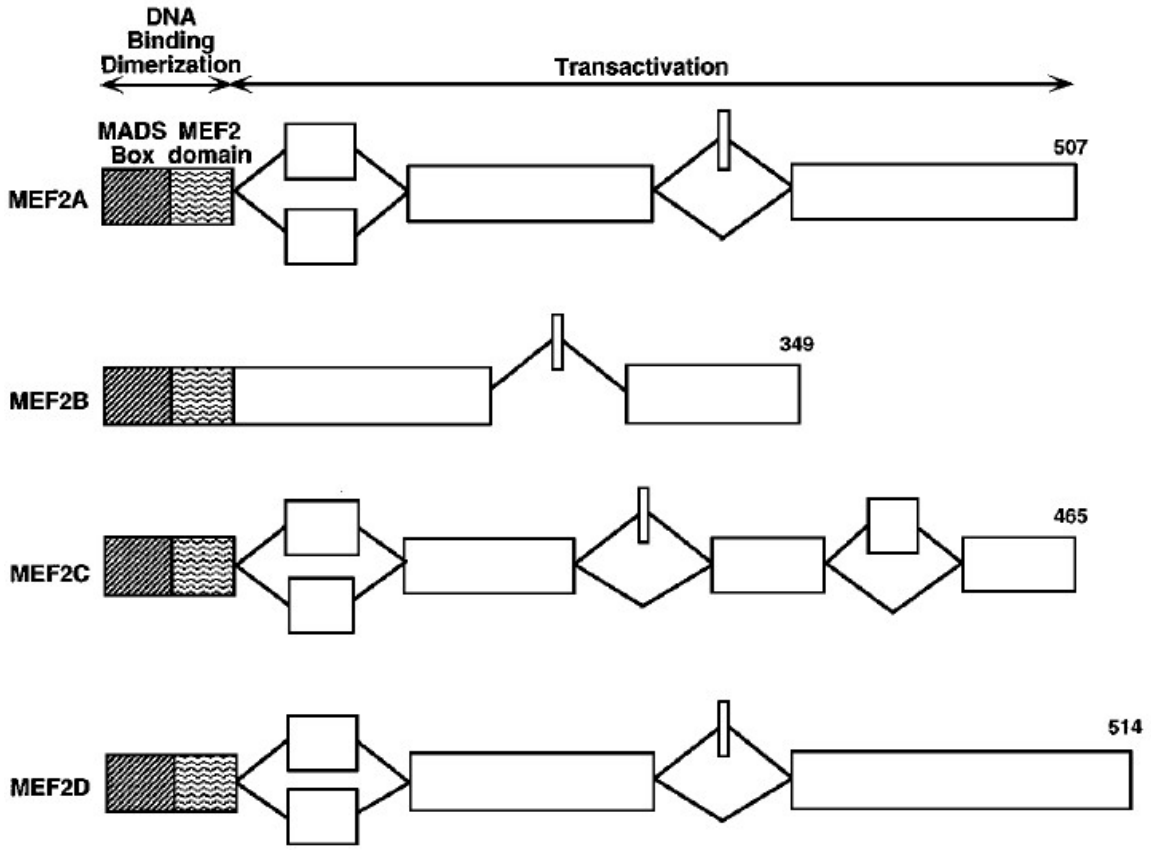

Figure 1. Schematic diagrams of MEF2 factors. Structures of the four vertebrate MEF2 gene products are shown. Alternative exons within the C-terminal activation domains are indicated, along with the number of amino acids in the longer form of each protein. This schematic has been adapted from [28].

2.2. MEF2 isoforms and their function in the heart

MEF2 is an essential regulator of cardiac morphogenesis and myogenesis. Previous studies showed that MEF2A knockdown in Zebrafish results in cardiac morphology defects, impairments of cardiac contractility and sarcomere assembly [29]. In addition, expression of cardiac contractile genes, including Troponin C, Troponin T, atrial myosin heavy chain (aMHC) and cardiac myosin light chain 2 (MLC2) which are involved in cardiac contractile organization were down-regulated. The expression of MEF2D was upregulated, possibly to compensate for the loss of MEF2A protein [29]. MEF2A and MEF2D are the primary MEF2 factors expressed in the adult heart. Mice deficient in MEF2A have post-natal dilation of the right ventricle, and deficiency of cardiac mitochondria and cardiac sudden death [30]. On the other hand, MEF2D knockout mice are viable, but are resistant to cardiac hypertrophy and pathological remodeling of the heart induced by stress [31]. Deletion of another MEF2 isoform, MEF2C, is associated with similar defects and myocardial impairment. MEF2C knockout mice die around E9.5 from cardiac looping defects, and disruption in right ventricle formation [15]. But the expression of MEF2B was enhanced, possibly to compensate for the loss of MEF2C [15]. MEF2B knock out mice are viable and its absence could be compensated by either MEF2A or MEF2C in cardiac development [15]. Thus, these studies clearly identify a functional role for MEF2 proteins in cardiac muscle cells development and cyto-architectural integrity.

2.3. MEF2 regulation by signaling pathways in cardiac

MEF2 transcriptional regulatory proteins play an important role in cardiac gene expression during pathologic and physiological adaptation of the heart [32]. Furthermore, MEF2 is crucial in activating diverse and often opposing genetic programs such as those that control cell proliferation, differentiation, morphogenesis, survival and apoptosis [33]. These different roles for MEF2 transcriptional factors are partly explained by the mechanisms that exist to regulate their activity. Therefore, regulation of MEF2 transcription factors by several kinase signaling cascades is important in understanding the molecular control of physiology and pathology of the heart.

MAPK-dependent phosphorylation enhances MEF2 transcriptional activity. The p38 MAPK is one of the MAPK phosphorylation cascades that can directly phosphorylate MEF2 and enhance its transcriptional activity (Figure 2) [34]. Previous studies have shown that MEF2A and MEF2C were directly phosphorylated and activated by p38 MAPK, however, MEF2D was phosphorylated to a much lesser extent [35,36]. The p38 phosphorylation of MEF2 transcriptional factors is important in normal development and post-natal hypertrophic growth and also in pathological hypertrophy of the heart [37,38].

The big MAP kinase 1 (BMK1) or ERK5 is the second MAP kinase that directly phosphorylates and activates MEF2 (Figure 2) [36,39]. ERK5 was found to associate with MEF2 through the N-terminal region, which contains the MADS-MEF2 domain and not the C-terminal domain, that p38 binds [36]. ERK5 phosphorylates MEF2C at Ser387, since Ser387 is a conserved residue in MEF2A and MEF2C, but not in MEF2B or MEF2D, stimulation of ERK5 only activates MEF2A and MEF2C [36,39]. In addition, insulin-like growth factor 1 (IGF-1) activates ERK5 in cardiomyocytes, and reduces

cardiac apoptosis through MEF2 [39]. ERK5 also play an important role in cardiac hypertrophy in which forced expression of ERK5 in cardiomyocytes induces eccentric hypertrophy [40]. Multiple calcium-regulated signaling proteins, calcineurin and calmodulin-dependent kinase (CaMK) are also involved in regulating MEF2 in cardiomyocytes (Figure 2). CaMK directly phosphorylates MEF2D and enhances its transcriptional activity [41].

One of the major MEF2 cardiac cofactors are class II histone deacetylases (HDACs). Calmodulin-dependent kinase (CaMK) disrupts MEF2-HDAC complexes by mediating nuclear export of the transcriptional repressor, HDACs II, which binds to chaperone protein 14-3-3. This event allows MEF2 to associate with histone acetylases (HATs) and to activate downstream genes [42]. In cardiomyocytes, MEF2 cooperates with NFAT in regulation of cardiac hypertrophy [10]. In this event, Calcineurin is involved in MEF2 target gene regulation, by activation and translocation of NFAT into the nucleus, where it can bind to MEF2 [43]. Calcineurin and CaMK signaling interact through the activation of NFAT and MEF2 [44], and activation of either calcineurin or CaMK promote cardiac hypertrophy [10].

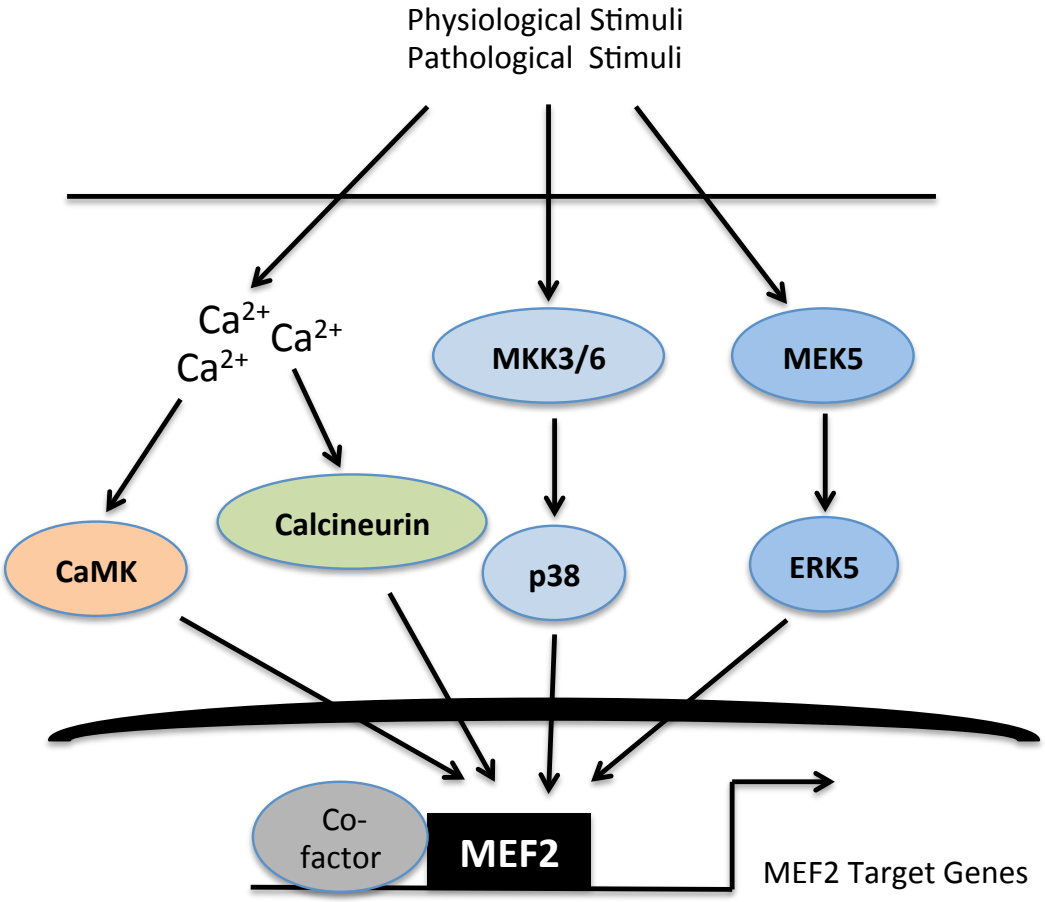

Figure 2. Signaling pathways regulating MEF2 in cardiac. MAP kinase cascades and the subfamilies include the extracellular regulated kinase 5 (ERK5) and the p38 MAPK activates MEF2. Calcium dependent signals also activate MEF2 by stimulating calcium-dependent kinases, calmodulin Kinase (CaMK) and calcineurin.

3. Myocardial remodeling

Cardiac diseases such as coronary artery disease, hypertension and heart failure are the major causes of death around the world [45]. Myocardial remodeling, a step on the progression to heart failure, refers to the changes in mass, shape and volume of the heart (left ventricular remodeling) in response to a variety of physiologic and pathophysiologic stimuli and classified as adaptive and maladaptive. Cardiac remodeling occurs due to a variety of pathological conditions in the heart such as myocardial infarction, pressure overload and volume overload hypertrophy. The underlying molecular and cellular processes leading to cardiac remodeling consist of myocyte growth (cardiac hypertrophy), myocyte death, and remodeling of the extracellular matrix (ECM) [46,47].

3.1. Cardiac hypertrophy

Cardiac hypertrophy refers to the enlargement of the heart due to an increase in cardiomyocyte size, resulting from enhanced protein synthesis and assembly of new sarcomeres. Cardiomyocyte hypertrophy occurs as a cellular response to increased mechanical and neurohumoral stimuli [48,49]. Cardiac hypertrophy has two forms; physiological hypertrophy and pathological hypertrophy (Figure 3) [49]. Physiological hypertrophy occurs during normal growth and development in conditions such as pregnancy and in response to chronic exercise training. The physiological hypertrophy is the proportional increase in the length and width of cardiomyocytes that leads to left ventricular hypertrophy and enhanced cardiac performance and is typically not associated with cardiac dysfunction, fibrosis, and heart failure [49]. Pathological

hypertrophy commonly occurs as a result of myocardial valve diseases, myocardial infarction and hypertension and it is commonly associated with fibrosis, cardiac dysfunction and alterations in cardiac gene expression and heart failure [48]. These processes lead to the activation of immediate early genes (c-jun, c-fos, c-myc) and increased expression of fetal genes such as beta myosin heavy chain (β-MHC), atrial natriuretic factor (ANF) and skeletal muscle α-actin [48,50]. There are two different pathological hypertrophy phenotypes, concentric hypertrophy and eccentric hypertrophy (Figure 3) [51]. Concentric hypertrophy, occurs when new sarcomeres are added in parallel, and is due to pressure overload in conditions such as aortic stenosis or hypertension. In contrast, eccentric hypertrophy, refers to the addition of sarcomeres in series resulting in longitudinal cell growth due to volume overload in conditions such as myocardial infarction [52,53]. The ventricular thinning and heart dilation in eccentric hypertrophy often leads to dilated cardiomyopathy (DCM) and heart failure [3].

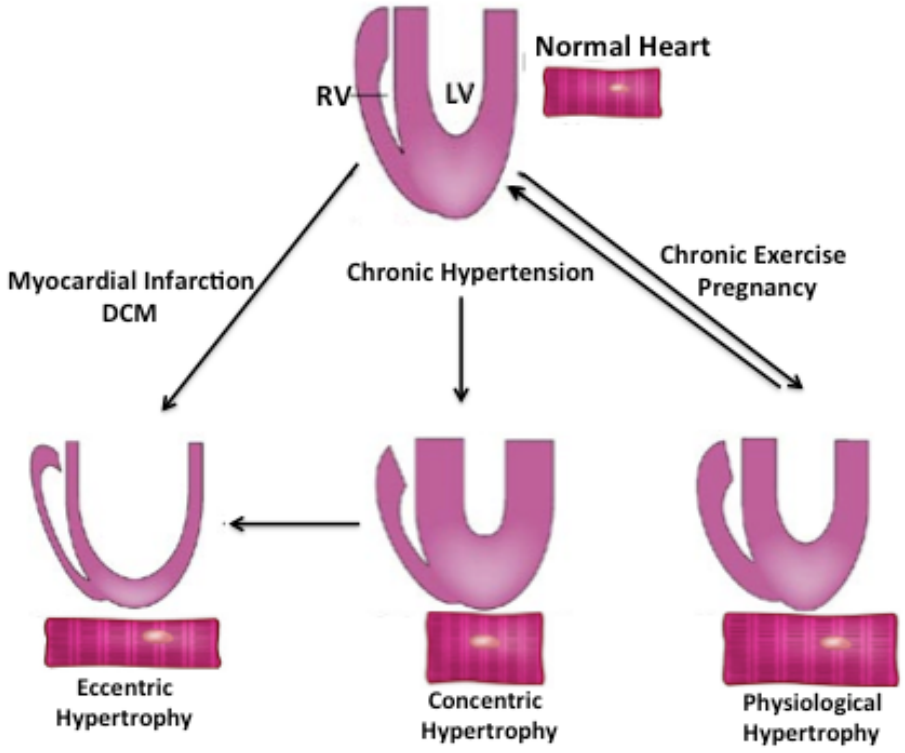

Figure 3: Different types of cardiac hypertrophy. The normal heart can lead to different types of hypertrophic remodeling depending on the stress. Physiological hypertrophy which is associated with exercise and pregnancy and pathological stress cardiac hypertrophy. Concentric hypertrophy, caused by chronic pressure overload, leads to ventricular wall thickness and eccentric hypertrophy, caused by volume overload, leads to thinning of the heart wall and possible dilated cardiomyopathy (DCM). This schematic has been adapted from [51].

3.1.1. Signaling pathway in cardiac hypertrophy

Disease of the adult heart activates a pathological response characterized by abnormal growth of cardiac myocytes. This cellular phenotype is the assembly of new sarcomeres and activation of a 'fetal' set of cardiac genes [48,50]. At the molecular level, these effects lead to activation of intercellular signaling pathways that ultimately affect nuclear factors and the regulation of pathological gene expression programs [54]. These signaling pathways do not function separately, but they participate in a more organized response that generates interdependent and cross-talking networks (Figure 4). Briefly, signaling pathways involved in cardiac hypertrophy include G-protein signaling, mitogen-activated protein kinase (MAPK), protein kinase A (PKA) and C (PKC) signaling, and Ca^{2+} dependent pathways; calcineurin and calmodulin-dependent kinase (CaMK) [46–48,55].

The most relevant myocardial G-protein coupled receptors (GPCRs) include α- and β-adrenergic receptors that are coupled to GTP-binding proteins, Gs, Gq/G11, and Gi. Stimulation of pathological cardiac hypertrophy agonists, Angiotensin II (AngII), Endothelin I (ET-1), and α-adrenergic, activates $G_q/_{11}$-coupled receptors, which activates phospholipase C (PLC), and downstream kinase PKC, and develop concentric cardiac hypertrophy [48,50]. Forced expression of a dominant-negative G_q in mice can almost completely block pathological hypertrophy [48]. Stimulation of the β-adrenergic receptors (βAR) activates Gαs and adenylate cyclase (AC) activity, accumulation of cAMP and subsequent activation of PKA. Acute stimulation of βAR in response to epinephrine and norepinephrine is associated with physiological hypertrophy and increased contractile function [48].

Chronic βAR stimulation results in pathological remodeling and the progression to heart failure [56]. Forced expression of PKA, the downstream effector of Gαs signaling, in the heart results in cardiomyopathy associated with cardiac hypertrophy and fibrosis [57]. An increase in intracellular Ca^{2+} concentration in cardiomyocyte activates several Ca^{2+}-dependent signaling pathways that are involved in the progression of heart failure. Calcineurin, a Ca^{2+}/calmodulin (CaM) -activated phosphatase regulating the activity of the nuclear factors of activated T cells (NFAT) transcription factor, is involved in pathological cardiac hypertrophy and failure [58,59].

Ca^{2+}/calmodulin-dependent protein kinase II (CaMKII) is also a Ca^{2+}-dependant kinase in cardiomyocyte. Activation of CaMKII can phosphorylate and dissociate Class II HDAC from binding to transcription factors in the nucleus, and resulting in progression of cardiac hypertrophy. CaMKII has also been shown to play a critical role in cardiac excitation-contraction coupling in response to β-adrenergic signaling [60]. However, sustained activation of cytoplasmic CaMKIIδ may phosphorylate proteins involved in cardiac apoptosis. It also has been shown that mice deficient in CaMKIIδ in the heart are protected from pathological hypertrophy following aortic banding [61].

ERK family members have also been shown to play a unique role in the signaling response to stress stimuli and are downstream effectors of the hypertrophic response [40,62]. P38 MAPK signaling pathways also participate in transducing cardiac hypertrophic signals in the heart. Published data existed about p38 MAPK function in cardiac hypertrophy, in that either promotion of hypertrophic growth in cultured cardiac myocytes, or progression to heart failure in animal models [63,64].

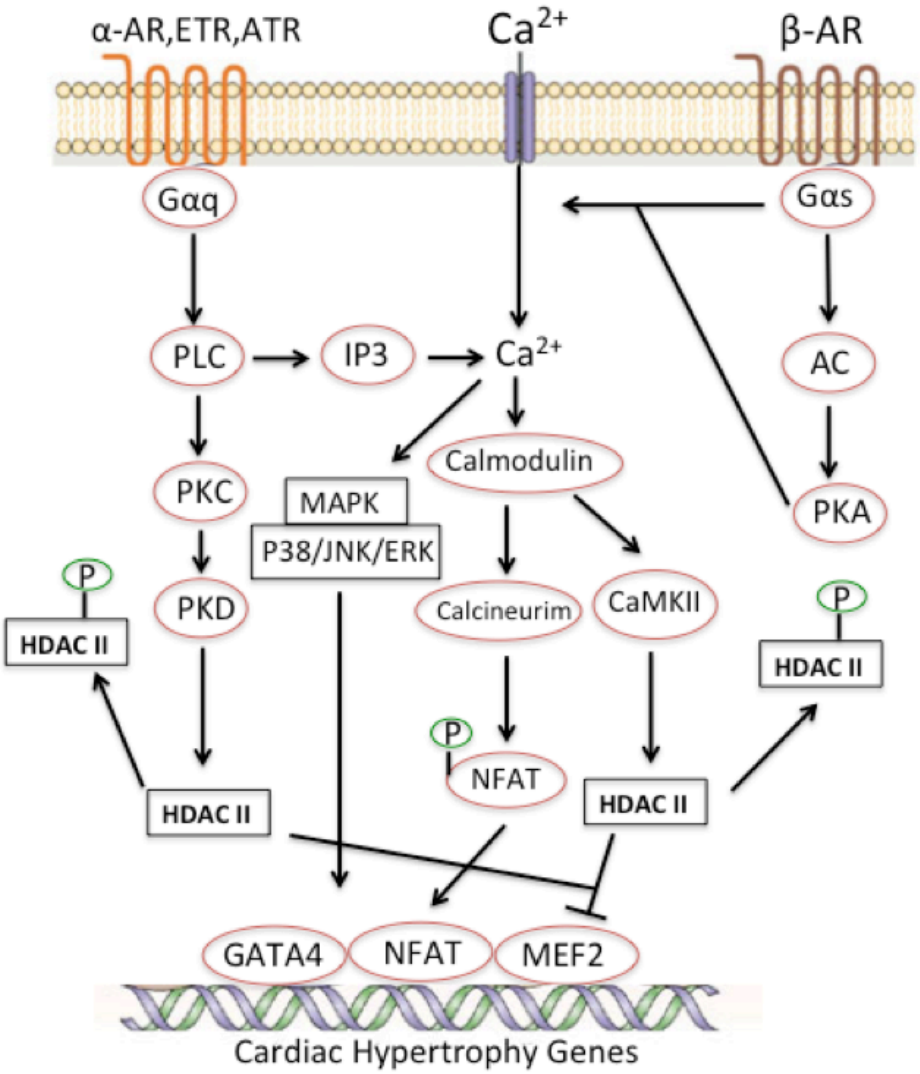

Figure 4: Signaling pathways involved in cardiac hypertrophy. Hypertrophic stimuli activate intracellular signaling pathways, such as G-proteins, Calcineurin, CaMKII, MAP-kinases, and others, in a receptor-dependent manner. The signaling enhancement results in phosphorylation, activation, and nuclear translocation of many transcription factors that are involved in cardiac hypertrophy gene expressions. This schematic has been adapted from [48].

3.2. Myocyte death

3.2.1. Introduction

To date, there are two well-recognized signaling pathways for cell death, apoptosis and necrosis. Apoptosis and necrosis are considered as two independent mechanisms; whereas apoptosis is a genetically controlled process, necrosis is a form of accidental death resulting from cellular injury [65].

Necrosis induces major damage at the cell membrane that results in loss of cellular homeostasis, rapid swelling, plasma membrane rupture and release of intracellular contents. In contrary, apoptosis is initiated by activation of endogenous proteases that results in cell shrinkage, chromatin cleavage, DNA fragmentation, and membrane blebbing. Apoptosis process is also involved in formation of membrane enclosed cellular organelles called "apoptotic bodies" that are either phagocytosed by tissue macrophages and neighbouring cells or undergoes degradation [65]. Both apoptosis and necrosis can be seen as a part of the pathogenesis of heart failure that result in loss of myocytes due to cell death. [66,67].

A programmed form of necrosis, necroptosis, is a form of cell death through regulated cell signaling pathways [68,69]. Whereas, apoptosis is defined as programmed cell death that responds to external and internal stimuli, activating separate signaling pathways resulting in cell death that does not involve an inflammatory reaction. When apoptosis is blocked by the inhibition of caspase activity, necroptosis can act as a backup mechanism, [70] ensuring cellular execution due to pathogen infections or cellular pathophysiology. Therefore, the induction of necroptotic cell death can be triggered by the same stimuli as apoptosis, namely death receptor activation [69].

3.2.2. Apoptosis

Since cardiomyocyte loss is the most important determinant of morbidity and mortality after heart pathophysiology, such as ischemia/reperfusion [71], myocardial infarction [72] and cardiomyopathies [73], preventing cardiomyocyte loss is important in management of heart dilation and failure [74,75]. Apoptotic cellular processes are often divided into two basic pathways, the “extrinsic” and “intrinsic” pathways (Figure 5).

In most cases, both pathways involve caspase activation. Caspases are a family of cysteine proteases that act as common death effector molecules in cell death pathways [76]. Caspases can activate each other, upon activation; initiator caspases (caspase-2, -8, -9 and -10) cleave and activate effector caspases (caspase-3, -6 and -7), which results in an increase of caspase activity through a protease cascade to cleave a number of different substrates in the cytoplasm or nucleus leading to cell death [76–78].

In the extrinsic pathway, caspases can be activated at the plasma membrane upon binding of extracellular death signal proteins (TNF-α, Fas L, TRAIL) to death receptors (receptor pathway). Binding of the ligand to death receptors results in recruitment of the death domain adaptor molecules (e.g. TRADD and FADD), form the death-inducing complex (DISC), further recruitment and activation of the initiator caspase-8 and the downstream effector caspase-3 [77].

The intrinsic pathway (mitochondrial pathway) is primarily activated by cellular stimuli, such as hypoxia, ischemia-reperfusion, and oxidative stress. The mitochondrial pathway is initiated by the release of apoptotic mediators such as cytochrome c [79], apoptosis inducing factor (AIF), Smac (second mitochondria derived activator of caspase) and endonuclease G (Endo G) from the mitochondrial intermembrane space. Once

cytochrome c is released into the cytosol, it triggers caspase-3 activation through formation of the cytochrome c/Apaf-1/caspase-9 “apoptosome” complex. Smac indirectly activates caspases, while release of Endo G and AIF from mitochondria results in direct or indirect DNA fragmentation [76,77,80,81]. A key step in the intrinsic pathway is the disturbance of the mitochondrial membrane integrity, which is usually regulated by the Bcl-2 protein family. Bcl-2 protein family contain both pro-apoptotic (Bax, Bad, Bid, Bik, Bim, Bak, Bnip3) and antiapoptotic (Bcl-2, Bcl-XL, bcl-W) members [82,83]. Activation of caspase-8 may result in cleavage of a pro-apoptotic Bcl-2 family, such as Bid, which leads to translocation to mitochondria to release cytochrome c thereby initiating the apoptotic pathway [76,77].

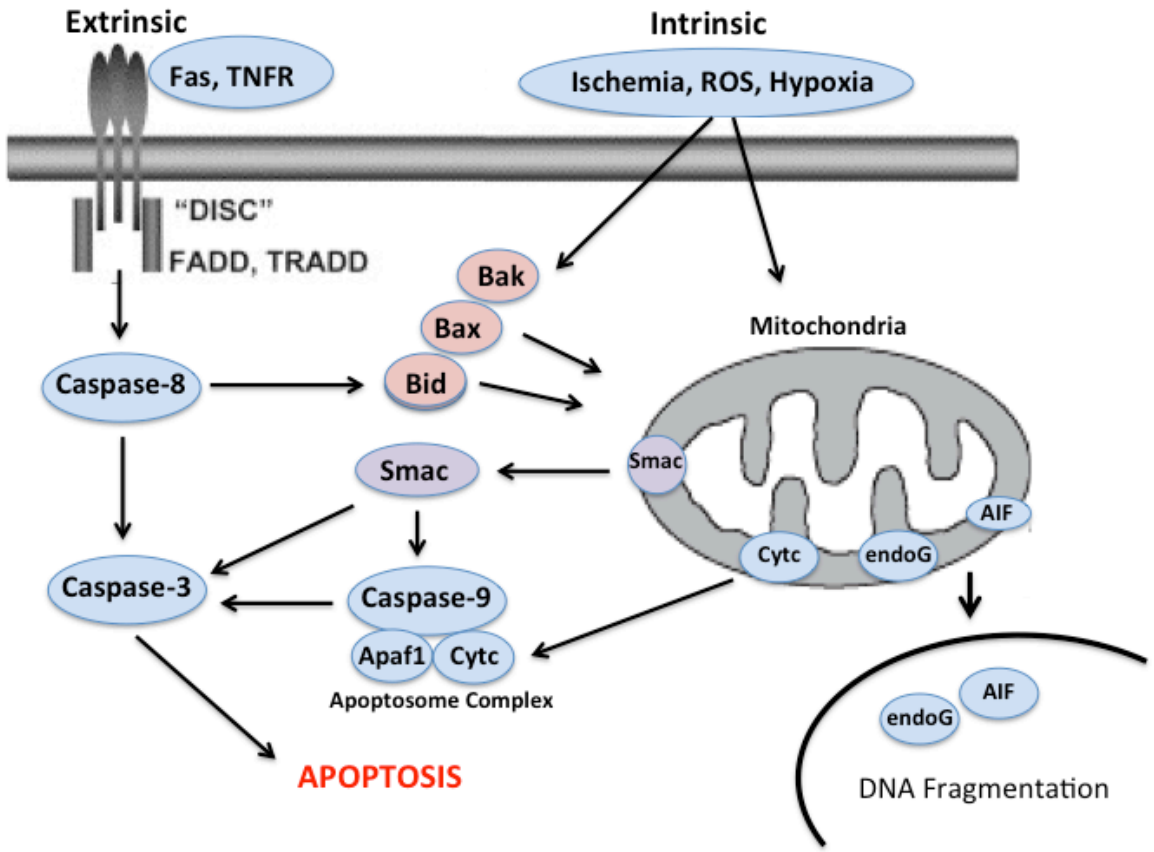

Figure 5: Programmed cell death, apoptotic pathways. The apoptotic pathways can be initiated through different entry sites, at the plasma membrane by death receptor ligation (extrinsic pathway) or at the mitochondria (intrinsic pathway). This schematic has been adapted from [77].

3.2.2.1 Signaling pathways in cardiac apoptosis

In the heart, a number of signaling pathways are essential for both pro- and anti-apoptotic effects in the myocardium. One of these signaling pathways is the MAP Kinase family. Mitogen activated protein kinases (MAPKs) are a group of kinases acting in succession to regulate cell growth, differentiation, and survival. The MAPK family is made up of three major branches: extracellular signal-regulated protein kinase (ERK), c-Jun N-terminal kinase (JNK), and p38 [84]. MAPKs could be activated in response to multiple agents, such as growth factors, cytokines, and stress. At first, G-protein coupled receptors activate MAPK kinase kinases (MAPKKKs), which target downstream MAPK kinases (MAPKKs) leading to subsequent activation of MAPKs. Upon their activation, they phosphorylate cytoplasmic, nuclear, and mitochondrial targets to regulate a variety of cellular processes including cell death [80].

In cardiac cells, JNKs were found to play critical roles in the regulation of cell death especially via the mitochondrial apoptotic pathway. For instance, in primary cardiomyocytes, expression of JNK or MKK4 inhibitory mutants increased ischemia-reperfusion-induced cardiomyocyte apoptosis, suggesting a protective role for JNK signaling [85]. On the other hand, inhibition of JNK1 was reported to actually protect cardiomyocytes from ischemia-induced apoptosis [86]. These findings demonstrate that JNKs can have both pro- and anti-apoptotic effects, although more experimental models prove induction of the pro-apoptotic pathways [87].

In the heart, MEK-ERKs have been shown to be part of the insulin-like growth factor-1 (IGF-1), basic fibroblast growth factor (bFGF), catecholamine and β2-adrenergic induced anti-apoptotic pathways [88–90]. For instance, ERK1/2 could antagonize apoptosis

through association with p90 ribosomal S6 kinase (RSK) by inactivation of the pro-apoptotic BAD protein and phosphorylation of GATA4 through its association with Bcl-XL upregulation [87,91]. P38 MAPK is thought to play a role in stress-induced apoptosis in cardiomyocytes. In contrast, some studies show a protective role of p38 signaling upon apoptotic stimulation. For instance, inhibition of p38 MAPK increased norepinephrine-induced apoptosis in cardiac myocytes [92]. On the other hand, *in vivo* study showed, inhibition of p38 promotes protection from ischemia-induced apoptosis [93].

Similar to the role of p38 MAPK in cardiac hypertrophy, there is also conflicting data with regard to p38 role in cardiac apoptosis. Several *in vivo* studies show the pro-apoptotic role of p38 in the heart, while in *vitro* studies support the protective role of p38 MAPK in cardiomyocytes.

3.2.3. Necroptosis

Necroptosis is a programmed cell death pathway similar to unregulated necrotic cell death [94]. In contrast to apoptosis, the necroptosis signaling pathway is completely caspase independent and relies on the stabilization and activation of the kinases RIP1 Receptor Interacting Protein 1 (RIP1) and Receptor Interacting Protein 3 (RIP3) [95]. Both kinases are regulated by caspase 8, in which they can be directly cleaved and inactivated by caspase 8 [96,97]. The cellular inhibitors of apoptosis proteins (cIAP) can also regulate RIP1. cIAP proteins are responsible for proteasomal degradation of RIP1. RIP3 can bind to RIP1 to form a complex called a Necrosome, and within the complex RIP3 is phosphorylated and activated by RIP1 [98]. Active RIP3 can phosphorylate the pseudo kinase, Mixed Lingase Kinase Ligase (MLKL) which results in the formation of

porous structures, leading to cell and plasma membrane disruption and execution [99].

The chemical compound necrostatin-1 (Nec-1) inhibits necroptosis without affecting apoptosis [100], which shows an independent caspase pathway of necroptosis. Moreover, studies in knockout mice have revealed that the regulation of the necroptotic pathway plays a direct role in viral infections inflammatory responses [101].

4. The role of β-adrenergic receptors in heart

4.1. Introduction

The autonomic (sympathetic) nervous system (ANS) is primarily involved in mediating the neuronal and hormonal stress response or fight-or-flight response (ex. increased heart rate). Activation of the symapathic nervous system in cardiovascular system releases 2 catecholamines, epinephrine (adrenaline) and norepinephrine (noradrenaline). Release of norepinephrine by the sympathetic nervous system and epinephrine by the adrenal medulla into circulation results in increase heart rate, contraction and blood vessel constriction.

In cells, epinephrine and norepinephrine mediate their effect by binding to adrenergic receptors, α1AR subtypes, α2AR and βAR subtypes. [102,103]. Regulation of β-adrenergic receptors (β-ARs) is important in understanding the mechanism of cardiac performance [104]. β-ARs belong to the superfamily of G-protein coupled receptors. In mammals three different subtypes have been distinguished: β1-, β2-, and β3-ARs [105,106]. β1-AR is predominately expressed in cardiac tissues (control of heart rate and contraction), the β2-AR is mainly expressed in the smooth muscle tissue (control of vasodilatory responses) and the β3AR is mainly expressed in adipose tissue. In the human heart, both β1- and β2-ARs exist and the ratio is 70%: 30% in the atria and 80%: 20% in the ventricles with β1-ARs being the dominant receptor [104]. When agonists such as epinephrine or norepinephrine bind to the receptor, GDP dissociates from the Gαs subunits, which then binds GTP. This causes the dissociation of G-protein into Gαs and Gβγ. Both β1 and β2ARs exert their physiological effects (increase cardiac contraction) by coupling to Gαs and activating adenylate cyclase enzyme, increasing intracellular

levels of cyclic adenosine monophosphate (cAMP) and stimulation of cAMP-dependent protein kinase A (PKA) [107,108]. In addition β2-ARs could also couple to inhibitory Gi proteins leading to reduction of adenylyl cyclases activity and subsequently cardiac contraction reduction and anti-apoptotic pathway initiation [108,109] (Figure 6).

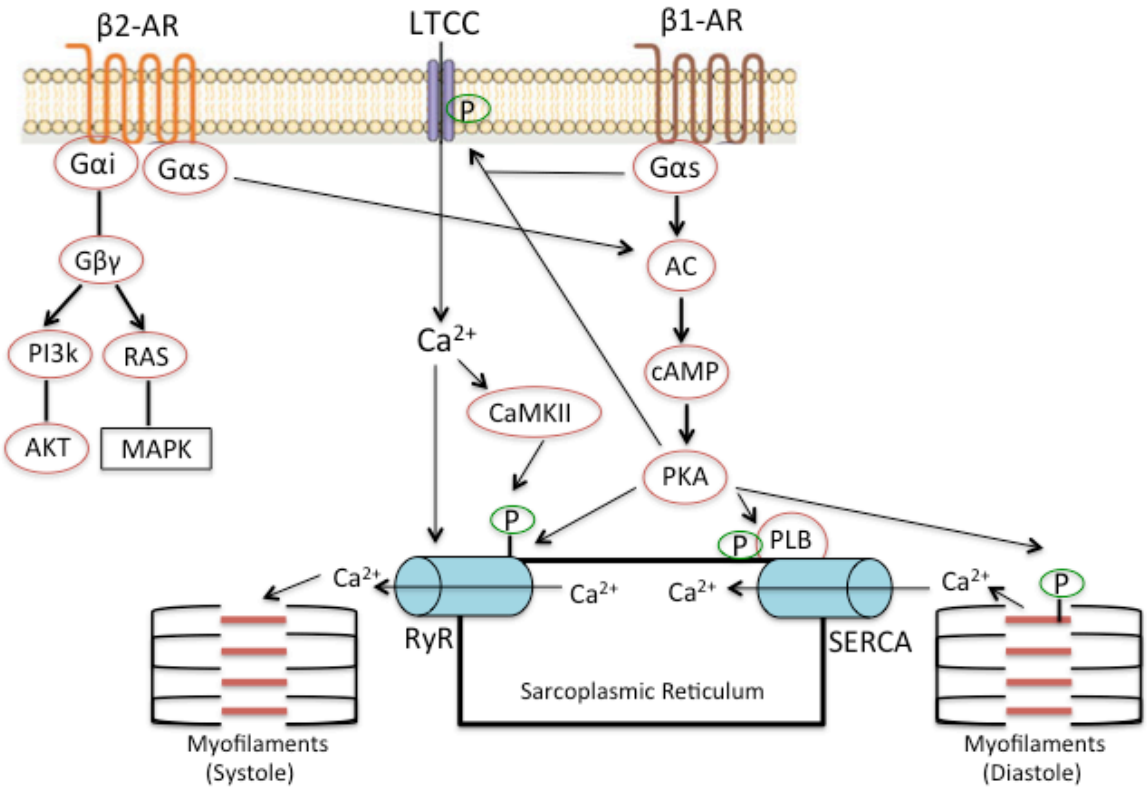

Figure 6: Adrenergic signaling in the heart. Within the heart, the β1-AR, β2-AR and induce unique, but overlapping signaling pathways to modulate cardiac contraction, survival and growth. This schematic has been adapted from [108].

4.2. Cardiac β1-adrenergic receptor function and signal transduction pathway

β1-ARs are the dominant receptor subtype in cardiac tissue, as mentioned above [104]. Under normal conditions, sympathetic activation (primarily by norepinephrine) of β1-ARs results in an increase in heart rate (chronotropy) and cardiac contractility (inotropy) [105]. Acute activation of β1-ARs represent the primary mechanism to increase cardiac output (CO) during the sympathetic fight or flight response [105]. However, chronic stimulation of the β1-AR is cytotoxic *in vitro*, leading to myocyte death and eccentric cardiac remodeling *in vivo*[108].

The β1-AR binds to Gαs subunits to stimulate the adenylyl cyclase enzyme and increase intracellular levels of an important secondary messenger, cAMP. cAMP binds to regulatory subunits on PKA, which release and activate the catalytic subunits to phosphorylate the downstream effectors that control the cardiac excitation and contraction pathway thus regulating chronotropy and inotropy [104] (Figure 7). β1-AR/PKA signaling acts on several proteins that are essential for cardiac function: L-type Ca^{2+} channels, ryanodine receptors, phospholamban, and the troponin complex. These mechanisms regulate intracellular Ca^{2+} concentrations, which in turn modulate myofilament Ca^{2+} sensitivity (troponin complex). Generally, increases in intracellular Ca^{2+} concentrations cause binding of the calcium to troponin C and initiate contraction (systole) while decreases in intracellular Ca^{2+} concentrations cause muscle relaxation (diastole) [110] (Figure 6) .

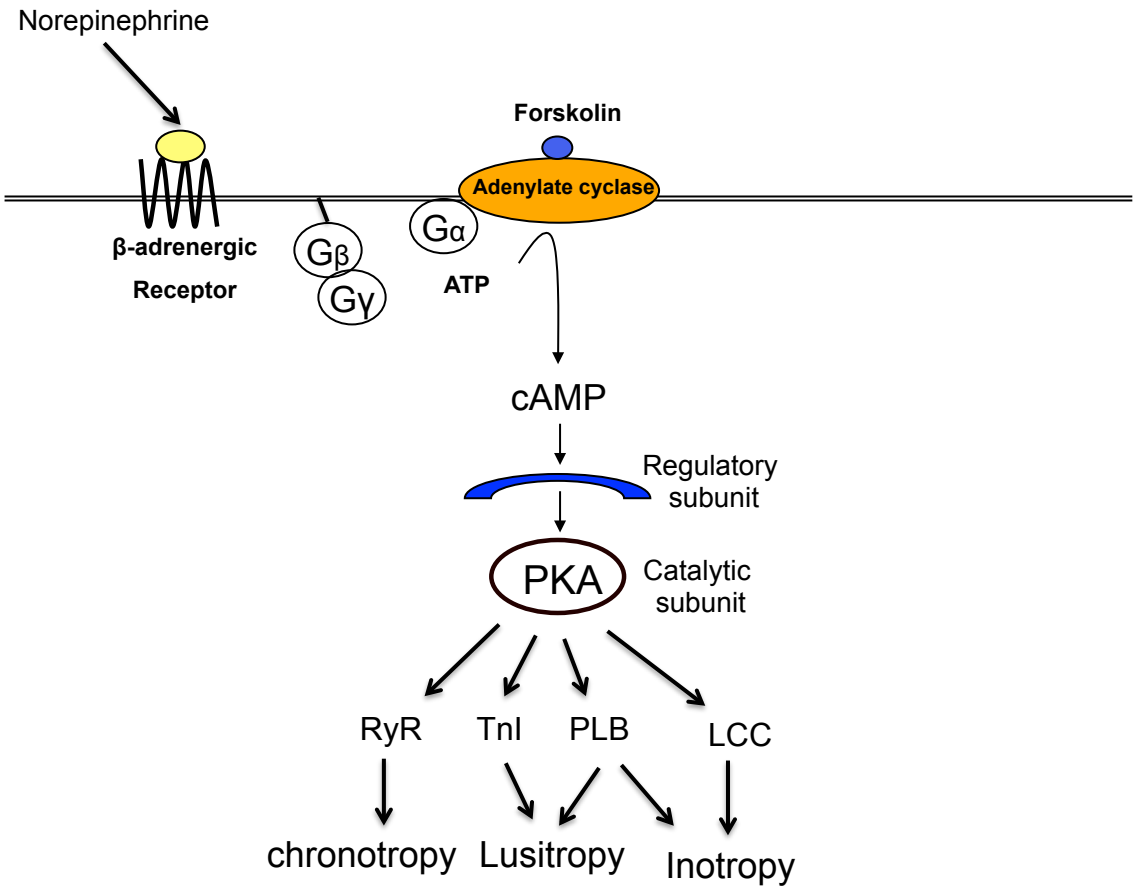

Figure 7: PKA signaling in the heart. Agonist binding to β-AR activates, via G_s, the plasma membrane bound adenylate cyclase (AC), which catalyzes the conversion of ATP to cAMP. cAMP activates PKA. Phosphorylation of PKA substrates causes change in cardiac inotropy, lusitropy and chronotropy.

In cardiomyocytes, the L-type Ca^{2+} channel (LTCC) is responsible for the conductance of the calcium current (ICa), which causes contraction [111]. PKA has been shown to be involved in phosphorylation of LTCC and activation of ICa [112]. Ryanodine receptors (RyRs) located on the sarcoplasmic reticulum are important in cardiac excitation-contraction coupling. The increase in intracellular calcium triggers further calcium release from the sarcoplasmic reticulum through the RyRs. β-AR/cAMP/PKA pathway play an indirect regulatory role on the function of RyRs, in which PKA-mediated phosphorylation of RyRs activates L-type Ca^{2+} channel and increase the release of sarcoplasmic Ca^{2+} through RyRs [113]. The regulation of RyRs is important for producing acute increases in the heart's pumping power [113]. PKA-mediated hyper-phosphorylation of RyRs might increase cytosolic Ca^{2+} levels and lead to the pathogenesis of heart failure [114]. An important target of PKA is phopholamban (PLB), a sarcoplasmic reticulum membrane protein that controls the sarcoplasmic reticulum Ca^{2+} uptake by inhibiting SERCA (The sarcoplasmic/endoplasmic reticulum Ca^{2+} ATPase). During rest, PLB is in a dephosphorylated state and inhibits SERCA. Activation of β-ARs leads to PKA-mediated phosphorylation of PLB, which increases sarcoplasmic reticulum Ca^{2+} uptake from cytoplasm. The overall results are important for cardiomyocyte relaxation (positive lusitropy). Further PKA targets are myosin-binding protein C and troponin, which reduce Ca^{2+} sensitivity of myofilaments. Although β1-AR stimulation is important in physiological excitation contraction coupling within the heart, chronic stimulation and acute over-stimulation can cause damage to myocardial tissue. Pharmacological studies have reported that stimulation of β1-AR leads to cardiac apoptosis [115]. The mechanisms of cardiac apoptosis appear to be both PKA-dependent and independent.

Some studies show that β1-AR mediated apoptosis was blocked by the PKA inhibitor (H89), and PKA activators (forskolin) induced apoptosis [90]. On the other hand, other studies demonstrated that β1-AR activation of CaMKII causes the release of mitochondrial cytochrome C and induces cardiac apoptosis in a PKA-independent pathway [116]. In addition, inhibition of PKA activity showed prevention of CaMKII activation and induction of cardiac apoptosis. This demonstrates the co-dependence of these two pathways[117].

4.3. β-adrenergic blockers and cardiac diseases

Since the Nobel Prize winning development of β-adrenergic antagonists (β-blockers) for the treatment of angina and cardiac arrhythmias by Sir James Black [118,119], this class of drugs has proved to be one of the most impactful in terms of contributions to pharmacology and medicine.

β-blockers are a class of drugs that are used to treat a wide range of cardiovascular diseases (hypertension, coronary artery disease, myocardial infarction (MI), and congestive heart failure as well as various non-cardiovascular diseases (glaucoma, migraine and anxiety) [120,121]. β-blockers block the effect of catecholamines (e.g. norepinephrine and epinephrine) on β1 and β2-subtypes of cardiac adrenergic receptors in patients with heart failure, and reduce heart rate and blood pressure by dilating blood vessels. Therefore, the enhanced sympathetic activation of the heart is inversely correlated with survival by β-blockers treatment, indicating one compelling reason why β-blockers are useful in heart disease.

β-blockers have been subsequently developed since the first generation of non-

selective (β1 +β2) β-blockers (propranolol), to the more cardio-selective β1-specific antagonists (atenolol, metoprolol, and bisoprolol). Selective β-blockers mainly act on the heart and do not affect airway passages. β-blockers that cross-react with β2-ARs such as propranolol can inhibit β2-AR mediated vasodilation and potentially shift the balance towards vasoconstriction, which leads to a reduction in tissue perfusion [122].

β-blockers protect the heart by balancing myocardial oxygen supply-demand and controlling heart rate [123]. Through this mechanism, β-blocker therapy has been used for patients after myocardial infarction (MI), as it is associated with a substantial reduction in the risk of re-infarction and mortality [120]. A randomized controlled trial evaluated treatment with atenolol (β1 selective blockade) in patients within hours after the MI, and found a significant decrease in mortality compared to no treatment. This shows clear benefits of early β-blocker therapy within 24 hours of MI symptoms [124–126].

As mentioned above, a healthy human heart contains 80% β1-ARs and 20% of the β2-ARs. In heart failure, the number of β1-AR decreases such that there are 60% β1 and 40% of the β2. There is also evidence that long-term activation of β1-ARs in mice is more toxic to the myocardium than activation of β2-ARs. Also, transgenic mice overexpressing β1-ARs develop cardiac failure and die, whereas β2-ARs overexpression is more tolerable. In humans, activation of β1-ARs is associated with an increase in mortality and they are restricted to short-term maintenance of cardiac output in intensive and coronary care units. The beneficial use of β-blocker treatment for heart failure was questionable at the beginning, but subsequent clinical trials proved that β-blockers are effective in reducing mortality in patients with heart disease [56,114].

CHAPTER 2: Statement of Purpose

The enhanced sympathetic drive due to binding of catecholamines, norepinephrine and epinephrine, to the β1 and β2-subtypes of cardiac adrenergic receptors in the heart is one factor contributing to the progression to heart failure. However, this adrenergic stimulus is also important in controlling cardiac inotropic, chronotropic and lusitropic physiological parameters.

There is a lack of information regarding how acute and chronic β-adrenergic signaling affects cardiac gene expression. Also, evidence indicates that regulation of the expression of a transcriptional regulatory protein can exert considerable control over the gene expression profile. MEF2 proteins are important transcription factors involved in cardiac gene expression in both physiological and pathological adaption of the heart. Therefore the overall purpose of this work was to identify an important link between the pharmacological blockade of β-adrenergic signaling in the heart and cardiac gene expression, particularly with respect to MEF2. We assessed whether this link is involved at an acute level, protection of cardiomyocytes from apoptosis in the early events post myocardial infarction and also in chronic conditions, in resistance to longer-term changes in cardiac gene expression leading to cardiac failure. This purpose was achieved experimentally through addressing the following specific objectives outlined below:

1) To determine how MEF2 activity is regulated during acute β-adrenergic blockade and determine whether this is protective against cardiomyocyte death.

2) To characterize changes in the cardiac gene transcriptome network and MEF2 activity during heart failure with and without β-adrenergic blockade.

3) To begin to assess the potential role of some of these differentially expressed genes in cardiomyocyte apoptosis and hypertrophy.

Considering human heart disease and therapy, this work would contribute in understanding the molecular events essential in how β-adrenergic receptor blockers have positive effects on heart pathology.

CHAPTER 3

PRO-SURVIVAL FUNCTION OF MEF2 IN CARDIOMYOCYTES IS ENHANCED BY β-BLOCKERS [χ]

Summary

β1-Adrenergic receptor (β1-AR) stimulation increases apoptosis in cardiomyocytes through activation of cAMP/protein kinase A (PKA) signaling. The myocyte enhancer factor 2 (MEF2) proteins function as important regulators of myocardial gene expression. Previously, we reported that PKA signaling directly represses MEF2 activity. We determined whether (a) MEF2 has a pro-survival function in cardiomyocytes, and (b) whether β-adrenergic/PKA signaling modulates MEF2 function in cardiomyocytes. Initially, we observed that siRNA-mediated gene silencing of MEF2 induces cardiomyocyte apoptosis as indicated by flow cytometry. β1-AR activation by isoproterenol represses MEF2 activity and promotes apoptosis in cultured neonatal cardiomyocytes. Importantly, β1-AR mediated apoptosis was abrogated in cardiomyocytes expressing a PKA-resistant form of MEF2D (S121/190A). We also observed that a β1-blocker, Atenolol, antagonizes isoproterenol-induced apoptosis while concomitantly enhancing MEF2 transcriptional activity. β-AR stimulation modulated MEF2 cellular localization in cardiomyocytes and this effect was reversed by β-blocker

[χ] Hashemi, S.[1,3,4], Salma, J.[1,3,4], Wales, S.[1,3,4], and McDermott, J.C.[1,2,3,4]

[1] Department of Biology, [2] Centre for Research in Mass Spectrometry (CRMS), [3] Muscle Health Research Centre (MHRC), [4] Centre for Research in Biomolecular Interactions (CRBI), York University.

treatment. Furthermore, Kruppel-like factor 6, a MEF2 target gene in the heart, functions as a downstream pro-survival factor in cardiomyocytes. Collectively, these data indicate that (a) MEF2 has an important pro-survival role in cardiomyocytes, and (b) β-adrenergic signaling antagonizes the pro-survival function of MEF2 in cardiomyocytes and β-blockers promote it. These observations have important clinical implications that may contribute to novel strategies for preventing cardiomyocyte apoptosis associated with heart pathology.

Introduction

Morbidity and mortality associated with heart disease remain a prevalent worldwide health concern [127]. In the diseased heart, the lack of capacity for tissue regeneration after injury contributes to diminished cardiac function and heart health. At the cellular level, irreversible loss of cardiac myocytes due to programmed cell death contributes to pathological ventricular remodeling and progression to heart failure [115,128]. Therefore, understanding the molecular genetic pathways that induce and also prevent myocardial cell apoptosis has potentially profound implications for understanding heart pathology and also therapeutic interventions for heart disease [128,129].

β-Adrenergic receptor (β-AR) antagonists, or β-blockers, are a class of highly effective front-line drugs for heart disease that, at the molecular level, block norepinephrine and epinephrine from binding to the β-ARs. β-Blockers primarily block β1 and β2 receptors and their efficacy in the heart is related to their capacity to influence both chronotropy and inotropy by reducing both heart rate and the force of myocardial contraction. Thus, this reduction in heart work by β-blockers has been effectively used to ameliorate

hypertrophy and cardiac dilation leading to heart failure [130]. Interestingly, one reported benefit of chronic β-blocker treatment is in reducing myocyte death in patients with heart failure [114,131]. Although activation of β1-AR, the predominant β-AR in the heart, has an important role in the regulation of normal heart function, prolonged activation of the β-adrenergic system in human heart disease or in experimental model systems results in dilated myopathy, cardiac fibrosis, cardiac myocyte apoptosis and heart failure [121,132]. Previous studies have suggested that the cAMP/PKA pathway downstream of β1-AR induces cardiac myocyte apoptosis which is supressed by β-blocker therapy [128,133]. However, the mechanism by which prolonged β-adrenergic activation compromises the survival of cardiac myocytes has not previously been elucidated. Recently, we have reported that one of the myocyte enhancer factor 2 (MEF2) proteins (MEF2D), which is a key transcriptional regulator of cardiac gene expression, is directly targeted by PKA signaling [134]. Although the role of MEF2 proteins in cardiovascular development and post-natal growth and hypertrophy has been extensively documented, [135–138] there has previously been no clear link between MEF2 and cell survival pathways in the heart. MEF2s belong to the MADS (MCM1, agamous, deficiens, serum response factor) superfamily of sequence specific DNA-binding transcription factors. The N terminus of MEF2 proteins is highly conserved among all family members and consists of a 58-amino acid MADS domain and an immediately adjacent 28-amino acid MEF2 domain. These two domains collectively mediate dimerization, co-factor interactions and DNA binding to the consensus DNA sequence (C/T)TA(A/T)4TA(G/A) found in the regulatory region of most cardiac-specific genes [139]. The two major isoforms of MEF2 in the adult heart are MEF2A and MEF2D, which form heterodimers [140]. Although a pro-survival role

of MEF2 has not been reported in striated muscle cells, a potent role of MEF2 in neuronal survival pathways has indeed been reported [16]. Moreover, we recently documented that PKA activation leads to abrogation of MEF2 activity and pro-survival mechanisms in primary hippocampal neurons [17]. This effect is mediated by a direct repressive effect of PKA phosphorylation of MEF2D at serines 121 and 190 leading to inhibition of its transactivation properties [134]. In view of the potent role of both MEF2 and β-adrenergic signaling in the molecular control of heart structure and function, we explored a possible connection between β-adrenergic signaling and MEF2 in cardiomyocyte survival. Here, we report, for the first time, that MEF2 has a pivotal prosurvival role in cardiomyocytes. Moreover, we observed that β-adrenergic activation directly antagonizes this MEF2 pro-survival role and β-adrenergic blockade restores this function, promoting cardiomyocyte survival. In addition, we document that the Kruppel-like factor 6 (KLF6) is an important downstream target of MEF2 in the cardiomyocyte survival pathway. These observations have important clinical implications for heart disease, firstly establishing that MEF2 has a key pro-survival role in the heart and secondly, documenting that β-adrenergic signaling intersects with this MEF2 survival pathway establishing a therapeutic node for intervention in cardiomyocyte apoptosis.

Results

MEF2 functions as a pro-survival factor in cardiac myocytes

MEF2 has previously been implicated in cell survival in primary embryonal hippocampal neurons [17] and in cerebellar granular neurons[141]. Although it is well documented that MEF2 functions as a key regulator of cardiac myocyte differentiation, [30,142] its role, as a possible survival factor has not been proven. Recently, we have identified some potentially novel aspects of MEF2 function in skeletal and cardiac muscle using high throughput genomic technologies such as ChIP-Exo and RNA-seq which based on gene ontology analysis, suggest a wider role for MEF2A than just cellular differentiation [143]. Interestingly, MEF2A-null mice exhibit an increase in cell mortality in the post-natal period [30]. Therefore, we sought to rigorously address the question of whether MEF2 has a direct role in cardiomyocyte survival. Initially, we used siRNA mediated gene silencing to downregulate MEF2A expression in primary cardiac myocytes followed by flow cytometry analysis to detect apoptotic cells. The efficacy of MEF2A silencing was tested by western blot analysis of primary cardiomyocytes that were transfected with two independent MEF2A siRNAs and a control scrambled siRNA (scRNA). As shown in Figure 8b, a robust reduction of MEF2A protein level was observed in cells expressing siMEF2A in contrast to cells expressing scRNA. To examine whether MEF2A silencing resulted in cardiomyocyte apoptosis, a combination of PI and annexin V-FITC fluorescence was used to determine necrosis and apoptosis by flow cytometry. An increase in the percentage of apoptotic cells with cardiomyocyte MEF2A silencing was observed as indicated in the lower right quadrant of the density plot (high Annexin V, low PI). Depletion of MEF2A enhanced the levels of cardiomyocyte apoptosis (27.67

and 25.70%) compared with the scRNA control condition (7.03%; Figure 8a). These data indicate that MEF2A has a pro-survival role in cardiomyocytes. Next, we interrogated the role of MEF2A depletion in cardiomyocyte gene expression in RNA-seq. A full description and bioinformatics analysis of these RNA-seq data will be published elsewhere (Hashemi and Wales, in preparation). However, with respect to apoptosis, we observed a significant enrichment of the gene ontology term, 'positive regulation of apoptotic process' in the data set. Using GeneMania, [144,145] the 20 genes with the lowest P-value were plotted to demonstrate the potential role MEF2A may have in regulating the expression of apoptosis-related genes. Several key apoptotic and tumor suppressor genes are upregulated including Bcl2l14, [146], Bnip3, [147,148] Rassf6 [149] and Ddit3 [150] (Figure 8c).

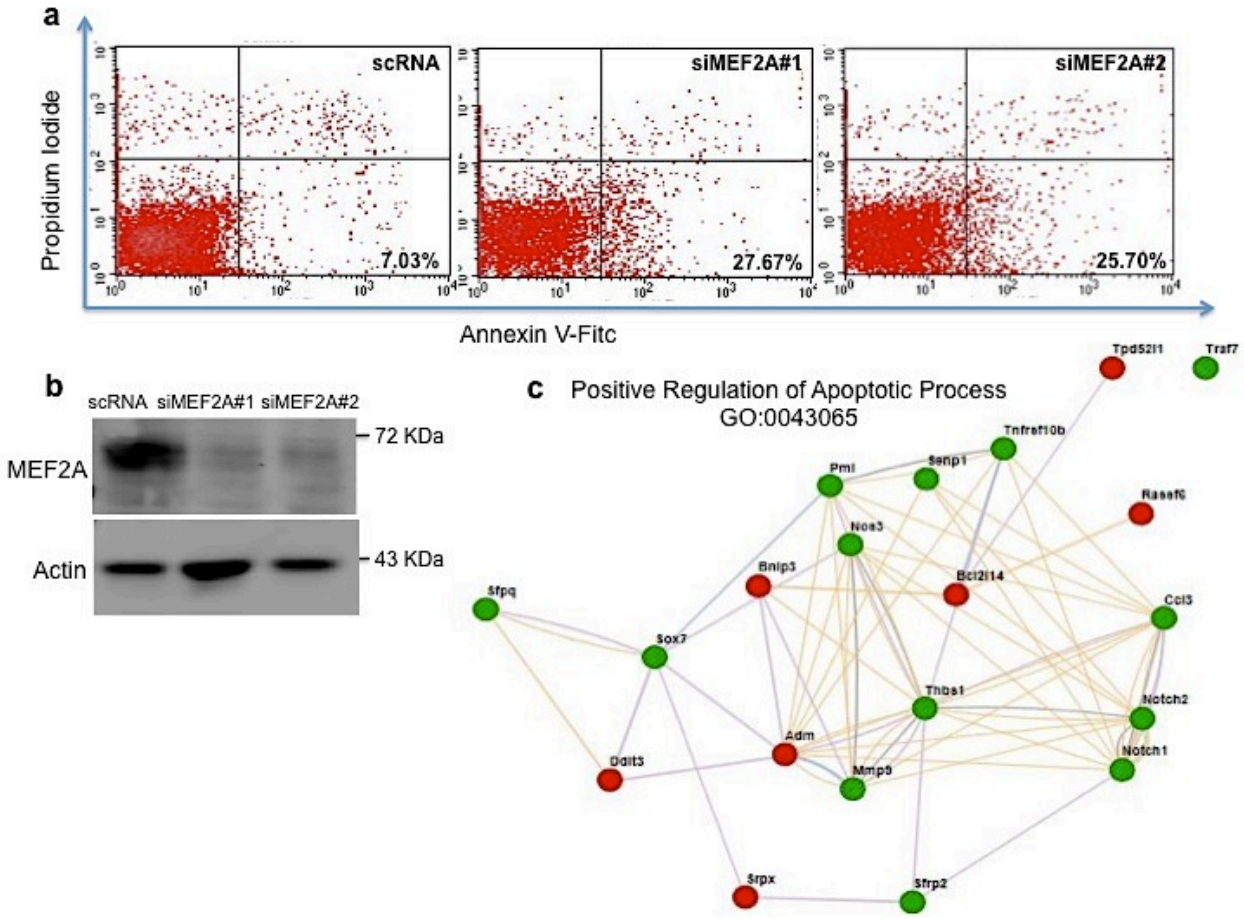
a
scRNA
siMEF2A#1
siMEF2A#2
Propidium Iodide
Annexin V-Fitc
7.03%
27.67%
25.70%
b
scRNA siMEF2A#1 siMEF2A#2
MEF2A
Actin
72 KDa
43 KDa
c
Positive Regulation of Apoptotic Process
GO:0043065
Tpd52l1
Traf7
Tnfrsf10b
Senp1
Pml
Rasef6
Noe3
Bnip3
Bcl2l14
Ccl3
Sfpq
Sox7
Thbs1
Notch2
Adm
Notch1
Ddit3
Mmp9
Srpx
Sfrp2

Figure 8

Figure 8. MEF2A knockdown induces apoptosis in cardiomyocytes. (a) Annexin V detection is upregulated in MEF2A-depleted cardiomyocytes. Primary cardiomyocytes were transfected with two independent MEF2A siRNAs or a control scRNA. Cells were stained with annexin V-FITC and PI using annexin V-FITC apoptosis detection kit 48 h after transfection. Apoptosis was measured using flow cytometry analysis (FACS analyzer). (b) siRNA-mediated gene silencing reduces MEF2A protein. Equal amounts of total protein were used for western blot analysis. The levels of the indicated proteins were assessed by a standard immunoblotting technique using specific primary antibodies for each as indicated. (c) RNA-seq analysis of MEF2A knockdown in cardiomyocytes. siMEF2A#1 or a control scRNA were transfected in cardiomyocytes in duplicate and prepared for RNA-seq analysis. The gene ontology (GO) term, positive regulation of apoptotic process, was observed. The 20 genes within this category with the lowest P-value are shown in a network created by the program GeneMania. Green and red nodes indicate down- and upregulated genes, respectively, whereas connections between nodes are as follows: purple, co-expression; orange, predicted; blue, co-localization; green, shared protein domains; gray, other.

Acute β1-AR signaling represses MEF2 activity leading to cardiomyocyte apoptosis

It has been documented that apoptotic cell death can be induced by β1-AR activation and is cAMP/PKA dependent [115,128]. In Skeletal muscle, we have previously shown that cAMP/PKA signaling is a potent repressor of MEF2D function and myogenic differentiation [134]. As the β-adrenergic system is such an important regulator of physiological and pathological heart function, we sought to determine whether acute β1-AR activation might impinge on the survival function of MEF2. Initially, we assessed activation of β1-AR-mediated apoptosis in primary cardiomyocytes by flow cytometry. Estimation of necrosis and apoptosis were again determined by a combination of PI and annexin V-FITC fluorescence, respectively. Substantial increases in apoptotic cells (cells appearing in the lower right quadrant of the density plot) were observed with isoproterenol (Iso; 10 μM) treatment (30.31%) when compared with control cells (10.77%; Figure 9a). To determine whether the mechanism leading to apoptosis is through cAMP–PKA pathway, we used a well-known pharmacological inhibitor of PKA, H89 (20 μM) before treatment with Iso (10 μM). Subsequently, reporter gene analysis demonstrated a reduction of MEF2 activity in Iso-treated cells, which was reversed by H89 treatment (Figure 9b). MEF2A and MEF2D are the two major isoforms of MEF2 in post-natal hearts that form heterodimers [140]. PKA was found to directly phosphorylate MEF2D in our previous work,[134] which also showed that this repressive effect was transdominant over MEF2A activity when MEF2A heterodimerized with MEF2D, as is the case in cardiomyocytes. PKA directly phosphorylates S121 and S190 on MEF2D and these sites were sufficient for repressive effects on skeletal muscle differentiation in

response to cAMP signaling [134]. To investigate this further, we determined whether a PKA-resistant MEF2D mutation (MEF2D S121/190A) could ameliorate β1-AR-PKA-mediated apoptosis in response to Iso. We noted a decrease in apoptotic cardiomyocytes when S121/190A was overexpressed with Iso (10 μM; 4.14%), compared with Iso alone (8.88%) in cardiomyocytes (Figure 9c). Conversely, phophomimic form of MEF2D (S121/190D) did not rescue Iso-induced cardiomyocyte cell death (Figure 9c). These results demonstrate that a PKA-resistant MEF2D (S121/190A) protects cardiomyocytes from Iso-induced apoptosis.

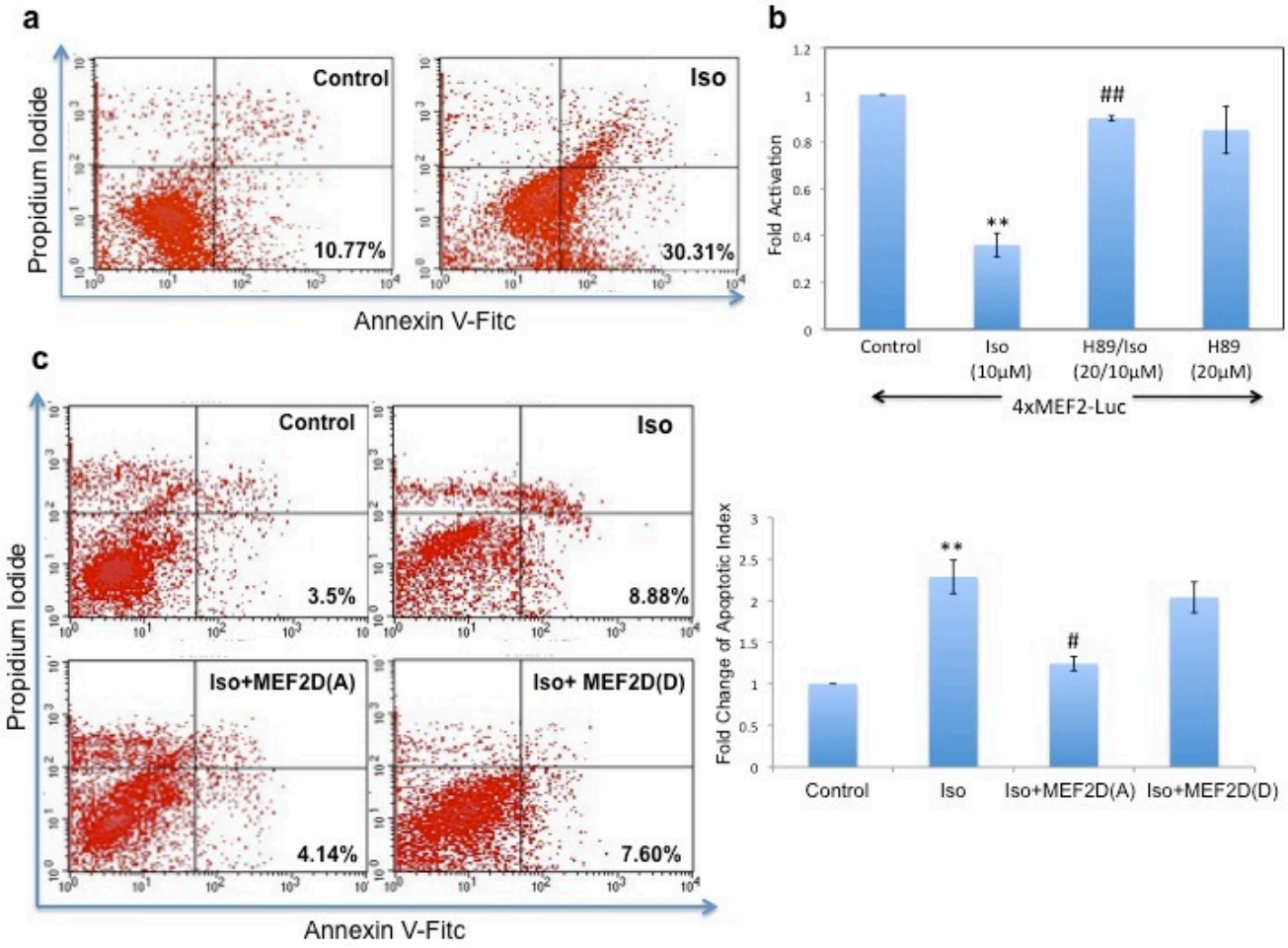
a
Propidium Iodide
Annexin V-Fitc
Control
10.77%
Iso
30.31%
b
Fold Activation
Control
Iso (10μM)
H89/Iso (20/10μM)
H89 (20μM)
4xMEF2-Luc
c
Propidium Iodide
Annexin V-Fitc
Control
3.5%
Iso
8.88%
Iso+MEF2D(A)
4.14%
Iso+ MEF2D(D)
7.60%
Fold Change of Apoptotic Index
Control
Iso
Iso+MEF2D(A)
Iso+MEF2D(D)

Figure 9

Figure 9. Activation of β1-AR induces cardiomyocytes apoptosis through the PKA pathway. (a) Primary cardiomyocytes were treated with Iso (10 μM) for 48 h and then stained with annexin V-FITC and PI using annexin V-FITC apoptosis detection kit. Apoptosis was measured using flow cytometry analysis. (b) Cardiomyocytes were transfected with 4xMEF2-Luc reporter gene and treated with Iso (10 μM) alone or in combination with PKA inhibitor (H89, 20 μM). Luciferase activity was assessed using the respective reporter gene and normalized to β-galactosidase (β-gal) activity. Data are the mean±S.E. The quantification data is between the same batch with n=3, **P≤0.01 comparing Iso with control, ##P≤0.01 comparing H89/Iso to Iso. (c) PKA-resistant MEF2D rescues cardiomyocytes. Primary cardiomyocytes were transfected with empty vector or mutated forms of MEF2D S121/190A (MEF2D (A), neutralizing) and S121/190D (MEF2D (D), phospho-mimetic) and then treated with with Iso (10 μM). Cells were prepared for FACS analysis as in a. n =3, **P ≤0.01 Iso versus control, #P ≤0.05 Iso+MEF2D (A) versus Iso.

A β1-selective adrenergic receptor blocker (Atenolol) enhances MEF2 transcriptional activity in primary cardiomyocytes

Given our data showing that β1-AR agonists activate PKA and induce apoptosis in cardiomyocytes, at least in part, by blocking the pro-survival role of MEF2A/D heterodimers, we next addressed the effects of β-blockers on MEF2 activity. As β-blocker therapy effectively is a first line treatment for most heart pathology, [115] we hypothesized that its impact on MEF2-mediated pro-survival, in conjunction with the well-known effects of β-blockers on cardiac contractility could contribute to the protective effects of pharmacological blockade of β1-AR in the heart. To test this hypothesis, we initially used an in vivo model a MEF2-LacZ sensor mouse [151–153] were treated with either β-blockers (Atenolol (Ate) 50 mg/kg per day) or solvent (water) for 48 h. The heart tissue was then stained with X-Gal (5-bromo-4-chloro-3-indolyl-β-d-galactopyranoside) and visualized for MEF2 activity. The data indicated a substantial enhancement of MEF2 activity in relatively acute β-blocker treatment in the hearts, as illustrated by X-Gal staining (Figure 10a). To document these effects in a more controlled manner, primary cardiomyocytes in vitro were transfected with a 4xMEF2-Luciferase construct (a synthetic reporter gene containing four copies of the MEF2 cis-element in tandem) and were treated with Ate (10 μM) alone and in combination with Iso (10 μM) for 48 h before determination of MEF2 transcriptional activity. These data illustrate that Ate enhances MEF2 transcriptional activity (Figure 10b). To further corroborate this, the effect of β-blockers on a natural heart promoter (atrial natriuretic factor—ANF), a previously well-characterized MEF2 target gene, [154] [154] was analyzed. Standard reporter gene analysis was performed using the ANF-Luc reporter gene with

Ate (10 μM) and Iso (10 μM) treatment. These experiments revealed that Iso (10 μM) treatment repressed Ate-Luc activity and this effect was abrogated with Ate, consistent with the idea that β-agonists repress ANF promoter activity through the MEF2 cis-element (Figure 10c, left panel). This was confirmed by utilizing an ANF-Luc reporter gene construct in which the MEF2 site was mutated by substitution of the A/T rich core of the MEF2 site with a GGG tri-nucleotide, which completely abrogates MEF2 binding (ANF-Luc ΔMEF2) (Figure 10c, right panel). Collectively, these data indicate that cardiomyocyte MEF2 activity on synthetic and natural promoters is repressed by Iso treatment and de-repressed by Ate treatment. These data demonstrate a potent level of control of cardiomyocyte MEF2 activity by β-adrenergic signaling.

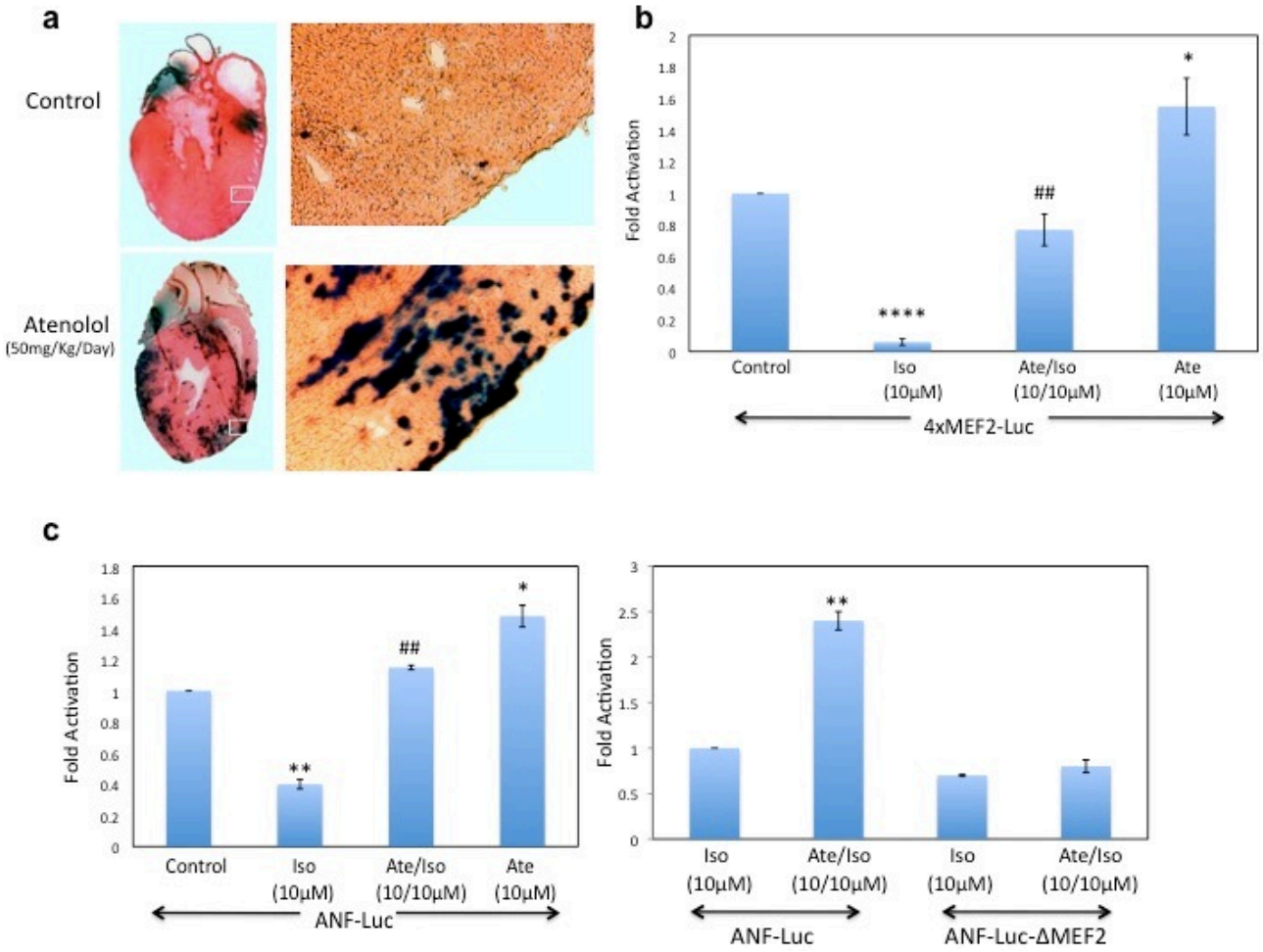
a
Control
Atenolol
(50mg/Kg/Day)
b
Fold Activation
Control
Iso
(10μM)
Ate/Iso
(10/10μM)
Ate
(10μM)
4xMEF2-Luc
c
Fold Activation
Control
Iso
(10μM)
Ate/Iso
(10/10μM)
Ate
(10μM)
ANF-Luc
Fold Activation
Iso
(10μM)
Ate/Iso
(10/10μM)
Iso
(10μM)
Ate/Iso
(10/10μM)
ANF-Luc
ANF-Luc-ΔMEF2

Figure 10

Figure 10. Ate enhances MEF2 transcriptional activity in cardiomyoytes. (a) Animal treatment with Ate in vivo. MEF2-LacZ transgenic mice were fed daily with Ate (50 mg/Kg per day) or water for 48 h. After treatment, mice were killed and hearts were fixed with 2% paraformaldehyde in PBS for 30 min. The samples were then incubated with X-Gal solution overnight and visualized for MEF2 activity. The dark blue stain indicates MEF2 activity. (b) Cardiomyocytes were transfected with 4xMEF2-Luc reporter gene and treated with Iso (10 μM), Ate (10 μM) alone or in combination. Luciferase activity was assessed using the respective reporter gene and normalized to β-galactosidase. Data are the mean±S.E. n=3, ****P≤ 0.0001 comparing Iso to control, **P≤0.01 comparing Ate/Iso to Iso, *P ≤0.05 comparing Ate to control. (c) Ate enhances transactivation of the ANF promoter through MEF2. The effect of Iso (10 μM), Ate (10 μM) alone and in combination was assessed on ANF-Luc or an analog with the MEF2 site mutated (ANF-Luc ΔMEF2) in cardiomyocytes. Data are the mean±S.E. n=3, ****P ≤0.0001 Iso versus control, ##P ≤0.01 Ate/Iso versus Iso, *P≤0.05 Ate versus control.

β-AR activation modulates MEF2D cellular localization in neonatal cardiomyocytes

In attempting to determine the mechanism by which MEF2 activity is repressed by β-adrenergic signaling, we determined the subcellular localization of MEF2D in cardiomyocytes that were treated with Iso (10 μM) alone and in combination with β-blockade Ate (10 μM) and ICI118551 (1 μM) using Immunofluorescence analysis. As shown in Figure 11 (top panel), MEF2D is mainly localized in the nucleus in solvent treated cells. However, we observed that in Iso-treated cells, MEF2D is mostly localized in the cytosol Figure 11 (middle panel). We further documented that with β-blocker treatment, MEF2D localization in the nucleus was restored Figure 11 (bottom panel). We observed a similar disruption of cellular localization patterns of MEF2A in cardiomyocytes treated with Iso alone and in combination with β-blockers (Figure S2).

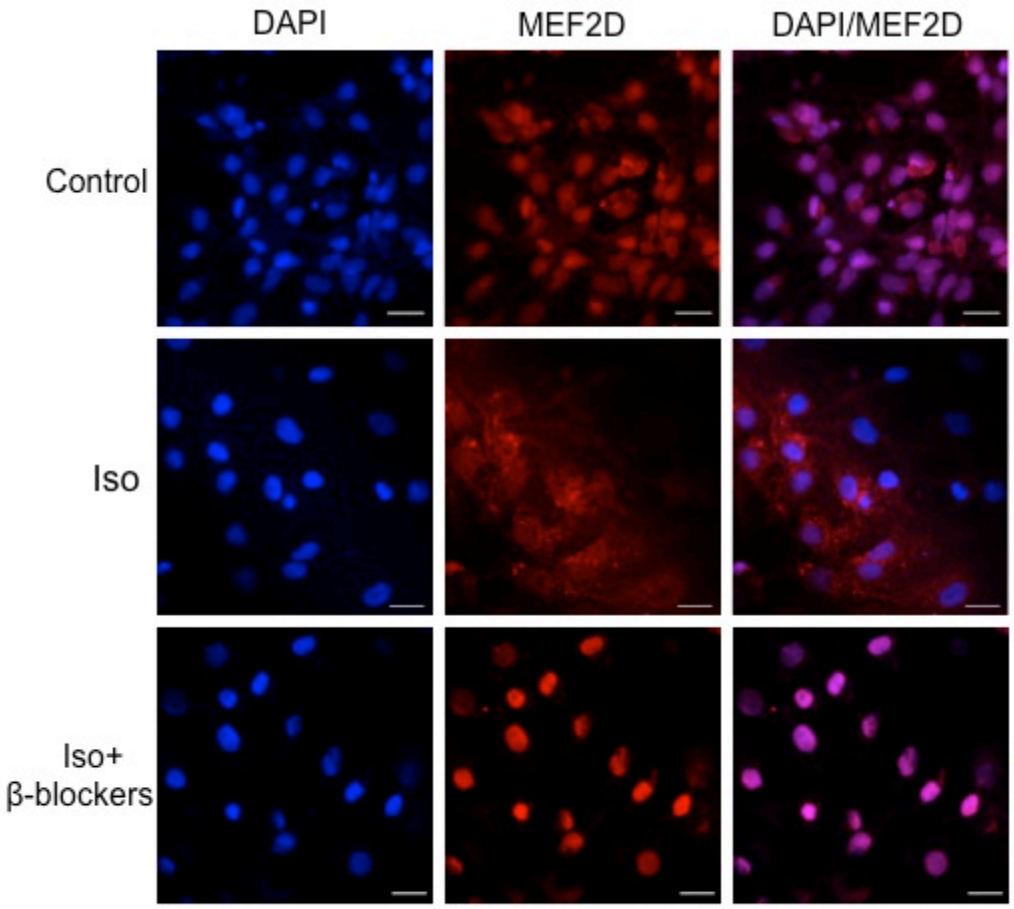

Figure 11

Figure 11. β-AR activation modulates cellular localization of MEF2D in cardiomyocytes. Primary cardiomyocytes were treated with solvent or Iso (10 μM) alone and in combination with β-blockers Ate (10 μM) and ICI118551 (1 μM). After treatment, cells were fixed with 4% paraformaldehyde and immunofluorescence analysis was performed using a primary antibody to MEF2D (red). DAPI (4,6-diamidino-2-phenylindole) was used to identify nuclei (blue). The merged pictures demonstrate localization of MEF2D (red) in respect to Iso (10 μM), β-blockers Ate (10 μM) and ICI118551 (1 μM) treatment, counterstained with DAPI. Scale bars, 20 μm.

KLF6 functions downstream of MEF2 as a pro-survival factor in cardiomyocytes

We previously observed that KLF6 is a key MEF2D target gene in primary hippocampal neurons, [17] and therefore sought to determine whether KLF6 might also function in cardiomyocytes. Endogenous expression of KLF6 was initially confirmed in primary neonatal cardiomyocytes and HL1 cells using western blot analysis (Figure 12a). Immunofluorescence analysis indicated expression of KLF6 in MEF2D positive primary cardiomyocytes. The data also indicate nuclear localization of both MEF2D (green) and KLF6 (red) in cardiomyocytes (Figure 12b). We also observed a similar cellular localization pattern of KLF6 and MEF2D in HL1 cells (Figure S3). Firstly, we assessed MEF2-dependent regulation of the KLF6 promoter in cardiomyocytes. To do this we used a number of KLF6 promoter reporter gene constructs containing different fragments of the KLF6 promoter, pROM6 (contains MEF2 cis-element), pROM3 (which has no MEF2 site), mut.pROM6 (contains MEF2-binding site mutation) and pGL3- basic empty vector which was used as a control (schematic in Figure 12c, lower panel). As shown in Figure 12c (upper panel), endogenous MEF2-induced pROM6 reporter transcriptional activity in contrast to pROM3, which lacks the MEF2-binding site. Furthermore endogenous MEF2 did not induce KLF6 reporter transcriptional activity when the MEF2 site is mutated, indicating that MEF2 is a transcriptional regulator of the KLF6 promoter. To further test if KLF6 is a potential MEF2 target gene in cardiac myocytes, we used siRNA targeting to reduce MEF2D and -A expression and then assessed KLF6 protein expression. Cardiomyocytes were transfected with three independent MEF2D siRNAs and scRNA. MEF2D silencing resulted in a concomitant repression of KLF6 protein expression (Figure 12d, left upper panel) corresponding with

a decrease in KLF6 promoter activation (pROM6; Figure 12d, lower panel). In addition, the reduction of KLF6 protein level was also observed in cells expressing siMEF2A in contrast to cells expressing the scRNA control (Figure 12d, right panel).

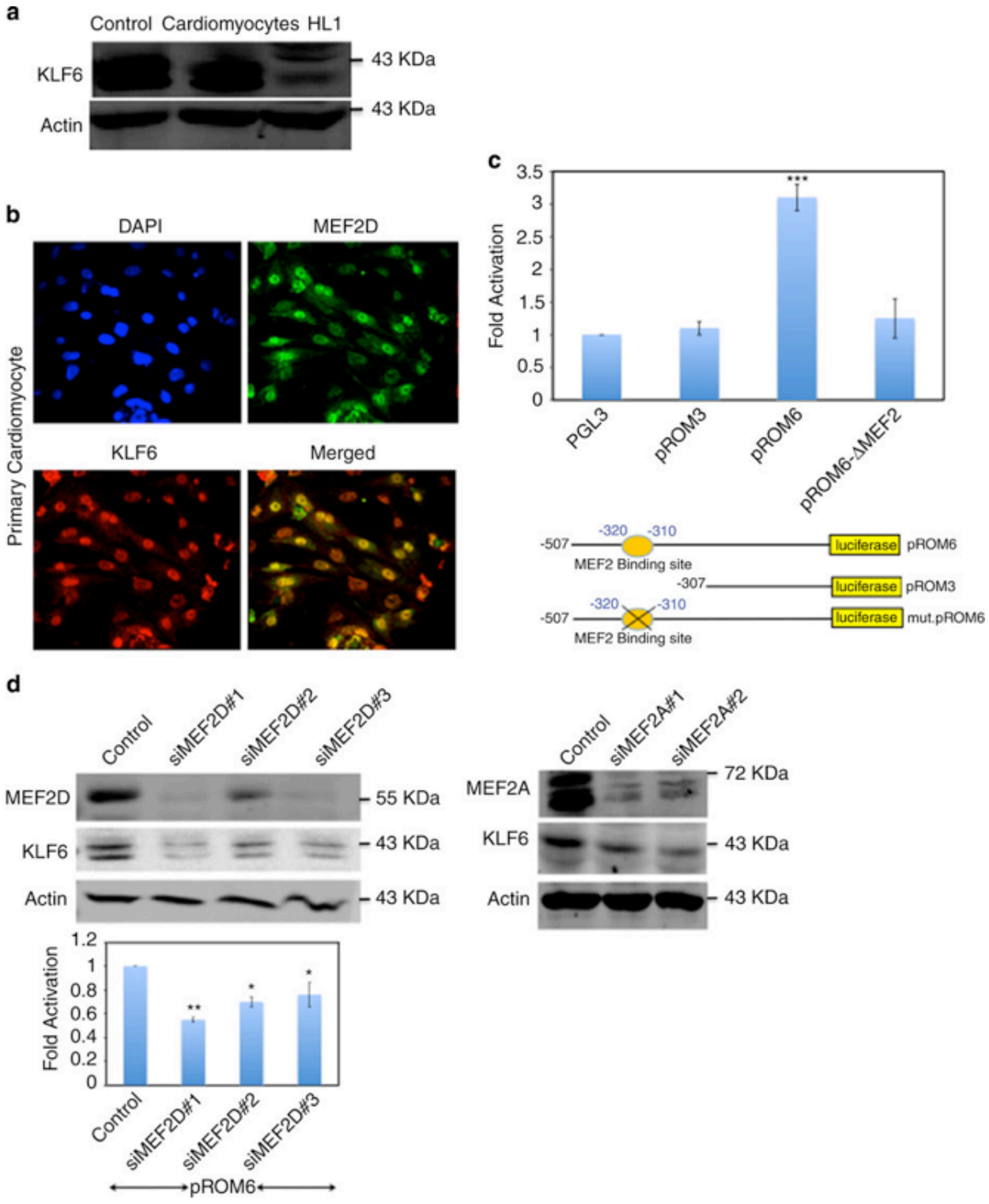
a
Control Cardiomyocytes HL1
KLF6
43 KDa
Actin
43 KDa
b
DAPI
MEF2D
Primary Cardiomyocyte
KLF6
Merged
c
Fold Activation
3.5
3
2.5
2
1.5
1
0.5
0
***
PGL3
pROM3
pROM6
pROM6-ΔMEF2
-507
-320
-310
MEF2 Binding site
luciferase
pROM6
-307
luciferase
pROM3
-320
-310
-507
MEF2 Binding site
luciferase
mut.pROM6
d
Control
siMEF2D#1
siMEF2D#2
siMEF2D#3
MEF2D
55 KDa
KLF6
43 KDa
Actin
43 KDa
Fold Activation
1.2
1
0.8
0.6
0.4
0.2
0
**
*
*
Control
siMEF2D#1
siMEF2D#2
siMEF2D#3
pROM6
Control
siMEF2A#1
siMEF2A#2
MEF2A
72 KDa
KLF6
43 KDa
Actin
43 KDa

Figure 12

Figure 12. MEF2 regulates KLF6 expression in cardiomyocytes (a) KLF6 protein expressed in cardiomyocytes. Cell lysates of primary cardiomyocytes and HL1 cells and C2C12 (as control) were prepared and equal amounts of total protein were used for western blot analysis. The levels of the indicated proteins were assessed by a standard immunoblotting technique using specific primary antibodies for each as indicated. (b) Cellular localization of MEF2D and KLF6 in cardiomyocytes. Primary cardiomyocytes were fixed with 4% paraformaldehyde. Double immunofluorescence labeling demonstrating KLF6 (red) and MEF2D (green) and DAPI (4,6-diamidino-2-phenylindole) was used to identify nuclei (blue). (c) MEF2-dependant induction of the KLF6 promoter in cardiomyocytes. Schematic illustrations of KLF6 reporter gene constructs used in reporter assays are indicated in the lower panel. All KLF6 promoter constructs were cloned into the pGL3-basic reporter vector (pGL3-KLF6-Luc). Primary cardiomyocytes were transfected with various constructs of the KLF6 promoter, pROM6, pROM3 and pROM6 with the MEF2 site mutated. Cell extracts were prepared and MEF2-mediated transcriptional activity was determined by luciferase and β-gal assays. n =3, ***P≤0.001 pROM6 versus pGL3. (d) KLF6 expression is reduced in MEF2 depleted cardiomyocytes. Primary cardiomyocytes were transfected with three independent MEF2D siRNAs (left panel) or two independent MEF2A siRNAs (right panel). Forty-eight hours after transfection equal amounts of total protein were used for western blot analysis. The levels of the indicated proteins were assessed by a standard immunoblotting technique using specific primary antibodies for each as indicated. KLF6 reporter gene expression is reduced in MEF2D depleted cells. Luciferase activity was assessed using KLF6 promoter driving luciferase (pROM6-Luc) and normalized to β-galactosidase. Data are the mean ±S.E. (n=3), **P ≤0.01, *P≤0.05 comparing to control.

KLF6 protects cardiomyocytes in β1-AR–PKA pathway

In an attempt to assess the functional role of KLF6 in cardiomyocytes, we silenced its expression using siRNA technology. Neonatal cardiomyocytes were transfected with three independent KLF6-siRNAs or scRNA and cardiomyocyte apoptosis was measured by flow cytometry analysis as described above (Figure 13a, left panel). Quantitative analysis shows depletion of KLF6 expression resulted in 2- to 3-fold increase in cardiomyocyte apoptosis compared with the control condition (Figure 13a, right upper panel). Reduction of KLF6 protein was observed in cells expressing siKLF6 in contrast to the scRNA (Figure 13b). Interestingly, we also observed that exogenous overexpression of KLF6 can reduce the amount of cell death provoked by Iso treatment (Figure 13c). To examine whether the expression of KLF6 is targeted when MEF2 activity is repressed by β1-AR–PKA signaling, cardiomyocytes were treated with Iso (10 μM) followed by western blot analysis of KLF6. As shown in Figure 13d, KLF6 protein expression level was suppressed by activation of β1-AR–PKA signaling. These data indicate that reduction in KLF6 expression by β1-AR activation occurs through MEF2 inhibition. Collectively, these data summarized in Figure 13, suggest that KLF6 functions downstream of MEF2 in a cardiomyocyte survival pathway.

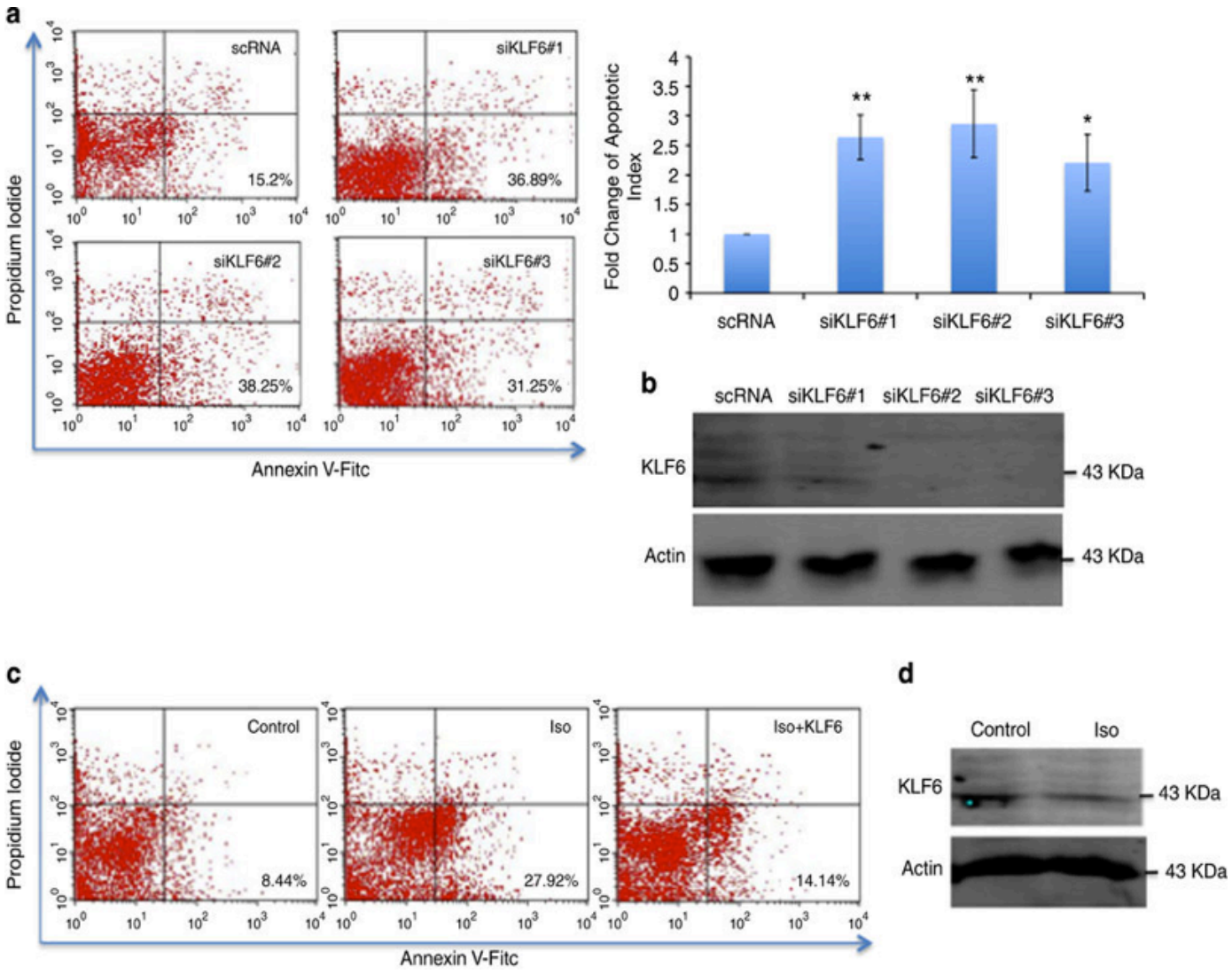
a
scRNA
15.2%
siKLF6#1
36.89%
siKLF6#2
38.25%
siKLF6#3
31.25%
Propidium Iodide
Annexin V-Fitc
Fold Change of Apoptotic Index
scRNA
siKLF6#1
siKLF6#2
siKLF6#3
b
KLF6
Actin
43 KDa
c
Control
8.44%
Iso
27.92%
Iso+KLF6
14.14%
d
Control
Iso

Figure 13

Figure 13. Role of KLF6 in cardiomyocyte survival. (a) siRNA-mediated depletion of KLF6 expression enhances apoptosis in primary cardiomyoytes. Primary cardiomyocytes were transfected with three independent KLF6 siRNAs and a control scRNA. Seventy-two hours after transfection, cells were stained with annexin V-FITC and PI using annexin V-FITC apoptosis detection kit. Cardiomyocytes apoptosis was measured using flow cytometry analysis (FACS analyzer). Changes in the number of apoptotic cells is indicated in a bar graph (left panel). n=3, **P ≤0.01,*P≤0.05 comparing to control. (b) Equal amounts of total protein were used for western blot analysis to validate KLF6 knockdown. The levels of the indicated proteins were assessed by a standard immunoblotting technique using specific primary antibodies for each as indicated. (c) Exogenous KLF6 expression rescues cardiomyocytes apoptosis. Primary cardiomyocytes were transfected with KLF6 expression vector or a control vector and then treated with Iso (10 μM). Cells were then prepared for FACS analysis. (d) Activation of β1-AR suppresses KLF6 protein expression. Primary cardiomyocytes were treated with Iso (10 μM) or solvent. Cells were prepared for western blot analysis as in b.

Discussion

Here, we present several lines of evidence documenting that MEF2 activity has an anti-apoptotic, pro-survival role in cardiac myocytes. Moreover, this pro-survival activity is antagonized by β-adrenergic signaling and, importantly, enhanced by β-adrenergic blockade (Figure 14). In view of the profound effects of myocyte loss in heart pathology, it is perhaps appropriate to consider possible contexts occurring in the cardiovascular system in which these observations have potentially important implications. One prominent context exists immediately after myocardial infarction, when the survival of cardiomyocytes in the myocardium is known to be severely compromised and also MEF2 activity is repressed by hyperactivation of β-adrenergic signaling and subsequent PKA-mediated phosphorylation. Our data indicate that β-blockade immediately post myocardial infarction could minimize cell death by promoting the cell survival mechanisms invoked by MEF2 and its downstream effectors. There are other conditions of acute hyper-adrenergic activation in humans, apart from myocardial infarctions, that have been linked with heart pathology [155]. In patients with stress cardiomyopathy a link between myocyte death and pronounced acute β-adrenergic activation has been postulated [155]. Certainly it is clear that one seminal feature of progressive heart failure is an elevation in catecholamine levels that results in myocyte death and concomitant hypertrophy in surviving cells, ultimately contributing to a worsening of left ventricular function [156–158].

Indeed, the general cardio-toxicity of high levels of catecholamine in the heart and more specifically the exact role of catecholamine mediated myocyte death is, to date, not well understood, although it has been reported that chronic hyper-activation of β-

adrenoreceptors leads to a PKA-mediated phosphorylation of the Ryanodine receptor that results in calcium leakage from the sarcoplasmic reticulum, possibly invoking cell death mechanisms [159]. Despite the link between cardiac pathology and elevated catecholamine levels documented in multiple, [155–159] our knowledge of the mechanisms leading to cell death in these contexts is still incomplete. On the basis of our observations, we propose that acute β-adrenergic stimulation mediates inactivation of the pro-survival function of MEF2 in cardiac myocytes, thereby contributing to myocyte cell death and left ventricular dysfunction in a variety of pathologies ranging from myocardial infarction to stress induced cardiomyopathy. Moreover, acute β-adrenergic blockade restores MEF2 activity thus facilitating cardiac myocyte survival.

We report here that the expression of a substantial number of apoptotic network related genes is affected by experimental manipulation of MEF2 activity (Figure 8). For example, in our experiments several key apoptotic and tumor-suppressor genes are upregulated in response to MEF2A suppression by siRNA technology, suggesting that MEF2 ordinarily represses these pro-apoptotic genes, including Bcl2l14,[146] Bnip3 (Bcl2- and 19KD-interacting protein-3), [147,148] Rassf6 [149] and Ddit4 (DNA damage-inducible transcript 4). Bnip3-mediated cardiomyocyte apoptosis contributes to post-infarction left ventricular remodeling [147,148]. Ddit4 is upregulated in response to ischemia/hypoxia-induced damage [150]. In addition, many genes that are broadly described as 'cardio-protective' were downregulated by MEF2A suppression including, notably, Notch 1; Thbs1 (thrombospondin 1) and NOS3 (nitric oxide synthase 3). It was previously shown that Notch 1 signaling reduces cardiomyocyte apoptosis in ischemic post- conditioning [160,161]. Thbs1 contributes to healing myocardial infarcts and also

protects against cardiac remodeling by regulating TGFβ signaling and promoting matrix preservation [162,163]. Exogenous NOS3 expression in myocardium protects the heart from arrhythmia [164].

Collectively, in general terms, it seems that loss of MEF2 function results in hyper-activation of genes involved in apoptotic induction and cell death while concomitantly leading to a reduction in the levels of genes involved in myocyte survival. The compound effects of these global gene expression changes for cardiac myocyte survival are clearly emphatic and of important clinical concern. Of note here is that in three independent large scale studies, the efficacy of β-adrenergic blockade in heart failure patients was reproducible and resulted in an approximate reduction by a third in the risk of death [165]. A statistic that is unparalleled by any other drug used to treat heart failure [165]. On the basis of our studies, our tenet is that there are no doubt multiple mechanisms contributing to this favorable outcome, one of which might be enhanced cardiac myocyte survival mediated by MEF2- dependent gene expression. Our observations, in combination with those of other groups, suggest the possibility of a general role for MEF2 in cell survival. In particular, MEF2 has been implicated in neuronal survival [17] and, in the current study, protection from cardiomyocyte cell death. Whether MEF2 has a general pro-survival role in other tissues is currently unknown. So far, MEF2 has been implicated in the control of gene expression and differentiation in neurons, cardiac, skeletal and smooth muscle, T and B cells, adipocytes and osteoblasts [13,18,96,166–169]. It will therefore be of interest to determine in these other MEF2-dependent cell types whether cell survival is anancillary function of its activity apart from its better-characterized role in cellular differentiation. Gene targeting studies

indicate that MEF2A has a role in cardiac metabolism, including regulation of fatty acid oxidation in the heart and maintenance of mitochondrial function [30]. Activation of caspase 9 and the role of mitochondria in catecholamine-induced apoptosis in cardiomyocytes has also been documented [115]. In view of these reports, it is likely that MEF2 protects against the mitochondrial-induced cell death pathway.

In view of the seemingly central role had by MEF2 in the control of gene expression in the heart, signal pathway regulated control of MEF2 activity could offer a broad target for therapeutic intervention. Research to date has indicated that MEF2 is a conduit for several signaling pathways that are regulated by a variety of cellular signaling pathways. To date MEF2 activity has been shown to be directly modulated by p38 MAP kinase [152,170], ERK5/BMK1 [36], PKA [134] and CDK4 [171] kinases, which are themselves, controlled by a myriad of signaling pathways. Therefore, there are many nodes that constitute potential rheostats in regulating MEF2 activity in the heart by means other than β-adrenergic blockade. One distinct and immediately applicable possibility is through the use of HDAC inhibitors. Several studies have indicated that class II HDACs are the most potent physiological repressors of MEF2 activity [172,173]. Since there are numerous well-characterized inhibitors of HDACs, some of which are in clinical trials, their utility to de-repress MEF2 activity in some cases may be worth consideration. Thus, signaling pathway diversity may provide considerable flexibility in targeting MEF2 under conditions in which it's activity is necessary or advantageous, such as during acute impending cardiomyocyte cell death, as well as under conditions when its activity needs to be restricted, such as under chronic conditions leading to cardiomyocyte

hypertrophy in which MEF2 contributes to cell enlargement by activation of fetal structural genes.

Summary

Our knowledge of the mechanisms controlling cardiac myocyte cell death is still quite incomplete. On the basis of our observations, we propose that the transcriptional regulator MEF2 fulfils a critical pro-survival function in cardiac myocytes having important implications for our understanding and therapeutic targeting of myocyte cell death and left ventricular pathology.

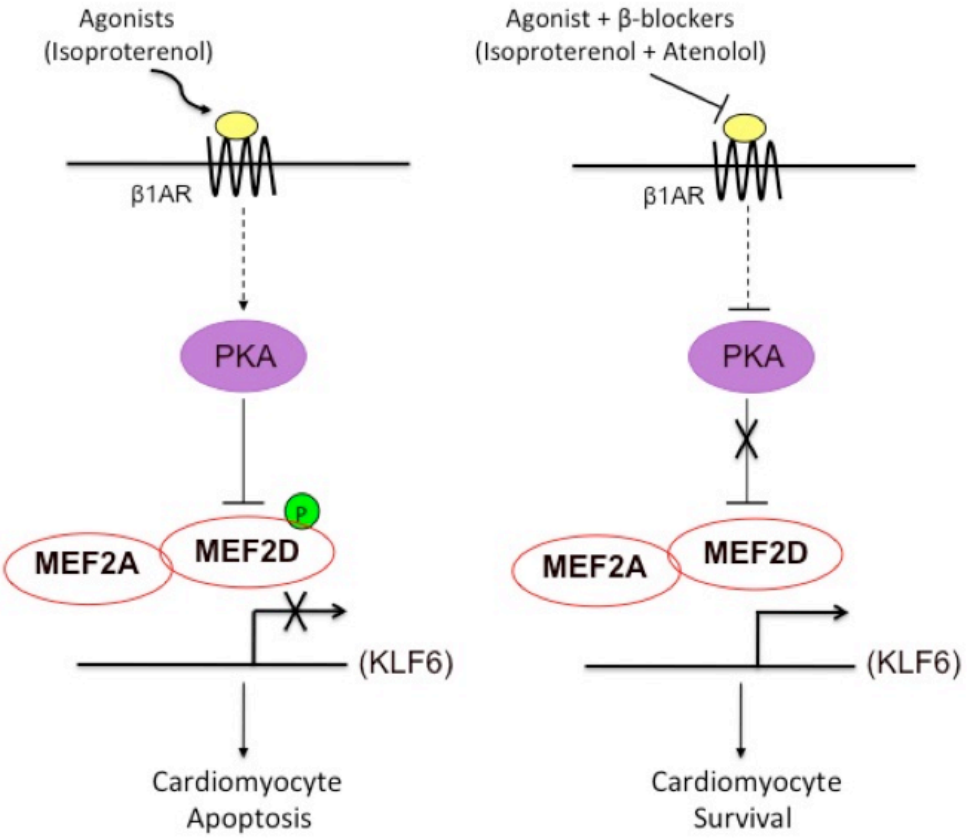
Agonists
(Isoproterenol)
β1AR
PKA
P
MEF2A
MEF2D
(KLF6)
Cardiomyocyte
Apoptosis
Agonist + β-blockers
(Isoproterenol + Atenolol)
β1AR
PKA
MEF2A
MEF2D
(KLF6)
Cardiomyocyte
Survival

Figure 14

Figure 14. Summary of MEF2 regulation by β-adrenergic signaling in cardiomyocyte survival. On the left side, acute activation of β-adrenergic receptors invokes cAMP-mediated PKA activation in cardiomyocytes, resulting in suppression of MEF2 transcriptional activity by direct phosphorylation. Expression of pro-survival genes such as KLF6 is prevented resulting in enhanced cardiomyocyte death. On the right side, β-blockers, such as Atenolol, competitively inhibit the activation of the β-adrenergic receptors by agonists resulting in enhanced MEF2 activity, thereby promoting cardiomyocyte survival.

Material and Methods

Cell culture

Primary neonatal rat cardiomyocytes were prepared from 1- to 3-day old Sprague Dawley rats using the Neonatal Cardiomyocyte Isolation System (Worthington Biochemical Corp, Lakewood, NJ, USA). Briefly, whole hearts were dissociated with trypsin (Promega, Madison, WI, USA) and collagenase (Worthington Biochemical Corp). The cells were re-suspended in Dulbecco's modified Eagle's medium F12 (Gibco, Burlington, ON, Canada) supplemented with 10% fetal bovine serum, 1% penicillin/ streptomycin and 50 mg/l gentamycin sulfate (Invitrogen, Burlington, ON, Canada). The isolated cells were plated for 60 min in 37 °C humidified incubator with a 5% CO2 in air, allowing differential attachment of non-myocardial cells. The cardiomyocytes were counted and transferred to gelatin-coated plates. The day after, medium was removed and replaced by fresh medium. For pharmacological treatments, cells were serum starved for the indicated time and replenished with fresh medium every 24 h.

Atenolol administration in vivo

MEF2-LacZ transgenic sensor mice, reported previously,[134,151–153] were used in this study. Two groups of male mice (n = 5/each group) at 6–7 weeks were used. β-Blockers were administered through drinking water (Atenolol; 50 mg/kg per day) or solvent (5 ml water) for 2 days. Mice were sacrificed by cervical dislocation. The apex of each heart was fixed with 2% paraformaldehyde in PBS for 30 min. After being washed three times with PBS, the samples were incubated at 37 °C with X-Gal staining solution (5mM ferrocyanide, 5mM ferricyanide, 2mM MgCl2, and 1 mg/ml X-Gal) to visualize β-Gal positive cells. Samples were examined using bright field microscopy.

Reagents and antibodies

Rabbit polyclonal MEF2A antibody was produced with the assistance of the York University (Toronto, ON, Canada) Animal Care Facility. MEF2D (BD Biosciences, Mississauga, ON, Canada, 610775), KLF6 (Santa Cruz, Dallas, TX, USA, R-173 and E-10), Actin (Santa Cruz, sc-1616), IRDye 680RD goat anti rabbit (LI-COR, Bioscience, Lincoln, NE, USA) and IRDye 680RD goat anti-mouse (LI-COR, Bioscience) were used for Immuno-blotting experiments. FITC- and TRITC-conjugated α-rabbit and α-mouse secondary antibodies and 4,6-diamidino-2-phenylindole (DAPI; D9542), H2O2 (H0904) and H89- dihydrochloride hydrate (B1427) were purchased from Sigma Aldrich (Toronto, ON, Canada). Atenolol (Sigma Aldrich, A7655), Isoproterenol hydrochloride (Sigma Aldrich, 1351005) and ICI 118551 hydrochloride (Abcam, Toronto, ON, Canada, ab1200808) were purchased for use in cell culture.

Plasmids

The firefly luciferase reporter gene plasmid pGL3–4xMEF2-Luc was made from pGL3-MEF2-Luc with three additional copies of the MEF2 site inserted.10 ANF and ANF ΔMEF2 reporter constructs (consist of the firefly luciferace cDNA driven by 700 bp of rat ANF promoter sequence), provided by Dr. M. Nemer (Faculty of Medicine, University of Ottawa). The expression plasmid of pCMV-β-galactosidase has been described previously [134]. The expression plasmid for pCIneo-KLF6 was a provided by Dr. S. Friedman (Mount Sinai School of Medicine, New York, NY, USA). KLF6 reporter constructs pROM6 and pROM3-Luc were provided by Dr. N.P. Koritschoner (Faculty of Bioquimica y Ciencias Biologicas, Universidad Nacional del Litoral, Santa Fe,

Argentina). pROM6 reporter construct containing the mutated MEF2-binding site (pROM6 ΔMEF2) has been described previously [17].

siRNA-mediated gene silencing

Gene silencing of target genes was done using siRNA technology; siRNAs were purchased from Sigma Aldrich. siMEF2A#1 (SASI_Mm01_00120787), siMEF2A#2 (SASI_Mm01_00120788) and siMEF2D#1 (SASI_Rn01_00057714), siMEF2D#2 (SASI_Rn01_00057709), and siMEF2D#3 (SASI_Rn01_00057717) were used at 100 nM concentrations. We also used siKLF6#1 (SASI_Rn01_ 00082277), KLF6#2 (SASI_Rn01_00082278) and KLF6#2 (SASI_Rn01_ 00082280) at 100 nM concentrations.

Transfections

Primary cardiomycoytes were transfected using Lipofectamine 2000 (Invitrogen) in a 1:2.5 mixture ratio of DNA to lipofectamine in Opti-MEM (Invitrogen) according to the manufacturer's instructions. Cells were re-feed and allow for recovery for 24 h before harvesting, or pharmacological treatments. For siRNA experiments, Lipofectamine RNAiMAX (Invitrogen) was used according to the manufacturer's instructions. Cells were harvested 48–72 h after transfection for western immunoblotting analysis to determine the efficacy of protein knockdown or flow cytometry analysis.

Protein extraction

Protein samples were kept on ice during the entire procedure. Cells were washed twice with cold 1x Phosphate buffered saline (PBS). After aspirating the last PBS wash, 1.0 ml of cold 1x PBS was added to cells. Cells were then gently scraped with a rubber policeman and transferred to a new tube and then centrifuged for 5 min at 4 °C. After

removing the PBS, the pellet was diluted with five times its volume in NP-40 lysis buffer (supplemented with 1mM sodium orthovanadate, 1mM PMSF and protease inhibitor cocktail (Sigma, P-8340). Cells were vortexed briefly every 10 min for a total of 40–45 min, and centrifuged at high speed and supernatant was transferred to a fresh tube. Protein concentrations were determined by Bradford assay (Bio-Rad) with bovine serum albumin as a standard.

Immunoblots

Cells were harvested using an NP-40 lysis buffer (0.5% NP-40, 50mM Tris, 150mM NaCl, 10mM sodium pyrophosphate, 2mM ethylene diamine tetra acetic acid and 100mM NaF), containing protease inhibitor cocktail (Sigma Aldrich), 1mM phenyl methyl sulfonyl fluoride (Sigma Aldrich) and 1mM sodium orthovanadate (Bioshop, Burlington, ON, Canada). Total protein extracts (20–25 μg) were diluted in sample buffer (SDS polyacrylamide) containing β- mercaptoethanol, boiled for 5 min and electrophoretically resolved by 10% SDS-polyacrylamide gels, then transferred onto Immobilon-FL polyvinylidene difluoride membrane (Millipore, Fisher Scientific (distributor) Ottawa, ON, Canada). Non-specific binding sites were blocked with Odyssey Blocking Buffer (LI-COR). Membranes were incubated with primary antibodies overnight at 4 °C in Odyssey Blocking Buffer. Primary antibodies included MEF2A (1:250), MEF2D (1:500), KLF6 (1:500) and actin (1:1000). The blots were then incubated with the appropriate secondary antibodies IRDye 680RD goat anti-rabbit (1:5000) and IRDye 680RD goat anti-mouse (1:5000) for 2 h at room temperature and were imaged using LI-COR Odyssey System.

Luciferase reporter gene analysis

Transcriptional assays were done using luciferase reporter plasmids. The cells were harvested for these assays using lysis buffer (20mM Tris, (pH 7.4) and 0.1% Triton X-100). Lysate was briefly vortexed and centrifuged at maximum speed for 15 min at 4 °C. Enzymatic activity was measured in each sample on a luminometer using luciferase assay substrate (E2820, Promega) and values obtained were normalized to β-galactosidase activity and expressed as fold activation by arbitrarily setting the control condition to 1. All measurements were made in triplicate for at least three independent experiments.

Statistical analysis

Data shown are mean ± S.D. All data were verified in three independent experiments using the same batch of cardiomyocyte isolation. Independent two sample t-tests of all quantitative data were conducted, whereas a one-way analysis of variance followed by a Tukey HSD post hoc test was performed on experiments with greater than two conditions. P-values are indicated with respect to controls where appropriate and $P < 0.05$ was considered statistically significant.

Flow cytometry

Flow Cytometry analysis was performed as previously described [17] using the annexin V-FITC apoptosis detection kit (APOAF, Sigma) following the manufacturer's instructions. Primary cardiomyocytes were washed, briefly trypsinized, and then washed twice with cold PBS. Cells were pelleted by centrifugation and re-suspended in binding buffer followed by incubation with staining solution (annexin V-FITC and PI) for 15 min in the dark at 4 °C. The cells were re-suspended in binding buffer. Samples were analyzed

immediately by flow cytometry fluorescence, respectively. Ten thousand cells from each sample were scanned and analyzed by FACS Calibur flow β-Blockers enhance MEF2 mediated cardiomyocyte survival cytometry (BD, Mississauga, ON, Canada) using the standard configuration and parameters. Data acquisition and analysis was performed using the Cell-Quest software (BD). Necrosis and apoptosis were determined by PI (FL2) and annexin V-FITC (FL1) fluorescence, respectively.

Immunofluorescence

Primary cardiomyocytes were fixed in 4% paraformaldehyde and permeabilized with 0.3% Triton X-100 in PBS for 5 min. Cells were blocked with 10% goat serum in PBS for 30 min at 37 °C and incubated overnight at 4 °C with primary antibodies MEF2D (1:100), MEF2A (1:100) and KLF6 (1:100) diluted in 1.5% goat serum. Cells were washed three times with PBS for 10 min and incubated with the appropriate TRITC- and FITC-conjugated secondary antibodies (1:500) in 1.5% goat serum for 2 hrs at room temperatur. DAPI staining (Sigma Aldrich) was carried out during the last 15 min. Cells were washed three times with PBS and images were captured using a Zeiss LSM confocal microscope (Carl Zeiss, ON, Canada).

CHAPTER 4

HEART FAILURE AND MEF2 TRANSCRIPTOME DYNAMICS IN RESPONSE TO β-BLOCKERS [χ]

Summary

Aims: Morbidity and mortality associated with cardiovascular disease (CVD) is a worldwide public health problem. β-blockers are a front-line treatment for heart failure (HF) yet the molecular characterization of their effects are incomplete. Transcription factor Myocyte Enhancer Factor 2 (MEF2) is an important mediator of cardiac remodelling and HF and is also a target of β- adrenergic signaling. The purpose of this study was to determine the global gene transcription networks that arise during HF with and without β-blocker treatment.

Methods: Experimental HF by transverse aortic constriction (TAC) in a MEF2 "sensor" mouse model (6 weeks), was followed by four weeks of β-blockade (Atenolol-AT) or solvent (Sol) treatment. Transcriptome analysis by RNA-seq from corresponding left ventricular RNA samples and MEF2A depleted cardiomyocytes was performed.

[χ] *Tobin, S.W.[1,3,4], *Hashemi, S.[1,3,4], Dadson, K.[1], Turdi, S. [1], Ebrahimian, K. [1,3,4], Zhao, J.[1,3,4], Sweeney, G.[1], Grigull, J.[1,5], and # J.C. McDermott [1,2,3,4]

*contributed equally to the work, # corresponding author

[1] Department of Biology, [2] Centre for Research in Mass Spectrometry (CRMS), [3] Muscle Health Research Centre (MHRC), [4] Centre for Research in Biomolecular Interactions (CRBI), [5] Department of Mathematics and Statistics, York University

Results: AT treatment resulted in an overall improvement in cardiac function of TAC mice and a decrease in cardiomyocyte size and fibrosis which was associated with repression of MEF2 activity. RNA-seq identified 65 differentially expressed genes (DEGs) due to TAC treatment with enriched GO clusters including cell proliferation, the immune system, cell migration and apoptosis. These genes were mapped against differentially expressed genes in cardiomyocytes in which MEF2A expression was suppressed. Non-coding RNA including lncRNAs were also assessed. Of the 65 TAC mediated DEGs, AT reversed the expression of a subset of 28 mRNAs and also 2 lncRNAs. *Rarres2* was identified as a novel MEF2 target gene that is upregulated with TAC *in vivo* and isoproterenol *in vitro* which has implications in cardiomyocyte apoptosis and hypertrophy.

Conclusions: Chronic β1-blockade inhibits myocardial MEF2 activity while also contributing to dynamic changes in heart failure associated transcriptome dynamics. These studies identify a cohort of genes with vast potential for disease diagnosis and therapeutic intervention in heart failure.

Introduction

Morbidity and mortality associated with cardiovascular disease (CVD) is a predominant global health problem occupying a prevalent position as the leading cause of death worldwide. Due to its universality, the multi-faceted progression of heart disease is therefore one of profound clinical importance. Progressive heart failure (HF), as one aspect of CVD, has a staggering prevalence of approximately thirty eight million diagnosed patients globally, a number which is growing due to the ageing population and the pervasiveness of HF in that age cohort [127,174]. Moreover, a HF diagnosis in many cases is an ailment with a poorer prognosis than most cancers [127,174]. Understanding and averting the progression of HF is therefore fundamental in the battle against CVD.

A significant body of cellular and molecular research has elucidated the many structural and signaling changes associated with HF, while current advances in transcriptional analysis have begun to unravel the underlying dysregulation of the cardiac transcriptome in the pathogenesis of CVD and heart failure. At the molecular level, transcription is orchestrated by a complex set of interwoven cellular signaling pathways that converge in the nucleus to activate various transcription factors that are involved in driving the expression of the ultimately pathological gene expression program [4,48,175]. Transcriptional circuits in post-natal vertebrate heart play a role in maladaptive cardiac hypertrophy and remodeling which are cardinal features of HF progression [4,48,175]. Congenital disorders of structural and contractile proteins of the myocardium also lead to hypertrophy and eventual heart failure [48]. Pathological remodeling of the heart is accompanied by increased apoptosis, fibrosis, alterations in cardiac gene expression,

assembly of new sarcomeres and activation of a 'fetal' set of cardiac genes [48]. Accordingly, we hypothesized that pathological events underlying HF are accomplished by transcriptional dysregulation of a battery of genes involved in multiple biological processes.

The regulation of the transcriptome in the heart is a primary determinant of its gene expression signature, phenotype and function [176–180]. Extensive work concerning the control of cardiac specific gene expression [4,135–137,181,182] and also loss of function analysis in gene targeted mice [15,30,183] has positioned Myocyte Enhancer Factor 2 transcriptional regulatory proteins (MEF2) at a nexus of control for cardiac and skeletal muscle gene expression. The MEF2 family of transcription factors (encoded by four genes labeled as MEF2A to D) have proved crucial in regulating cardiac [12], skeletal [13,135] and smooth muscle differentiation [96], neuronal survival and plasticity [16,17] and T cell activation [18]. The requirement for MEF2 is evolutionarily conserved for cardiac and skeletal muscle development from flies to humans [135]. The N-terminus of MEF2 proteins (A-D) is conserved among all family members and consists of a 58-amino acid MADS domain and an immediately adjacent 28-amino acid MEF2 domain. These two domains collectively mediate dimerization, co-factor interactions and DNA binding to the consensus DNA sequence (C/T)TA(A/T)$_4$TA(G/A) found in the regulatory region of most cardiac-specific genes [139]. Interestingly, transgenic mice that express a constitutively active CaMKIV gene exhibit cardiac hypertrophy and, when cross-bred with a MEF2 "sensor" mouse model, show markedly enhanced MEF2 activity [10]. There is further molecular and correlative data that MEF2 activity is enhanced during cardiac hypertrophy, but to date how this modulates the progression of disease *in vivo* is

unclear. MEF2 is highly responsive to several signal transduction cascades, and post-translational regulation by covalent modification by PKC [184], p38 MAPK [152,170,184], ERK5 [36,185] and PKA have been documented by ourselves [134] and others [186,187]. In view of the central role of MEF2 in the control of cardiac transcription we view MEF2 activity as a barometer of extensive transcriptional changes in the heart. Moreover, because of the role of β-adrenergic signalling in heart disease and its associated control of cardiac MEF2 activity, we postulated that this may be of potential relevance in the pathology of the heart.

Clinically, β-adrenergic receptor (βAR) antagonists, or β-blockers, reduce heart rate (chronotropy) and the force (inotropy) of myocardial contraction. Chronic heart failure in humans has been associated with impaired cardiac function, structural alteration, neurohormonal activation and use of β-blockers in humans with heart failure results in decreased mortality [114,130]. Despite the well characterized effects of β-adrenergic blockers in modulating cardiac inotropic and chronotropic parameters and improving overall cardiac function, there is a surprising lack of information concerning how acute and, particularly, chronic β-blocker treatment affects cardiac gene expression.

To date, the impact of pharmacologic treatment by β-blockers, a first line HF treatment, on global transcription changes during HF has not been reported. Therefore, we have begun to assess the relationship between global gene transcription and heart failure, particularly in response to β1-adrenergic blockade. Here, we report dynamic changes in cardiac gene transcription and MEF2 activity in response to HF, and document a subset of these genes that respond to pharmacologic manipulation by β1-adrenergic blockade.

Methods

Induction of pressure overload by transaortic constriction (TAC) in mice. Six to eight week old MEF2-LacZ transgenic male sensor mice, reported previously [151], were used in this study. Under general anesthesia (i.p. xylazine: 0.03 mg/g; ketamine: 0.15 mg/g), hair from the chest was removed and the surgical area disinfected with betadine. A skin incision was made along the midline from the neck to the rib cage and the chest cavity was opened. The rib cage and thymus were retracted to expose the transverse aorta. A 27g needle was used to calibrate a microclip applicator. A titanium microligation clip was applied between the origins of the innominate and left common carotid arteries, constricting the transverse aorta to the gauge of the needle. The rib cage, muscles, and skin were closed with a 6-0 USP non-absorbable silk suture. The animals were then administered s.c. 0.03 μg/mg Buprenorphine and allowed to recover on a heating pad until fully awake. Sham surgeries were performed as above except the microligation was not applied to the transverse aorta. All mice were monitored after the procedure for normal behaviour in accordance with Canadian Council on Animal Care regulations.

Atenolol administration in vivo and β galactosidase staining. β-blockers were administered through drinking water (Atenolol; 50mg/kg/day) or solvent (5 ml water) for 10 weeks. Mice were sacrificed by cervical dislocation and the apex of each heart was fixed with 2% paraformaldehyde in PBS for 30 minutes. The samples were washed three times with PBS, and incubated at 37 °C with X-Gal (5-bromo-4-chloro-3-indolyl-β-d-galactopyranoside) staining solution (5 mM ferrocyanide, 5 mM ferricyanide, 2 mM MgCl2, and 1 mg/ml X-Gal) to visualize β-Gal positive cells. Then all the samples were examined using bright field microscopy.

Analysis of cardiac function using high-frequency ultrasound imaging technology. All mice were subjected to transthoracic echocardiographic analysis to measure heart function 6 and 10 weeks following aortic banding or sham surgery. Cardiac function and heart morphology were evaluated using echocardiography (Vevo 2100, VisualSonics). The animals were sedated using 3% isoflurane and maintained with 1~2% isoflurane. The parasternal long axis view (B-mode, M-mode) was obtained and measurements of cardiac structure and function were determined as described previously [188]. The individuals performing echocardiographic analysis of heart function were blinded to surgical group and genotype.

Cardiac tissue collection, H&E, Masson's Trichrome, and wheat germ agglutinin staining (WGA) staining. Following echocardiography, mice were weighed and euthanized using cervical dislocation. Hearts were excised and quickly perfused with 30mM KCl to induce diastolic arrest. Hearts were then weighed and divided for further analysis. Mid-ventricular cross-sections of freshly dissected heart tissue were fixed in 10% formalin solution for 1 hour then stored in 70% ethanol at 4^{o}C until further processing. Fixed heart tissues were dehydrated to xylene and embedded in pure paraffin wax blocks. Paraffin-embedded sections were deparaffinized and rehydrated first with descending concentrations of ethanol and then brought into double distilled water. The sections were then subjected to H&E or Masson's Trichrome staining per manufacturer's instructions, or incubated with wheat germ agglutinin (WGA; Alexa Fluor 488 conjugated) for 2 hours in the dark, briefly washed with PBS and then mounted on microscopy slides with ProLong Gold. Fluorescent images were captured with an Olympus confocal microscope and analyzed with NIH ImageJ software (v.147).

Cardiomyocyte cross-sectional area data from at least 100 cells were determined per group from representative triplicate experiments.

Primary cardiomyocyte isolation. Primary neonatal rat cardiomyocytes were prepared from 1- to 3-day old rats (Sprague Dawley) using the Neonatal Cardiomyocyte Isolation System (Worthington Biochemical Corp). Neonatal rat pups were sacrificed by decapitation. In brief, whole hearts were dissociated and digested with trypsin (Promega) and collagenase (Worthington Biochemical Corp). Cardiomyocytes were re-suspended in culture medium with (DMEM/F12 (Gibco) with 10% fetal bovine serum (FBS), 1% Penicillin/Streptomycin and 50 mg/L gentamycin sulphate). The isolated cells were plated on 10 cm dishes for 60 minutes in 37^{o}C humidified incubator with a 5% CO2 in air to remove non-myocardial cells. The cardiomyocytes were then seeded into gelatin-coated 6-well plates. The day after, medium was removed and replaced by fresh medium.

Cardiomyocyte transfection. Neonatal cardiomyocytes were transiently transfected with siRNA using Lipofectamine RNAiMAX (Invitrogen). For each well, according to the manufacture's instruction, Lipofectamine RNAiMAX reagent was diluted into 150 µl in Opti-MEM medium, and in a separate tube, siRNA (100nM) was also diluted in 150 µl Opti-MEM medium, mixed and incubated for 5 minutes at room temperature. The 250 µl of siRNA/Lipofectamine mixture was added to cells and incubated at 37°C overnight. Following the incubation, media was replaced and harvested 48 hours later for experimental procedures. The siRNAs purchased from Sigma Aldrich were, siMEF2A#1 (SASI_Mm01_00120787) or scrambled control (SIC001). The siRNA purchased from Thermo Fisher Scientific were, siRarres2 (ID: 252512, ID: 252511), siJunb (ID: 59715,

ID: 51454), siAlas2 (ID: 468000, ID: 46614), siKLF2 (ID: 218080, ID: 218079) and siligp1 (ID: 76220, ID: 76128). Isoproterenol hydrochloride (Sigma Aldrich, 1351005) (10μM) was used to induce apoptosis in primary cardiomyocytes. Caspase 3 (Cell signaling, 9662) and cleaved caspase 3 antibodies (Cell signaling, 9661) were used for western blot analysis and to measure apoptosis a ratio of cleaved caspase3 to total caspase3 was used.

HL1 Cell Culture and Transfection. The HL-1 cardiac cell line was cultured in Claycomb Medium (SigmaAldrich) supplemented with 100μM norepinephrine (Sigma Aldrich), 10% FBS and 4 mM L-glutamine (Invitrogen). Cells were maintained in a humidified 37 °C incubator with 5% CO2. The HL-1 cell line was originally established from an AT-1 subcutaneous tumor excised from an adult female Jackson Laboratory inbred C57BLy6J mouse. Transient transfections were performed using lipofectamine 2000. A 1:2.5 mixture ratio of DNA to lipofectamine in 250 μl Opti-Medium (Gibco) was prepared and incubated overnight. The day after medium was removed and replace by fresh medium. The HL-1 transfected cells incubated with wheat germ agglutinin (WGA; Alexa Fluor 637 conjugated) for 2 hours in the dark, briefly washed with PBS and then mounted on microscopy slides. Fluorescent images were captured with an Olympus confocal microscope and analyzed with NIH ImageJ software.

RNA preparation for sequencing. Total RNA was isolated from the mouse left ventricle or primary rat cardiomyocytes using the Qiagen Universal RNA kit. Five μg of RNA was sent to the McGill University and Genome Quebec Innovation Centre (MUGQIC) for cDNA library preparation (Illumina Truseq mRNA kit). Paired reads were generated using Illumina HiSeq 2000 sequencer (100 bp paired-end reads). RNA-seq

data has been deposited in the NCBI's Gene Expression Omnibus (GEO) accession number: GSE75213

Differential expression analysis of transcripts from TAC+AT experiments. For mRNA mouse reads were aligned to mm10 as previously reported [143]. Differentially expressed mRNA transcripts were filtered and identified with edgeR, using the following options: i) Transcripts are represented by 5 or more reads per million in at least 6 among the 12 experiments. Transcripts are identified as differentially expressed in 5 comparisons ii) Transcripts which are up-or downregulated by 50%, for a False-Discovery-Rate (FDR) of 20% or less (in the output of edgeR's glmLRT function) are selected. Clustering heatmaps were generated with Matlab's Bioinformatics toolbox. Primary miRNA transcripts were identified using edgeR (adjusted p-value<0.2). To find lncRNA, short paired-end reads were mapped with RSEM/ Bowtie to the reference index (mm9) which was built for the 2073 mouse lncRNAs [189]. All uniquely mappable short reads are included by using the bowtie-m 1 option in the rsem-calculate-expression command. For identifying differentially expressed lncRNAs we used options that differed slightly from the analysis of protein-encoding transcripts: i) Transcripts are represented by 5 or more reads per million in at least 5 among the 12 experiments. ii) Reads were multiplied by coefficients assuming equal library sizes for each of the 12 experiments. iii) A two-factor generalized linear model design matrix was specified to estimate dispersion parameters. The Huber function with k=1.03 was used for robust statistics in the estimation of the tagwise dispersion parameters by the edgeR software [190]. LncRNAs are identified as differentially expressed in 5 different comparisons and by

using a False-Discovery-Rate (FDR) cut-off of 20% in the output of edgeR's glmLRT function.

Differential expression analysis of transcripts in primary rat cardiomyocytes. NGS short reads were mapped to the rat genome with the RSEM/ Bowtie software (Dewey Lab) and an index generated for 17349 mature transcripts in Rnor_6 coordinates. Raw counts were analysed with edgeR using similar identical parameters as in above: requiring that transcripts are represented by 5 or more reads in at least 3 out of 4 experiments (2 siMEF2A replicates and 2 controls). In the MEF2A-depleted cardiac cells, 168 genes, excluding MEF2A, were significantly up- or downregulated, using an FDR of 25%.

Quantitative real-time PCR. Total RNA was extracted using the RNeasy Plus Mini kit (Qiagen) according to manufacturer's protocol. RNA was converted to cDNA using Superscript III (Invitrogen) according to the manufacturer's instructions. Note that cDNA was combined with iTaq universal SYBR Green supermix (Bio-Rad) and 500 nM primers in a final volume of 20 µl**.** Each sample was prepared in triplicate and analyzed using Rotor-GeneQ (Qiagen) according to the manufacturer's protocol. All values were normalized to GAPDH (internal control) mRNA levels.

Statistics. Data are reported as mean±SEM. Independent two sample t-tests of all quantitative data were conducted, whereas a one-way analysis of variance followed by a Tukey HSD post hoc test was performed on experiments with greater than two conditions. P-value of less than 0.05 was considered statistically significant. All data were done on technical triplicate and biological triplicate. The n=3 in the caption indicates the biological replicate.

Study Approval. All mouse experiments were approved by the York University Animal Care Committee in accordance with Canadian Council of Animal Care regulations.

Results

β-adrenergic blockade attenuates the hypertrophic response to TAC, enhances cardiac function and reduces MEF2 activity

Transverse aortic constriction (TAC) is a widely used *in vivo* model that mimics disease associated with cardiac hypertrophy and heart failure [191]. The β1 selective β-adrenergic antagonist, Atenolol, is historically one of the most frequently prescribed of all medicines, and in experimental models such as TAC, Atenolol can prevent cardiac hypertrophy [192,193]. Since MEF2 regulates a large battery of cardiac genes we were intrigued to further pursue these observations since it may have important clinical relevance for understanding the effects of chronic β-blocker treatment, which has been, and continues to be carried out in many millions of patients with cardiovascular disease. To study the effects of TAC and chronic treatment with Atenolol on MEF2 activity we initially utilized a MEF2-lacZ reporter transgenic mouse model. These mice harbour a synthetic transgene containing three MEF2 sites from the desmin gene distal to a heterologous promoter and exhibit MEF2 activity during development in the heart and somites [151]. Similar to previous studies with CAMKII activation [10], we observed that MEF2 activity is markedly enhanced by TAC during cardiac hypertrophy (Figure 15A) as we reported previously [194]. Long term Atenolol (>10 weeks) treatment also reduced MEF2-activity in non-treated mice (Figure 15A). Mice at 6-8 weeks of age were randomized to receive either TAC surgery to induce left ventricular (LV) pressure

overload, or a sham operation. Assessment of heart function by transthoracic echocardiography six weeks after surgery demonstrating that TAC mice had developed physiological readouts characteristic of cardiac hypertrophy and the onset of heart failure: increased LV posterior wall thickness (PWDd) and LV mass, and decreased ejection fraction (EF) and fractional shortening (FS) (Figure S4). TAC or sham, mice were then treated with Solvent (Sol) or the β-blocker Atenolol (AT; 50mg/kg/day) for four additional weeks. After which time a series of comprehensive physiological, biochemical and genomic analyses were carried out. The four experimental conditions were therefore: Sham+Sol; Sham+AT; TAC+Sol; and TAC+AT (Figure 15A).

After 4 weeks of treatment, TAC+Sol mice continued to exhibit signs of cardiac dysfunction and LV hypertrophy: reduced EF and FS, and increased PWDd, end systolic diameter (ESD), end systolic volume (ESV) and LV mass compared to Sham+Sol (Figure 15B). End diastolic diameter (EDD) and volume (EDV) were similar between the TAC+Sol and Sham+Sol groups. Atenolol treatment in the sham group (Sham+AT) induced no statistically significant change in heart function when compared to the control group (Sham+Sol). However, four weeks of Atenolol treatment in the TAC group (TAC+AT) resolved changes to LV geometry and reversed indices of LV hypertrophy induced by pressure overload as indicated by a reduction in ESD, PWDd and LV mass compared to TAC+Sol, and this was associated with an overall improvement in cardiac function, as evidenced by a significant increase in FS and EF in TAC+AT compared to TAC+Sol (Figure 15B).

To further document the changes occurring in TAC mice treated with Atenolol, tissue sections were stained for wheat germ agglutinin (WGA) to visualize and quantitate

cellular hypertrophy (Figure 15C). TAC+Sol had larger cardiomyocytes than control (*P<0.05). Cardiomyocyte size in the TAC+AT group, however, was significantly smaller than in the TAC+Sol group indicating a reversal of the hypertrophic phenotype (#P<0.05). TAC and LV pressure overload is known to be associated with increased collagen deposition leading to fibrosis resulting in increased wall stiffness and ultimately decreased cardiac function [194,195]. Masson's trichrome staining showed increased fibrosis in the TAC+Sol group which was reduced in the TAC+AT group, as shown in representative images in Figure 15D. Together, these results demonstrate major positive effects of chronic Atenolol treatment on cardiac hypertrophy and heart failure progression.

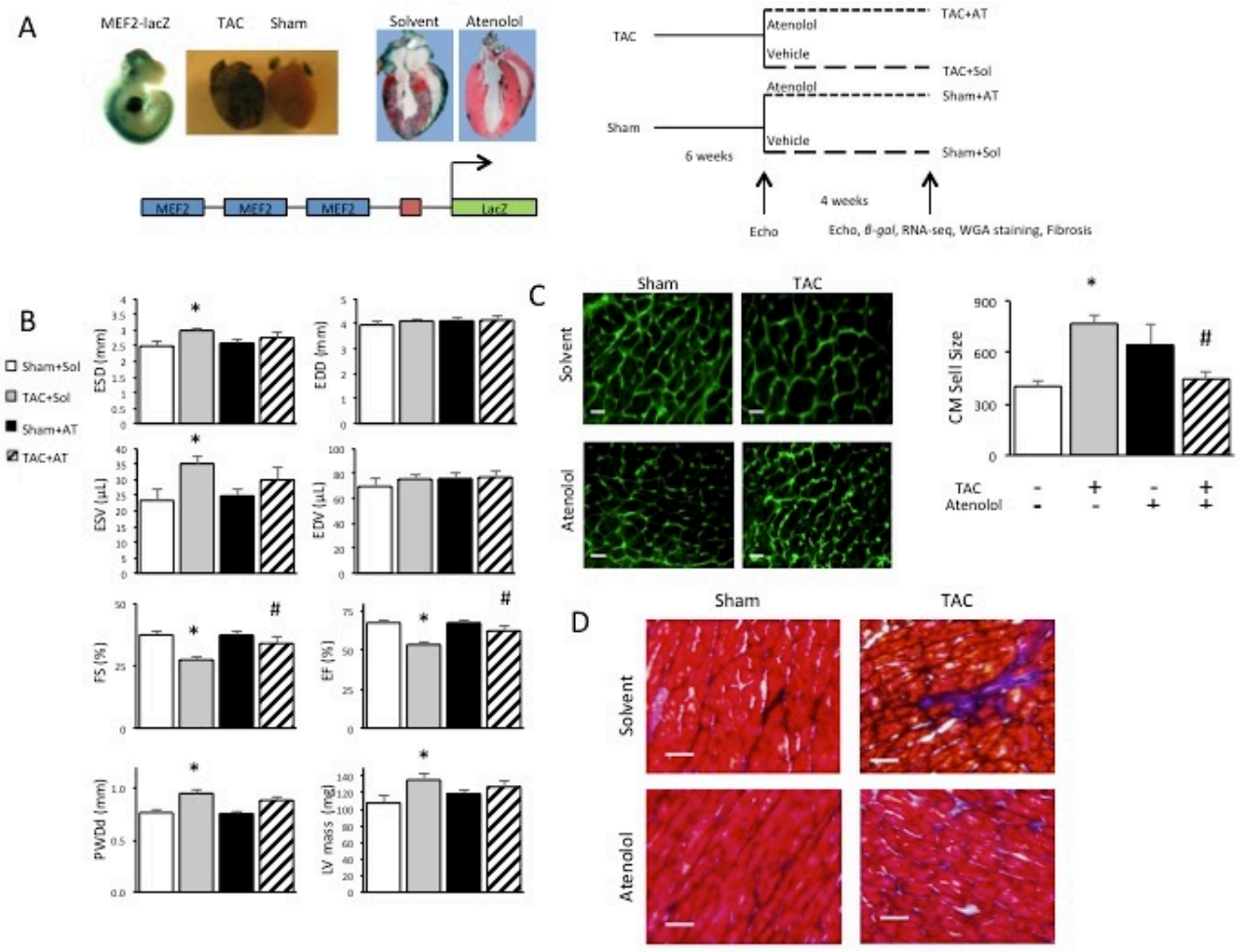
A
MEF2-lacZ
TAC
Sham
Solvent
Atenolol
MEF2
MEF2
MEF2
Lac2
TAC
Atenolol
TAC+AT
Vehicle
TAC+Sol
Sham
Atenolol
Sham+AT
Vehicle
Sham+Sol
6 weeks
4 weeks
Echo
Echo, ß-gal, RNA-seq, WGA staining, Fibrosis
B
Sham+Sol
TAC+Sol
Sham+AT
TAC+AT
ESD (mm)
EDD (mm)
ESV (µL)
EDV (µL)
FS (%)
EF (%)
PWDd (mm)
LV mass (mg)
C
Sham
TAC
Solvent
Atenolol
CM Sell Size
TAC
Atenolol
D
Sham
TAC
Solvent
Atenolol

Figure 15

Figure 15. Atenolol reverses heart failure symptoms in TAC mice. A) Experimental design overview. Left panel: MEF2-lacZ mice (6-8 weeks old) underwent transverse aortic constriction (TAC) or sham treatments, followed by Solvent or Atenolol (50mg/kg/day) treatment (n=9). Right panel: MEF2-LacZ activity in heart with chronic 10 week β-blocker (Atenolol) treatment (50mg/kg/day). B) Functional analysis of TAC or Sham mouse hearts after four weeks of Atenolol or Solvent treatment. End systolic diameter (ESD), end diastolic diameter (EDD), ejection fraction (EF), fractional shortening (FS), end systolic volume (ESV), end diastolic volume (EDV), left ventricular mass (LV), and left ventricular posterior wall depth (PWDd) were assessed by ultrasound echocardiography. Data are presented as mean ±SEM. *P < 0.05 vs Sham+Sol. # P < 0.05 vs TAC+Sol C) WGA stain depicting cardiac hypertrophy. Images are representative of an average of n≥10 images per heart, 4 animals per group. Scale bar: 25 μm. Graph below shows cardiomyocyte size (CM cell size), quantified based on an average of ≥10 cell measurements per mouse (n=4). Data are presented as mean ±SEM. *P < 0.05 vs Sham+Sol. # P < 0.05 vs TAC+Sol. D) Masson's Trichrome stain depicting fibrosis. Images are representative of n=10 images per heart, 4 animals per group. Cardiomyocytes appear red, nuclei appear black and collagen appears blue. Scale bar: 100 μm.

Dynamic changes in gene expression provoked by TAC are reversed by β-adrenergic blockade

To further understand the underlying changes in gene expression during these conditions, the left ventricle was isolated from each condition (n=3 mice per condition) and RNA was prepared for subsequent RNA-Seq analysis to document transcriptome changes associated with the experimental treatments and potentially identify differentially expressed genes (DEGs). Across all conditions, 1571 DEGs were detected (Figure 16A). In particular, we documented 65 DEGs in TAC+Sol mice compared to Sham+Sol (Figure 16B). In parallel, some genes affected by Sham+Sol had a reversed pattern of expression in TAC+AT (Figure 16A, blue boxes). A complete list of all DEGs is in Dataset 1. Most importantly, one predominant feature of the data is that the pattern of differentially expressed genes in TAC+Sol was in general reversed in TAC+AT (Figure 16A, yellow boxes).

To identify the potentially most biologically relevant DEG's we focused on genes that were differentially expressed in both TAC+Sol vs Sham+Sol and TAC+AT vs TAC+Sol comparisons (32 genes), which comprised of nearly half of all DEGs in the TAC+Sol condition (Figure 16C). Figure 16D depicts the dynamic regulation of a sub-set of the 32 genes identified in Figure 16C. In general, genes that were upregulated in TAC+Sol relative to Sham+Sol were downregulated in TAC+AT vs TAC+Sham, and vice versa for downregulated genes, demonstrating that Atenolol reverses the effect of TAC on gene expression in the heart. Among these genes were *Klf2*, *Junb*, *Ier2* (immediate early response 2), *Alas2* (delta-aminolevulinic acid synthase 2, two ubiquitin related proteins *U*be2l6 (E2 ubiquitin ligase) and *Usp53* that are upregulated in TAC, while Atenolol

reduces their expression in response to TAC. The upregulation of a and b chains of hemoglobin seen in TAC+Sol were also reversed by Atenolol treatment, an important feature since elevated hemoglobin has been associated with cardiac death [196]. On the other hand *Ifrd1* (also known as PC4; Tis7) is a known co-factor of MEF2 in skeletal myoblasts that contributes to skeletal myogenesis [197] is downregulated with TAC, but atenolol treatment induces expression relative to TAC+Sol. Down-regulation of tissue inhibitors of metalloproteinases (Timps) and upregulation of matrix metalloproteinases is also associated with extracellular matrix remodelling during heart failure [198,199]. In our data, *Timp*-4, was downregulated with TAC and upregulated with Atenolol treatment. *Timp*-4 downregulation has also been associated with left ventricular dilatation in heart failure in humans [200].

lncRNAs are non-coding RNAs greater than 200 nucleotides long and have increasingly been connected to cardiac development [189]. Using a compiled network of lncRNAs [189] we characterized DE lncRNA in our samples. The percentages of reads, which mapped to lncRNAs varied in a narrow range from 2.8% to 3.4% (Figure S5). It is important to point out that our analysis isolated poly-A containing transcripts, so any lncRNA without this modification would not be detected. However, our analysis showed that there are 84 differentially expressed lncRNA across all conditions (Figure S5). Matkovich et al. [189] found that expression in lncRNAs was most dynamically regulated during heart development in the embryo, and less so in a TAC model of cardiac hypertrophy. Similarly, we found 6 lncRNAs to be significantly regulated in TAC+Sol conditions, and 12 were DE in TAC+AT vs TAC+Sol (Figure S5). An emerging role for lncRNA in cardiac hypertrophy is apparent, however to study the function of individual lncRNA will

take time because of the highly variant mechanisms proposed for their function. To initially identify some potential biological associations we assessed the five most abundant lncRNA in each condition and identified a lncRNA name in the literature (if present) (Figure S5). In all conditions, n413706, n415312 and n413977 were most abundant. n415312 has recently been identified as lncRNA Myheart (*Mhrt*) and is associated with regulation of *Mhy7* [201]. *Mhrt* has a reported cardio-protective role through inhibition of the Brg1 chromatin remodeling factor [201]. n424047, lncRNA *M*SUR1, was abundant in Sham+Sol but downregulated in all other conditions. *MSUR1* was able to prevent SOD1-mediated cell death [202]. It may therefore be possible that *MSUR1* also has a role in heart failure.

We used a functional annotation clustering tool [203,204] to group terms with related biological meaning into annotation clusters. Annotation terms were manually selected from the list of representative terms generated within each cluster. The ten clusters with the highest enrichment score from each treatment are shown in Figure 17. TAC+Sol (Figure 17A) contained clusters enriched for cell proliferation, the immune system, cell migration and apoptosis. The most critical comparison was between TAC+Sol and TAC+AT (Figure 17B). Annotation clusters were related to the extracellular matrix, collagen and heparin binding, and also muscle protein.

To draw out a more gene specific comparison, two representative GO clusters from Figure 17B are illustrated in Figure 17C corresponding to the 'muscle protein' (left) and 'heparin binding' (right) identifiers. Terms within each annotation are on the X axis, while each gene associated with these terms is on the Y axis. Genes that were upregulated are red and genes that were downregulated are green. Fourteen genes were associated

within the ‘muscle protein’ cluster. Some upregulated genes of note include *Mybpc2*, *Myh7*, *Acta1* and *Des*. Interestingly two of the affected genes were E3 ubiquitin ligases *Trim63* and *Trim72*. *Trim63*, (also called MuRF1) was downregulated and has been previously associated with muscle atrophy [205]. *Trim72* (or MG53) was upregulated and is associated with membrane stability has been reported to target the insulin receptor for degradation [206]. In general genes associated with the heparin-binding cluster were downregulated in TAC+AT compared to TAC+Sol. Consistent with the high glycosaminoglycan binding properties of the protein products of these genes, several genes within this cluster are related to the extracellular space. Ccn1 is a matricellular protein whose expression has been associated with heart failure [207]. Mice deficient for Col15a1 (type XV collagen) also have heart defects [208,209]. Adamts1 and 8, two matrix metalloproteinases, are also known to be anti-angiogenic [210]. Precise expression of Adamts1 during embryogenesis is involved with trabeculation of the heart but its role in the adult heart is not yet clear [211].

In general, these data demonstrate that during TAC+Sol treatment genes associated with apoptosis and remodeling of the extracellular matrix are upregulated and Atenolol treatment remarkably reverses many of these transcriptome changes. In addition, TAC+AT resulted in an upregulation of muscle protein genes that are collectively associated with improved muscle function.

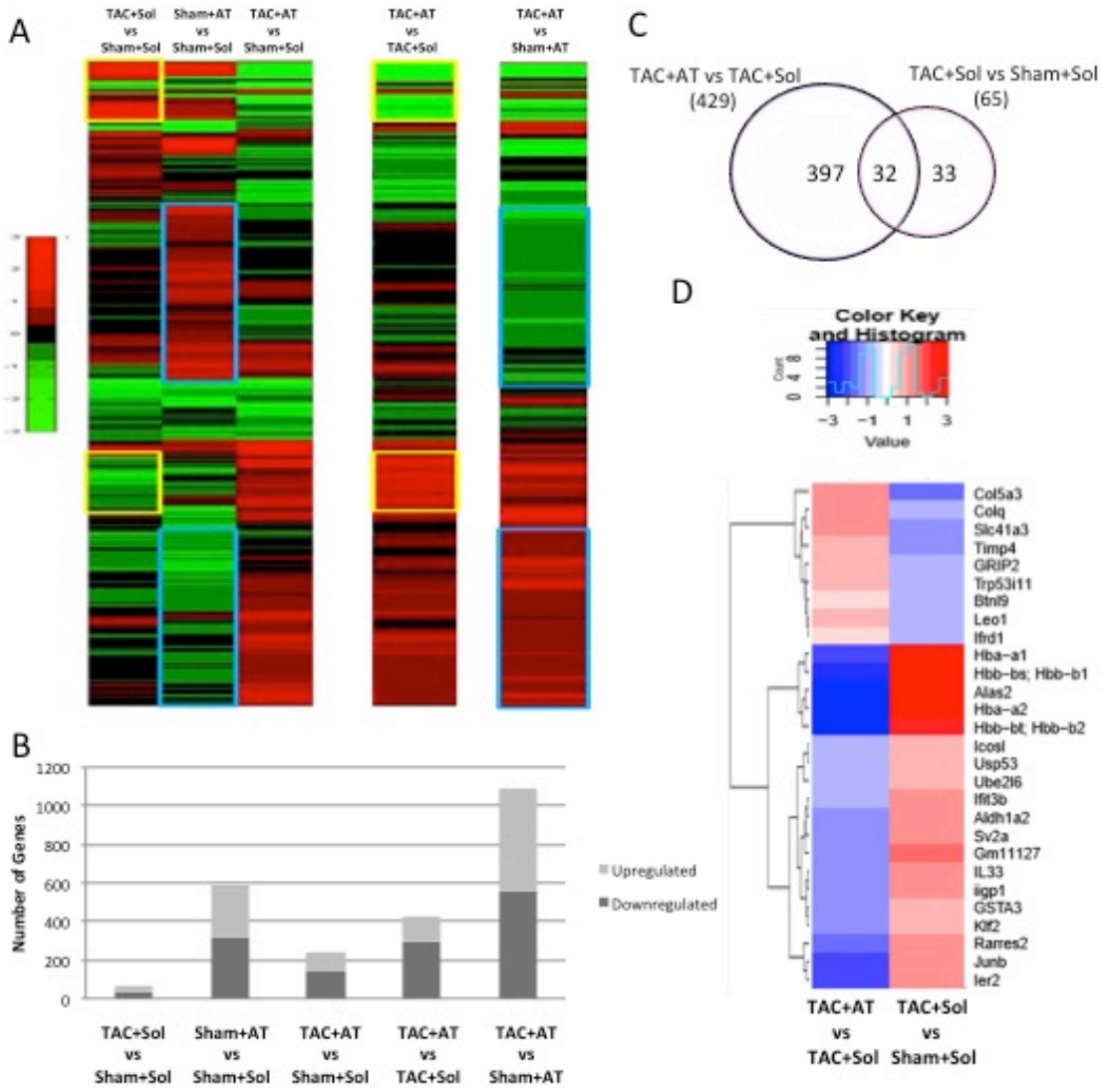
A
TAC+Sol vs Sham+Sol
Sham+AT vs Sham+Sol
TAC+AT vs Sham+Sol
TAC+AT vs TAC+Sol
TAC+AT vs Sham+AT
B
Number of Genes
1200
1000
800
600
400
200
0
TAC+Sol vs Sham+Sol
Sham+AT vs Sham+Sol
TAC+AT vs Sham+Sol
TAC+AT vs TAC+Sol
TAC+AT vs Sham+AT
Upregulated
Downregulated
C
TAC+AT vs TAC+Sol (429)
TAC+Sol vs Sham+Sol (65)
397
32
33
D
Color Key and Histogram
Count
0 4 8
−3 −1 1 3
Value
Col5a3
Colq
Slc41a3
Timp4
GRIP2
Trp53i11
Btnl9
Leo1
Ifrd1
Hba−a1
Hbb−bs; Hbb−b1
Alas2
Hba−a2
Hbb−bt; Hbb−b2
Icosl
Usp53
Ube2l6
Ifit3b
Aldh1a2
Sv2a
Gm11127
IL33
iigp1
GSTA3
Klf2
Rarres2
Junb
Ier2
TAC+AT vs TAC+Sol
TAC+Sol vs Sham+Sol

Figure 16

Figure 16: C**hanges in gene expression caused by aortic constriction is reversed by atenolol treatment.** RNA-seq analysis was completed on the left ventricle of mice that had undergone TAC or Sham operation for 6 weeks followed by either solvent or Atenolol treatments (n=3 in each group). A) Heatmap depicting changes in gene expression of 1571 protein coding genes. Genes are ordered based on hierarchical clustering. Genes up- or down-regulated by TAC alone, relative to control (leftmost column; yellow box). Effects of β-blocker (2^{nd} leftmost column; blue box). B) Total change in up and downregulated genes in each condition. C) A select group of genes (32) were differentially regulated in both the TAC+Sol vs Sham+Sol and TAC+AT vs TAC+Sol conditions. D) Heatmap depicting the Fold Change values of TAC+AT vs TAC+Sham and TAC+Sol vs Sham+Sol.

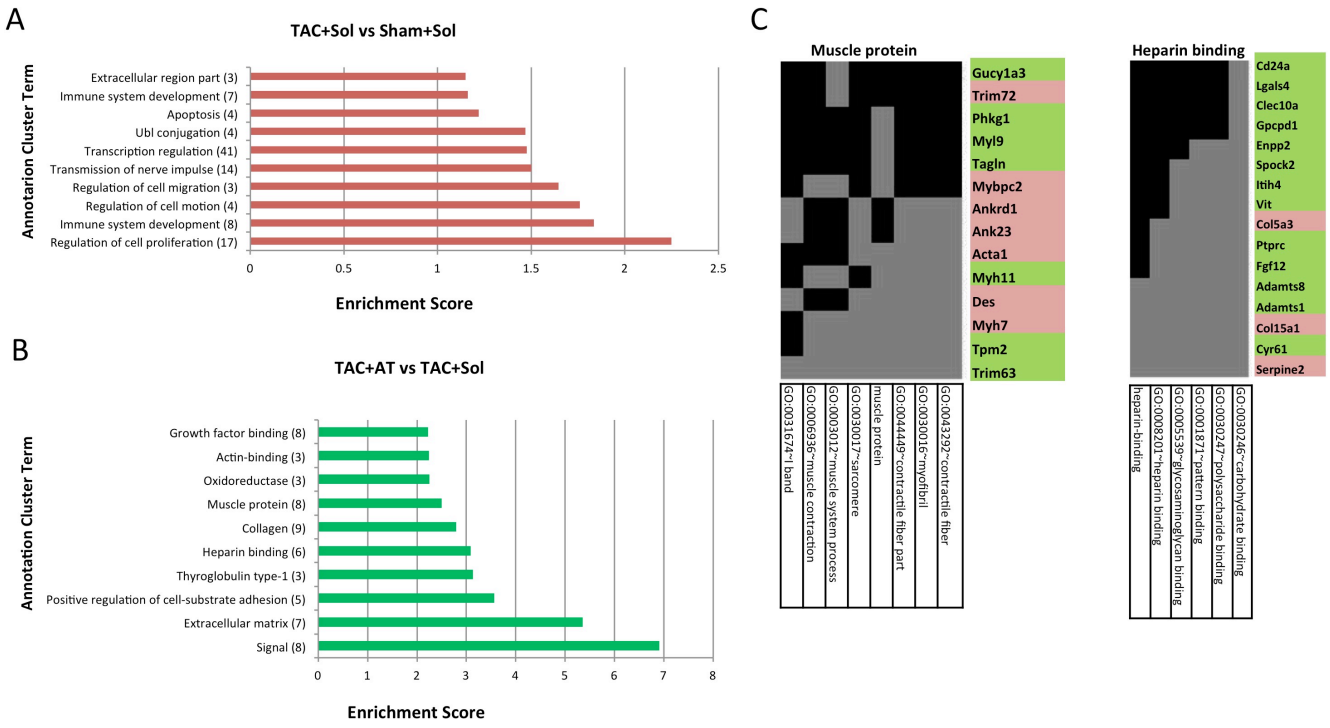
A
TAC+Sol vs Sham+Sol
Annotation Cluster Term
Extracellular region part (3)
Immune system development (7)
Apoptosis (4)
Ubl conjugation (4)
Transcription regulation (41)
Transmission of nerve impulse (14)
Regulation of cell migration (3)
Regulation of cell motion (4)
Immune system development (8)
Regulation of cell proliferation (17)
0
0.5
1
1.5
2
2.5
Enrichment Score
B
TAC+AT vs TAC+Sol
Annotation Cluster Term
Growth factor binding (8)
Actin-binding (3)
Oxidoreductase (3)
Muscle protein (8)
Collagen (9)
Heparin binding (6)
Thyroglobulin type-1 (3)
Positive regulation of cell-substrate adhesion (5)
Extracellular matrix (7)
Signal (8)
0
1
2
3
4
5
6
7
8
Enrichment Score
C
Muscle protein
Gucy1a3
Trim72
Phkg1
Myl9
Tagln
Mybpc2
Ankrd1
Ank23
Acta1
Myh11
Des
Myh7
Tpm2
Trim63
GO:0031674~I band
GO:0006936~muscle contraction
GO:0003012~muscle system process
GO:0030017~sarcomere
muscle protein
GO:0044449~contractile fiber part
GO:0030016~myofibril
GO:0043292~contractile fiber
Heparin binding
Cd24a
Lgals4
Clec10a
Gpcpd1
Enpp2
Spock2
Itih4
Vit
Col5a3
Ptprc
Fgf12
Adamts8
Adamts1
Col15a1
Cyr61
Serpine2
heparin-binding
GO:0008201~heparin binding
GO:0005539~glycosaminoglycan binding
GO:0001871~pattern binding
GO:0030247~polysaccharide binding
GO:0030246~carbohydrate binding

Figure 17

Figure 17. Biological implications based on functional annotation gene clustering. **A**) TAC+Sol vs Sham+Sol. B) TAC+AT vs TAC+Sol. Function annotation clusters identified by DAVID using default settings with medium stringency. Annotation terms were chosen from the list of representative terms generated within each cluster. If present, the first SP_PIR_KEYWORDS was used as the annotation. If SP_PIR_KEYWORDS was not present the first BP term to occur in the cluster was used. Beside each annotation is the number of representative terms associated within each cluster. C) Two representative clusters from TAC+AT vs TAC+Sham. Representative terms within each cluster are on the X axis. Genes within each GO term are on the Y axis. Left: 'Muscle protein' (7 genes up, 7 down, 14 total). Right 'Heparin binding' (3 up genes, 13 down, 16 total). Grey indicates association of a gene with a representative term. Genes shaded red or green were up- or down-regulated, respectively.

The role of *Klf2*, *Junb*, *Rarres2* and *Alas2* in cardiomyocyte hypertrophy and apoptosis.

To verify the differential regulation of individual genes in response to TAC and Atenolol, as depicted in Figure 19C and 19D in the transcriptomics data, we performed individual qRT-PCR on RNA samples from the same treatment conditions on 24 of the identified genes (Figure 18A, Figure S6, S7). Next, we selected 5 genes upregulated in TAC+Sol relative to Sham+Sol and downregulated in TAC+AT vs TAC+Sham (*Klf2*, *Junb*, *Rarres2*, *Iigp1* and *Alas2*) for further analysis in the context of cardiac hypertrophy and apoptosis. Since two prominent features of progressive heart failure are cardiomyocyte hypertrophy and apoptosis, we decided to further test the capacity of the identified genes to affect these parameters in our *in vitro* models using gain and loss of function analysis. For the gain of function (GOF) analysis we chose to exogenously express the genes of interest. For loss of function (LOF) we used siRNA mediated depletion of the target genes. We then assessed GOF or LOF in two models: a) apoptotic induction by high-level Isoproterenol (Iso) induction in primary cardiomyocytes; and b) induction of hypertrophy in the cardiac HL-1 cell line. The rationale for choosing the particular genes that we did was that they were dysregulated under TAC conditions and, importantly, their expression pattern was substantially reversed with Atenolol treatment indicating that they may be involved in pathological changes that can be potentially altered by drug therapy. First, RT-PCR analysis confirmed that *Klf2*, *Junb*, *Rarres2*, and *Alas2* are upregulated in response to TAC, and Atenolol treatment reverses this effect (Figure 18A) similar to what was observed with TAC and Atenolol treatment *in vivo* in the transcriptome data (Figure 16*)*.

Next, cardiac HL-1 cells were transfected with GFP and expression plasmids for a number of genes of interest individually or in combination and the cells were stained for Wheat Germ Agglutinin (WGA) to visualize and quantitate the cell surface area as an index of cellular hypertrophy (Figure 18B). Only GFP+ cells were quantified in this analysis. The bar graph indicates the mean size of HL-1 cells transfected with the indicated expression plasmids individually or in combination compared to the vector alone control. These preliminary data indicate that, of the genes tested, *Alas2*, *Junb* and *Klf2* may have a role in promoting cardiomyocyte hypertrophy since their exogenous expression in cultured HL-1 cells led to a trend towards increased cell surface area although *Klf2* was the only significantly different treatment ($p<0.05$). To assess the potential role of Junb, *Klf2*, *Rarres2*, *Alas2* and *Iigp1* genes in cardiac apoptosis using LOF, we silenced their expression using siRNA technology and treated cardiomyocytes with isoproterenol (10μM) for 48 hours to induce increased levels of cardiac apoptosis as we have previously published [212]. Protein expression of caspase 3 and cleaved caspase 3 (active form of caspase 3) was then determined as an indicator of apoptotic induction. Of the genes tested, expression of the active form of caspase 3 was reduced in siRNA-mediated depletion of *Junb*, *Rarres2* and *Klf2* treated with Iso compared to the control but depletion of *Alas2* or *Iigp1* had no effect (Figure 18C and Figure S8).

These results demonstrate a possible pro-apoptotic role of *Junb*, *R*arres2 and *Klf2* genes in primary cardiomyocytes. In summary, these preliminary *in vitro* data on the possible function of the genes identified in the *in vivo* transcriptomics data reveal a putative involvement of *J*unb, *R*arres2 and *Klf2* in apoptotic induction and a potential hypertrophic influence of *Alas2*, *Junb* and *Klf2* in hypertrophy. Further *in vivo* studies of

these genes are thus warranted to determine their role in cardiac pathology.

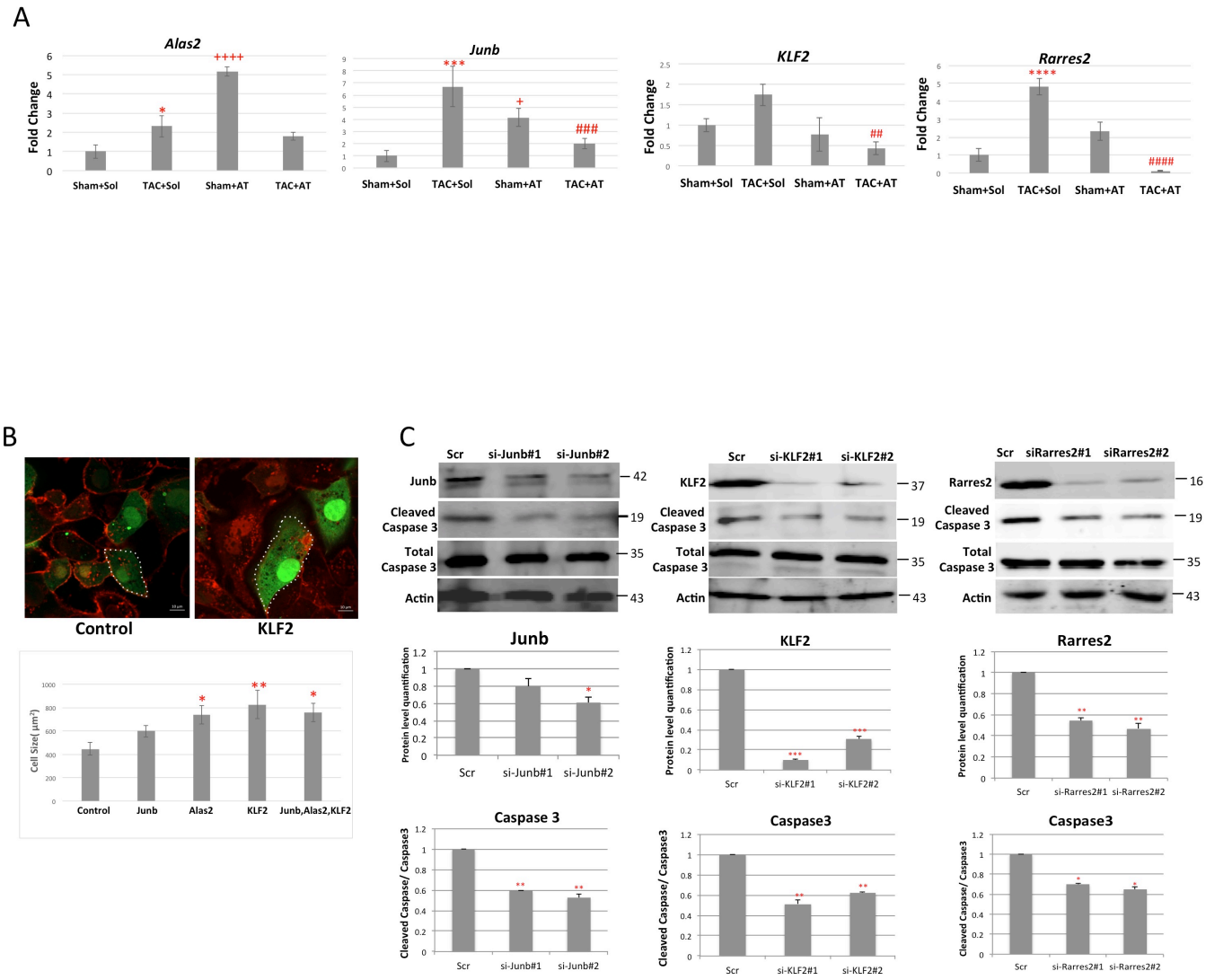
A
Alas2
Junb
KLF2
Rarres2
Fold Change
Sham+Sol
TAC+Sol
Sham+AT
TAC+AT
B
Control
KLF2
Cell Size(μm²)
Control
Junb
Alas2
KLF2
Junb,Alas2,KLF2
C
Scr
si-Junb#1
si-Junb#2
si-KLF2#1
si-KLF2#2
siRarres2#1
siRarres2#2
Junb
KLF2
Rarres2
Cleaved Caspase 3
Total Caspase 3
Actin
Protein level quantification
Caspase 3
Caspase3
Cleaved Caspase/ Caspase3

Figure 18

Figure 18. Role of KLF2, Junb, Rarres2 and Alas2 in cardiomyocyte hypertrophy and apoptosis. A) Modulation of *KLF2*, *Junb*, *Rarres2* and *Alas2* expression in response to TAC and Atenolol as depicted in Figure 2C, was confirmed using qRT-PCR. cDNA was analyzed via qRT-PCR using SYBR Green master mix. Data were normalized to Gapdh and are presented as fold change using the delta delta Ct method (n=3, *P<0.05 **P<0.01 Sham+Sol vs TAC+Sol, ++P<0.01 Sham+Sol vs Sham+AT, ##P<0.01 TAC+Sol vs TAC+AT). B) WGA staining depicts cardiac hypertrophy. Cardiac HL-1 cells were transfected with GFP and Alas2, Junb, or KLF2 expression plasmids individually or in a mixture and stained with Wheat Germ Agglutinin (WGA) in red. The bar graph indicates that cell size of GFP positive HL-1 cells, quantified based on 5 cell measurements per image. Data are presented, as mean ±SEM. Scale bar is 10μm. C) Primary cardiomyocytes were transfected with two independent siRNAs, Junb siRNA, Rarres2 siRNA, KLF2 siRNA, (top panel), or with scramble siRNA control and treated with isoproterenol (10μM) for 48 hours. Equal amounts of total protein were used for western blot analysis and the levels of the indicated proteins were assessed by a standard immunoblotting technique using specific primary antibodies for each as indicated. Bar graph represents the quantified data, Caspase 3 bar graph represents cleaved Caspase 3 normalized to total caspase 3 (bottom panel).

Transcriptome profiling in MEF2A depleted cardiomyocytes and its relation to β-blockade associated transcriptome changes.

To determine how TAC and Atenolol influence MEF2 activity, MEF2 sensor mouse hearts were stained for LacZ expression. These data indicate that MEF2 activity was strongly induced in TAC+Sol mice and, in parallel with the positive reversal of other TAC induced changes, Atenolol treatment substantially reduced MEF2 activity (Figure 19A). We then assessed potential regulation of these differentially expressed genes (429) from the TAC+AT vs TAC+Sol analysis using oPossum 3.0 to find transcription factor consensus sequences within ±5kb of the transcription factor start site (data not shown). MEF2A consensus sequences were identified at 159 (37%) of differentially expressed genes. Next, we assessed predicted MEF2 consensus sequences from 32 overlapping genes upregulated in Figure 16D. RNA expression (FPKM) of these genes in heart muscle (Female, age 40-50) was also analyzed in Human Protein Atlas program (Figure S9). MEF2A, as a positive control, with FPKM >20 is highly expressed (+++) in heart muscle. In comparison, RNA levels (FPKM), *R*arres2, *J*unb and *Slc41a3* (++) have high heart muscle expression and *Aldh1a2*, *Ifrd1*, *Klf2*, *Leo1* have lower expression (+).

Since MEF2 activity was potently regulated by TAC and AT we next took a more reductionist approach by using siRNA-mediated MEF2 gene silencing to determine whether genes affected in the *in vivo* experiments were also influenced by MEF2A suppression in primary isolated cardiomyocytes. We reasoned that this approach might provide insight into the number of direct cardiomyocyte DEGs that were altered by β-adrenergic blockade that were a consequence of altered MEF2 function. siRNAs targeting MEF2A were transfected into primary cardiomyocytes and prepared for RNA-

sequencing in duplicate. In total there were 168 DEGs, where 107 of which were upregulated and 68 were downregulated (Figure 19B). Figure 5C demonstrates the log2FoldChange of the differentially expressed genes in a volcano plot. The overall features of this plot reveal an extensive re-patterning of cardiomyocyte gene expression when MEF2A is depleted. Of note, *M*ef2a downregulation was coincident with downregulation of cytokines *Cxcl6* (rat homologue to mouse *Cxcl5*) and *Cxcl10* while *Bnip3*, which is involved in apoptotic induction, was upregulated. We have previously identified a protective role of MEF2A in cardiomyocyte survival [212]. It will be interesting to determine if upregulation of *Bnip3* is involved in apoptotic induction when MEF2A is silenced- a condition that does occur with acute β-adrenergic stimulation [115].

Next we assessed the biological significance of the function of these genes using Gene Ontology analysis. Figure 19D shows the ten most enriched Biological Processes associated with MEF2A depletion. Interestingly, a number of these terms are related to cell death and the inflammatory response.

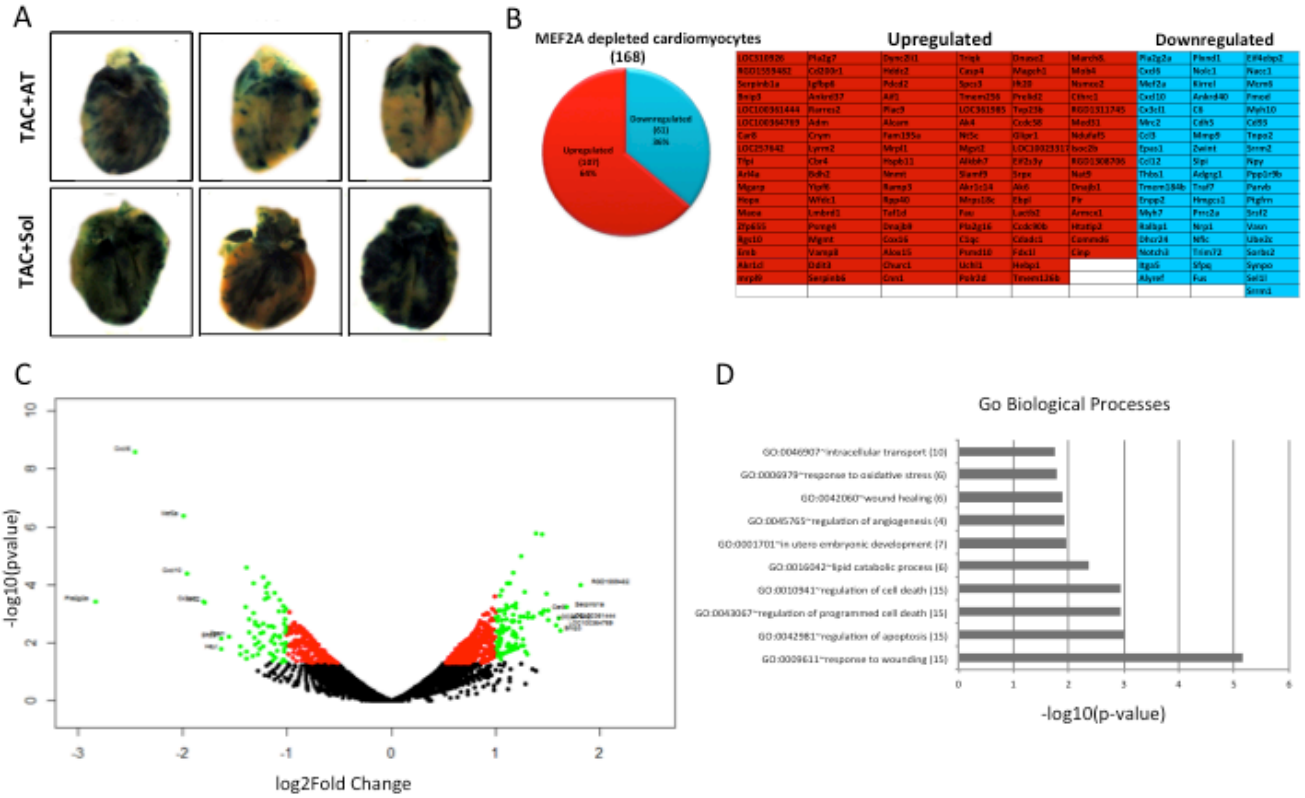
A
TAC+AT
TAC+Sol
B
MEF2A depleted cardiomyocytes
(168)
Upregulated
Downregulated
C
-log10(pvalue)
log2Fold Change
D
Go Biological Processes
-log10(p-value)

Figure 19

Figure 19. Involvement of MEF2 in cardiac hypertrophy and death. A) Hearts from TAC+Sol and TAC+AT (n=3) were stained for LacZ expression. B) The number of genes up or downregulated in response to MEF2A knockdown in primary cardiomyocytes. Table of genes regulated by MEF2, (upregulated are in red, downregulated are in blue). C) Volcano plot depicting up and downregulated genes identified in RNA-seq in response to MEF2A knockdown in primary cardiomyocytes. Black if p-value>0.05, red if p-value<0.05, green if log2FoldChange>1 or <-1 and p-value<0.05. Labels are present only on logFC>±1.5. E) GO Biological Processes associated with up or downregulated genes. The number of genes is in parentheses beside each term.

Rarres2 is a novel MEF2 target gene regulated by β-adrenergic signaling.

In comparing our transcriptome profiles from Figure 16D to those affected by MEF2A knockdown in vitro we were particularly interested in the identification of the Rarres2 mRNA. This gene encodes a protein for the adipokine Chemerin that is mainly produced in liver and adipose tissue, and is also highly expressed in heart muscle based on the Human Protein Atlas analysis in Supplementary Figure S6. Previous studies have shown that treatment of cardiomyocytes with Chemerin affects caspase 9 activity and induction of apoptosis [213]. The expression (FPKM) of Mef2a and Rarres2 from the RNA-seq data is shown in Figure 20A indicating efficacy of the gene silencing and an upregulation of Rarres2. From our in silico analysis using oPossum, we found a putative MEF2 consensus sequence approximately 1 kb upstream from the transcription start site. Using primers flanking this region we performed ChIP-qPCR and validated MEF2A recruitment in primary cardiomyocytes to this locus (Figure 20B). We also determined that loss of MEF2A and MEF2D had a similar effect on Rarres2 induction (Figure 20C). Figure 20C depicts cardiomyocyte treatment with the p38MAPK inhibitor (SB 203580) for 24 hours which led to upregulation of Rarres2 expression and this effect is reduced when cardiomyocytes were transfected with a MEF2A mutation (MEF2A-T312, 319A) which is refractory to p38MAPK phosphorylation. We also observed that Rarres2 is upregulated in cardiomyocytes by β-adrenergic signalling activation (Isoproterenol treatment-Figure 20D), similar to what was observed with TAC treatment in vivo (Figure 16, 18A). Taken together, these data indicate that Rarres2 is a p38 MAPK/MEF2 regulated gene that is induced in heart failure.

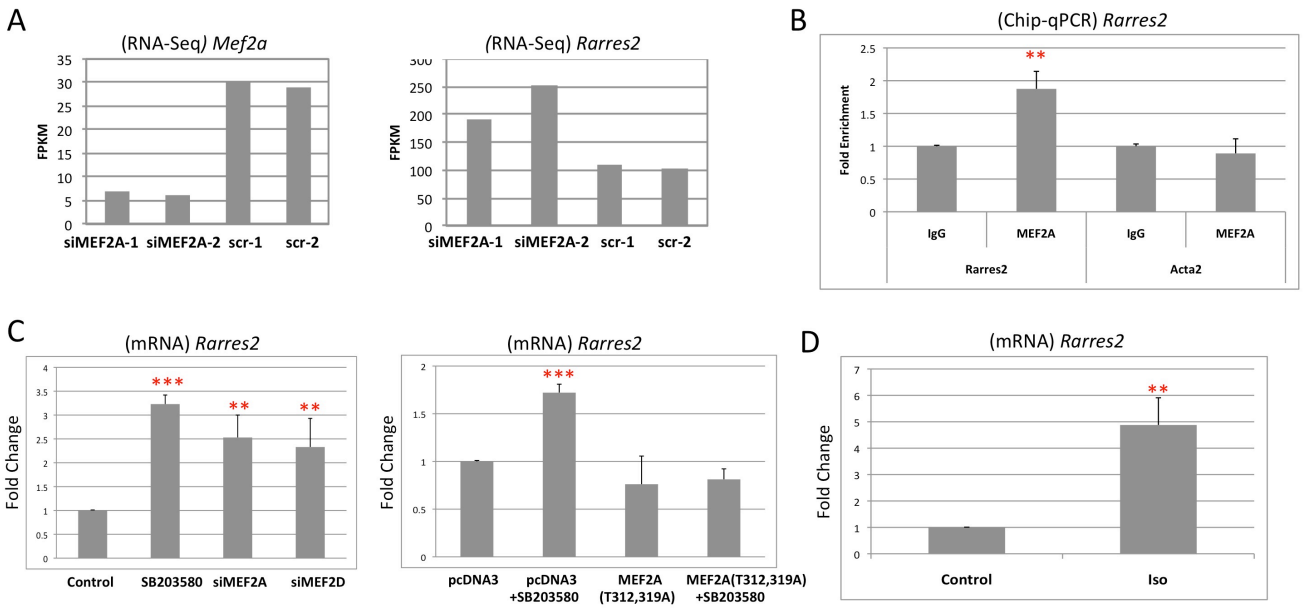
A
(RNA-Seq) Mef2a
FPKM
35
30
25
20
15
10
5
0
siMEF2A-1
siMEF2A-2
scr-1
scr-2
(RNA-Seq) Rarres2
FPKM
250
200
150
100
50
0
siMEF2A-1
siMEF2A-2
scr-1
scr-2
B
(Chip-qPCR) Rarres2
Fold Enrichment
2.5
2
1.5
1
0.5
0
**
IgG
MEF2A
IgG
MEF2A
Rarres2
Acta2
C
(mRNA) Rarres2
Fold Change
4
3.5
3
2.5
2
1.5
1
0.5
0
***
**
**
Control
SB203580
siMEF2A
siMEF2D
(mRNA) Rarres2
Fold Change
2
1.5
1
0.5
0
***
pcDNA3
pcDNA3 +SB203580
MEF2A (T312,319A)
MEF2A(T312,319A) +SB203580
D
(mRNA) Rarres2
Fold Change
7
6
5
4
3
2
1
0
**
Control
Iso

Figure 20

Figure 20. Rarres2 is regulated by MEF2. A) Expression of Mef2a and Rarres2 in RNA-seq analysis of MEF2A depleted cardiomyocytes (fragments per kilobase of exon per million fragments mapped). B) MEF2A recruited to the Rarres2 promoter in primary cardiomyocytes. Data are presented as fold enrichment (n=3, *P<0.05). Acta2 was used as a negative control. C) Rarres2 expression is negatively regulated by MEF2 in a p38 MAPK dependant manner in primary cardiomyocytes. Cardiomyocytes were transfected with siRNA targeting MEF2A or MEF2D. Cells were also transfected with scramble siRNA control (left panel) and empty vector (pcDNA3) or MEF2A mutated form MEF2A (T312, 319A) (right panel) and treated with SB 203580 (5 μM) for 24 hours and analyzed for changes in Rarres2 mRNA. Control cells were treated with an inactive analogue, SB 202474. Data were normalized to Gapdh and are presented as fold change using the delta delta Ct method (n=3, *P<0.05, **P<0.01). D) Isoproterenol (Iso; 10 μM) treatment for 24 hours, upregulates Rarres2 expression. Data were normalized to Gapdh and are presented as fold change as was done in 6C (n=3, **P<0.01).

Discussion

Understanding the global gene networks associated with heart failure will provide critical insight into the underlying aetiology of heart disease while also providing an unprecedented array of molecular targets for therapeutic intervention. In the work presented here we have used next generation RNA sequencing based approaches coupled with bioinformatics to document transcriptome changes associated with experimental heart failure. Moreover, we have documented gene expression changes mediated by β−adrenergic antagonism that result from a partial reversal of a heart failure associated gene signature that is coupled with improved cardiac function.

Underlying the transcriptome changes that we have observed are dynamic changes in the activity of a fundamental cardiac transcriptional regulator, MEF2. The potent influence of β-adrenergic blockade in regulating MEF2 function in the heart has been highlighted recently [212]. However, the influence of β-blockers on MEF2 function in the heart is complex and requires attention to context since MEF2 responsiveness to β-blockade depends on the temporal nature of the treatment. Firstly, short term β-blockade leads to an acute upregulation of MEF2 activity [212]. Mechanistically this is well understood since β-adrenergic signalling promotes PKA activity and HDAC nuclear retention [214]. Both of these have strong repressive effects on MEF2 activity since PKA phosphorylates two residues in MEF2D (S121/190) that repress MEF2 function and HDAC retention in the nucleus enhances the formation of a MEF2/HDAC repressor complex [134]. We have recently reported that acute β-blockade essentially reverses this effect and upregulates MEF2 activity promoting a pro-survival function of MEF2 in cardiac myocytes that has potentially important clinical implications, particularly after

myocardial infarction [212]. In support of this idea, we and others recently documented that experimental suppression of MEF2 expression in rodent cardiomyocytes using siRNA technology promotes apoptosis [212,215]. Conversely, as we have shown here and somewhat unexpectedly, MEF2 activity under conditions of chronic (>4 weeks) β-adrenergic blockade leads to a downregulation of MEF2 activity, particularly under conditions where the heart is stressed as exhibited under conditions of TAC in mice. In our experiments long term (>6 weeks) TAC in mice leads to cardiac hypertrophy, progression to heart failure, and pronounced activation of MEF2 activity. Treatment of mice at 6 weeks after TAC by four weeks of β-adrenergic blockade reduces the adverse impact on heart function and concomitantly suppresses chronic MEF2 activity while also invoking major transcriptome changes. In view of reports that MEF2 is a fundamental regulator of cardiac hypertrophy [31,182] and our results documenting the transcriptomic effects of MEF2 suppression in cardiomyocytes, we suspect that alterations in MEF2 activity are a major determinant of the transcriptome changes observed in response to TAC and also the positive outcome associated with β-adrenergic blockade.

Of particular interest in our studies are the gene expression changes that are induced by experimental heart failure and subsequently reversed by β-blockade since, in our view, some of these genes most likely mediate the protective effects of β-blockers in the heart. Cardiac hypertrophy is initially an adaptive compensatory mechanism to maintain cardiac output, however, prolonged hypertrophic conditions such as those seen during hypertension ultimately contribute to the progression towards heart failure [216]. Although β−blocker treatment in humans post-MI is undoubtedly effective in preventing or slowing the progression to heart failure, the molecular mechanisms involved are unclear. Here

we provide the first steps in characterizing the molecular genetic basis of beneficial β−adrenergic antagonists in the heart. In this cohort we have identified 32 genes that are differentially regulated by TAC whose expression pattern is reversed when TAC mice are treated with β-blockers. We explored the role of Junb, Alas2, Klf2, and Rarres2 in cardiomyocyte hypertrophy and apoptosis as they were induced by TAC in vivo but their expression was repressed by Atenolol (Figure 18A). Two of these (Junb and KLF2) are transcription factors whereas Alas2 regulates heme synthesis and Rarres2 (which encodes Chemerin) is an adipokine. Interestingly, these four different genes potentiate different aspects of heart failure including oxidative stress, hypertrophy, cardiac remodelling, vascular remodelling and apoptosis. Alas2 was shown to be upregulated in failing human hearts, resulting in oxidative stress and cell death [217]. In our experiments loss of Alas2 in primary cardiomyocytes did not reduce apoptosis as cleaved caspase 3 was unaffected (Figure S8), indicating that Alas2 may promote cardiomyocyte death through alternate pathways. Junb is directly responsible for the upregulation of Mmps which mediate cardiac remodelling in ischemia-reperfusion studies [218] therefore it is important that Atenolol can reverse its expression. Klf2 has been shown to be activated in endothelial cells by shear stress [219]. In our TAC model, constriction of the aorta results in increased hemodynamic stress, and likewise results in Klf2 induction which is reversed by Atenolol. Lastly, Rarres2 was also upregulated in MEF2A knockdown cardiomyocytes in vitro, and has been previously associated with cardiac apoptosis and coronary artery disease [213]. It would be of interest to study β-adrenergic and MEF2 regulation of Rarres2 in more detail in human heart disease. Taken together, these data indicate a potential involvement of these genes in the failing mouse heart that may have

implications in human heart failure. Furthermore, the identification of genes associated with heart failure that are downregulated by Atenolol (such as Junb, Klf2, Alas2, and Rarres2) demonstrates the underlying molecular changes responsible for improved heart function, which may lead to new downstream targets for treating heart failure.

Overall, we contend that the cohort of DEGs reported here represent vast potential for the diagnosis and treatment of heart disease. Interestingly, we have noted considerable identification of genes and GO processes associated with the immune system. These observations support recent developments reflecting the involvement of the immune system and inflammatory responses in the progression of heart disease [220–222]. It will be of interest to further analyze these immune system related protein coding genes and non-coding RNAs to determine if they do indeed contribute to heart disease. Herein, we report broad categories of biological processes and also individual genes and non-coding RNAs that are differentially regulated under conditions of experimental heart failure that can be reversed by pharmacological treatment with β-adrenergic antagonists. The next steps will be to determine whether these changes are mirrored in human heart disease and to develop a flexible array of therapeutics that can detect and potentially target these processes with the ultimate aim of reducing pathological changes in the myocardium, enhancing cardiac function, and improving patient morbidity and mortality associated with heart disease.

Funding. This work was supported by an operating grant to JCM from the Canadian Institutes of Health Research (CIHR). JCM is supported by the McLaughlin Research Chair, Faculty of Science, York University. Work in GS laboratory was supported by an operating grant from the Canadian Diabetes Association. GS is supported by a Career Investigator Award from the Heart and Stroke Foundation of Ontario, Canada.

CHAPTER 5: Summary and Discussion

The focus of this dissertation was to investigate a potential clinically important link between the pharmacological blockade of β-adrenergic signaling in the heart and MEF2 transcriptional regulators as global regulators of cardiac gene expression. The influence of β-blockers on MEF2 function in the heart is complex since MEF2 responsiveness to β-blockade depends on the temporal nature of the treatment. In the first manuscript, the short-term effect of β-blockade in regulating MEF2 function in the heart has been investigated. In the first set of experiments, it was observed that β-blockade antagonizes β-adrenergic mediated apoptosis while concomitantly enhancing MEF2 transcriptional activity promoting a MEF2 pro-survival function in cardiomyocytes. In addition, β-adrenergic mediated apoptosis was abrogated in cardiomyocytes expressing a PKA-resistant form of MEF2D (S121/190A). Mechanistically this is well understood since β-adrenergic signaling enhances PKA activity and also nuclear retention of HADCII. Both of these mechanisms repress MEF2 activity since PKA phosphorylates two residues in MEF2D (S121/190) that repress MEF2 function and increased HDACII retention in the nucleus enhances the formation of a MEF2/HDAC repressor complex [134]. Furthermore, KLF6, a MEF2 target gene in the heart, functions as a downstream pro-survival factor in cardiomyocytes (Figure S1, News and Commentary, [223]). Also in support of this idea, siRNA depletion of MEF2 expression promotes cardiomyocytes apoptosis and up-regulation of apoptotic genes as assessed by RNA-Seq analysis. Based on this evidence I propose that increased adrenergic drive and PKA signaling in pathological remodeling inhibits MEF2 pro-survival activity, which contributes to cardiomyocyte cell death post myocardial infarction (MI). Interestingly, β blockade

inhibits PKA activation and reduces infarct mediated cell death post MI and, based on our data, this may result from MEF2 pro-survival activity. This needs to be clarified in an *in vivo* model of MI. It would therefore also be interesting to investigate alternative ways of activating MEF2 transcriptional activity acutely through different mechanisms in the infarcted heart. Recently we also reported that adiponectin can contribute to MEF2 activation in the heart by p38 MAPK activation, indicating another possible pathway to activate MEF2 that might allow pharmacological involvement of Adiponectin [194]. In general, such an approach would allow β-blockade to be maintained for other aspects of its function while recruiting MEF2 pro-survival activity by alternate routes in the acute phase.

Furthermore, it would be interesting to find out if another mechanism of cardiac cell death, necroptosis, is regulated by MEF2. Recent studies have shown that necrostatin-1 (Nec-1) is a chemical compound that inhibits necroptosis without affecting apoptosis [100] Since Nec-1 reduces infarct-mediated cell death post ischemic/reperfusion [224],therefore it is interesting to see if Nec-1 has an effect on MEF2 transcriptioal activity. In particular using a MEF2-Lacz transgenic mice as an *in vivo* model post MI and to see if this is associated with increase in MEF2 pro-survival activity.

In the second study, the mechanisms of how MEF2 activity is down- regulated during chronic β-blockade and determine whether this is protective against pathological heart remodeling was investigated. This study indicated that chronic β-blocker treatment leads to dynamic changes in the heart failure associated cardiac gene transcriptome, and this is accompanied by repression of MEF2 activity. In this category we have identified 32 genes that are differentially regulated by TAC whose expression pattern is

reversed when the TAC mice are treated with β-blockers. Of particular interest was *Rarres2* (which encodes Chemerin) an adipokine that was also upregulated in MEF2A knockout cardiomyocytes. Previous studies have shown that *Rarres2* is associated with cardiac apoptosis and coronary artery disease [213]. Our experiments revealed that P38 MAPK/MEF2 regulates *Rarres2* in cardiomyocytes through MEF2. Also data from this thesis indicates *Rarres2* may play a pro-apoptotic role in cardiomyocytes, as siRNA mediated depletion of Rarres2 following isoproterenol treatment reduced cleaved caspase-3 expression in cardiomyocytes. It would thus be interesting to further study MEF2 regulation of *Rarres2* in human heart disease. Inhibition of Chemerin binding to its receptor or Loss of function analysis of *Rarres2* in experimental animal models of myocardial infarct and pressure overload would elucidate its function in adult myopathy. In our study, we implicated GO terms associated with the immune system, inflammation and apoptosis, it would be interesting to further analyze the involvement of these inflammatory/immune system genes in human heart disease.

One other aspect of our data sets that warrants consideration is the identification of a number of non-coding RNAs. Some miRNAs such as miR-133 and miR-208 are expressed in the mammalian heart and have been linked with the development of cardiac hypertrophy in several studies [225,226]. Since we know that miRNAs regulate an extensive and complex regulatory network of gene expression involving many protein-coding genes, it will be of interest to determine the extent of miR involvement in the gene expression changes involved in heart failure and in response to β-adrenergic blockade to understand their role in protection from or progression to heart failure.

Collectively, these data further define the role of β-blockade on MEF2 regulation in

heart, which is important in cardiac muscle gene expression during physiological and pathological adaptation of the heart. Activation of MEF2 is necessary for preventing cardiac apoptosis and regulation of cardiac survival gene expression in conditions of acute β-adrenergic signaling but blockade of chronic β-adrenergic signaling also leads to inhibition of myocardial MEF2 activity and also likely contributes to the reversal of the effects of heart failure associated transcriptome dynamics. This can, at least partially, be explained due to acute and chronic β-adrenergic signalling effects that have been associated with the PKA and CaMK signalling pathways, respectively [227], which target MEF2 in different ways. The impact of these basic studies for cardiac pathology and therapeutics will require many years of further study in additional clinically relevant models and in human heart tissue.

REFERENCES

1. Kohli S, Ahuja S, Rani V. Transcription factors in heart: promising therapeutic targets in cardiac hypertrophy. *Curr Cardiol Rev* 2011;**7**:262 271.

2. Olson EN. Gene Regulatory Networks in the Evolution and Development of the Heart. *Science (80-)* 2006;**313**:1922–1927.

3. Hunter JJ, Chien KR. Signaling Pathways for Cardiac Hypertrophy and Failure. *N Engl J Med* Massachusetts Medical Society; 1999;**341**:1276–1283.

4. Doevendans PA, Bilsen M van. Transcription factors and the cardiac gene programme. *Int J Biochem Cell Biol* 1996;**28**:387–403.

5. Hogan PG, Hogan PG, Chen L, Chen L. Transcriptional regulation by calcium, calcineurin. *NFAT Genes Dev* 2003;**17**:2205–2232.

6. Molkentin J. Calcineurin?NFAT signaling regulates the cardiac hypertrophic response in coordination with the MAPKs. *Cardiovasc Res* 2004;**63**:467–475.

7. Pikkarainen S, Tokola H, Kerkelä R, Ruskoaho H. GATA transcription factors in the developing and adult heart. *Cardiovasc Res* 2004;**63**:196–207.

8. Patient RK, McGhee JD. The GATA family (vertebrates and invertebrates). *Curr Opin Genet Dev* 2002;**12**:416–422.

9. Olson EN, Perry M, Schulz R a. Regulation of muscle differentiation by the MEF2 family of MADS box transcription factors. *Dev Biol* 1995;**172**:2–14.

10. Passier R, Zeng H, Frey N, Naya FJ, Nicol RL, McKinsey TA, Overbeek P, Richardson JA, Grant SR, Olson EN. CaM kinase signaling induces cardiac hypertrophy and activates the MEF2 transcription factor in vivo. *J Clin Invest* American Society for Clinical Investigation; 2000;**105**:1395–1406.

11. Desjardins CA, Naya FJ. The Function of the MEF2 Family of Transcription Factors in Cardiac Development, Cardiogenomics, and Direct Reprogramming. 2016;**3**:1–23.

12. Black BL, Cripps RM. Myocyte Enhancer Factor 2 Transcription Factors in Heart Development and Disease. *Hear Dev Regen* 2010;673–699.

13. Edmondson DG, Lyons GE, Martin JF, Olson EN. Mef2 Gene-Expression Marks the Cardiac and Skeletal-Muscle Lineages during Mouse Embryogenesis. *Development* 1994;**120**:1251–1263.

14. Black BL, Olson EN. Transcriptional control of muscle development by myocyte enhancer factor-2 (MEF2) proteins. *Annu Rev Cell Dev Biol* Annual Reviews 4139 El Camino Way, P.O. Box 10139, Palo Alto, CA 94303-0139, USA; 1998;**14**:167–196.

15. Lin Q, Schwarz J, Bucana C, Olson EN. Control of mouse cardiac morphogenesis and myogenesis by transcription factor MEF2C. *Science* 1997;**276**:1404–1407.

16. Heidenreich KA, Linseman DA. Myocyte enhancer factor-2 transcription factors in neuronal differentiation and survival. *Mol Neurobiol* 2004;**29**:155–165.

17. Salma J, McDermott JC. Suppression of a MEF2-KLF6 Survival Pathway by PKA Signaling Promotes Apoptosis in Embryonic Hippocampal Neurons. *J Neurosci* 2012;**32**:2790–2803.

18. Woronicz JD, Lina A, Calnan BJ, Szychowski S, Cheng L, Winoto A. Regulation of the Nur77 Orphan Steroid-Receptor in Activation-Induced Apoptosis. *Mol Cell Biol* 1995;**15**:6364–6376.

19. Yu YT, Breitbart RE, Smoot LB, Lee Y, Mahdavi V, Nadal-Ginard B. Human myocyte-specific enhancer factor 2 comprises a group of tissue- restricted MADS box transcription factors. *Genes Dev* 1992;**6**:1783–1798.

20. Molkentin JD, Black BL, Martin JF, Olson EN. Mutational analysis of the DNA binding, dimerization, and transcriptional activation domains of MEF2C. *Mol Cell Biol* 1996;**16**:2627–2636.

21. Potthoff MJ, Olson EN. MEF2: a central regulator of diverse developmental programs. *Development* 2007;**134**:4131–4140.

22. Gossett L a, Kelvin DJ, Sternberg E a, Olson EN. A new myocyte-specific enhancer-binding factor that recognizes a conserved element associated with multiple muscle-specific genes. *Mol Cell Biol* 1989;**9**:5022–5033.

23. Akazawa H, Komuro I. Roles of cardiac transcription factors in cardiac hypertrophy. *Circ Res* 2003;**92**:1079–1088.

24. Kuisk IR, Li H, Tran D, Capetanaki Y. A Single MEF2 Site Governs Desmin Transcription in Both Heart and Skeletal Muscle during Mouse Embryogenesis. *Dev Biol* 1996;**174**:1–13.

25. Chambers AE, Logan M, Kotecha S, Towers N, Sparrow D, Mohun TJ. The RSRF/MEF2 protein SL1 regulates cardiac muscle-specific transcription of a myosin light-chain gene in Xenopus embryos. *Genes Dev* 1994;**8**:1324–1334.

26. Bhavsar PK, Dellow KA, Yacoub MH, Brand NJ, Barton PJR. *J Mol Cell Cardiol* Elsevier; 2016;**32**:95–108.

27. Czubryt MP, McAnally J, Fishman GI, Olson EN. Regulation of peroxisome proliferator-activated receptor γ coactivator 1α (PGC-1α) and mitochondrial function by MEF2 and HDAC5. *Proc Natl Acad Sci* 2003;**100**:1711–1716.

28. Molkentin JD, Olson EN. MADS-box transcription. 1996;**93**:9366–9373.

29. Wang YX, Qian LX, Yu Z, Jiang Q, Dong YX, Liu XF, Yang XY, Zhong TP, Song HY. Requirements of myocyte-specific enhancer factor 2A in zebrafish cardiac contractility. *FEBS Lett* 2005;**579**:4843–4850.

30. Naya FJ, Black BL, Wu H, Bassel-Duby R, Richardson J a, Hill J a, Olson EN. Mitochondrial deficiency and cardiac sudden death in mice lacking the MEF2A transcription factor. *Nat Med* 2002;**8**:1303–1309.

31. Kim Y, Phan D, Rooij E Van, Wang D-Z, McAnally J, Qi X, Richardson JA, Hill JA, Bassel-Duby R, Olson EN. The MEF2D transcription factor mediates stress-dependent cardiac remodeling in mice. *J Clin Invest* 2008;**118**:124–132.

32. Doevendans PA, Bilsen M Van. Transcription factors and the cardiac gene programme. *Int J Biochem Cell Biol* 1996;**28**:387–403.

33. Pon JR, Marra MA. MEF2 transcription factors: developmental regulators and emerging cancer genes. *Oncotarget* 2015;**7**.

34. Cox DM, Du M, Marback M, Yang ECC, Chan J, Siu KWM, McDermott JC. Phosphorylation motifs regulating the stability and function of myocyte enhancer factor 2A. *J Biol Chem* 2003;**278**:15297–15303.

35. Zhao M, New L, Kravchenko V V, Kato Y, Gram H, Padova F di, Olson EN, Ulevitch RJ, Han J. Regulation of the MEF2 family of transcription factors by p38. *Mol Cell Biol* 1999;**19**:21–30.

36. Yang CC, Ornatsky OI, McDermott JC, Cruz TF, Prody CA. Interaction of myocyte enhancer factor 2 (MEF2) with a mitogen-activated protein kinase, ERK5/BMK1. *Nucleic Acids Res* 1998;**26**:4771–4777.

37. Wang Y, Huang S, VP S. Cardiac muscle cell hypertrophy and apoptosis induced by distinct members of the p38 mitogen-activated protein kinase family. *J Biol Chem* 1998;**273**:2161–2168.

38. Kolodziejczyk SM, Wang L, Balazsi K, DeRepentigny Y, Kothary R, Megeney LA. MEF2 is upregulated during cardiac hypertrophy and is required for normal post-natal growth of the myocardium. *Curr Biol* 1999;**9**:1203–1206.

39. Kato Y. BMK1/ERK5 regulates serum-induced early gene expression through transcription factor MEF2C. *EMBO J* 1997;**16**:7054–7066.

40. Nicol RL, Frey N, Pearson G, Cobb M, Richardson J, Olson EN. Activated MEK5 induces serial assembly of sarcomeres and eccentric cardiac hypertrophy. *EMBO J* 2001;**20**:2757–2767.

41. Blaeser F, Ho N, Prywes R, Chatila TA. Ca2+-dependent Gene Expression Mediated by MEF2 Transcription Factors. *J Biol Chem* 2000;**275**:197–209.

42. McKinsey TA, Zhang C-L, Lu J, Olson EN. Signal-dependent nuclear export of a histone deacetylase regulates muscle differentiation. *Nature* Macmillian Magazines Ltd.; 2000;**408**:106–111.

43. Molkentin JD, Lu J-R, Antos CL, Markham B, Richardson J, Robbins J, Grant SR, Olson EN. A Calcineurin-Dependent Transcriptional Pathway for Cardiac Hypertrophy. *Cell* Elsevier; 2016;**93**:215–228.

44. Ramirez MT, Zhao XL, Schulman H, Brown JH. The nuclear deltaB isoform of Ca2+/calmodulin-dependent protein kinase II regulates atrial natriuretic factor gene expression in ventricular myocytes. *J Biol Chem* 1997;**272**:31203–31208.

45. Rosamond W, Flegal K, Furie K, Go A, Greenlund K, Haase N, Hailpern SM, Ho M, Howard V, Kissela B, Kittner S, Lloyd-Jones D, McDermott M, Meigs J, Moy C, Nichol G, O'Donnell C, Roger V, Sorlie P, Steinberger J, Thom T, Wilson M, Hong Y. Heart disease and stroke statistics-2008 Update: A report from the American heart association statistics committee and stroke statistics subcommittee. *Circulation* 2008;**117**.

46. Barry SP, Townsend PA. Chapter Three - What Causes a Broken Heart—Molecular Insights into Heart Failure. In: Biology KWJBT-IR of C and M, ed. Academic Press; 2010. p. 113–179.

47. Kehat I, Molkentin JD. Molecular pathways underlying cardiac remodeling during pathophysiologic stimulation. *Jorunal Amerian Hear Assoc Circ* 2011;**122**:2727–2735.

48. Frey N, Olson EN. Cardiac hypertrophy: the good, the bad, and the ugly. *Annu Rev Physiol* 2003;**65**:45–79.

49. Czubryt MP, Olson EN. Balancing contractility and energy production: the role of myocyte enhancer factor 2 (MEF2) in cardiac hypertrophy. *Recent Prog Horm Res* 2004;**59**:105–124.

50. Sadoshima J, Izumo S. THE CELLULAR AND MOLECULAR RESPONSE OF CARDIAC MYOCYTES TO MECHANICAL STRESS. *Annu Rev Physiol* Annual Reviews; 1997;**59**:551–571.

51. Calderone A, Takahashi N, Izzo Jr NJ, Thaik CM, Colucci WS. Pressure- and Volume-Induced Left Ventricular Hypertrophies Are Associated With Distinct Myocyte Phenotypes and Differential Induction of Peptide Growth Factor mRNAs. *Circulation* 1995;**92**:2385 LP-2390.

52. Frey N, Katus HA, Olson EN, Hill JA. Hypertrophy of the Heart. *Circulation* 2004;**109**:1580 LP-1589.

53. Lorell BH, Carabello BA. Left Ventricular Hypertrophy. *Circulation* 2000;**102**:470 LP-479.

54. Heineke J, Molkentin JD. Regulation of cardiac hypertrophy by intracellular signalling pathways. *Nat Rev Mol Cell Biol* Nature Publishing Group; 2006;**7**:589–600.

55. Lips DJ, deWindt LJ, Kraaij DJW van, Doevendans PA. Molecular determinants of myocardial hypertrophy and failure: alternative pathways for beneficial and maladaptive hypertrophy. *Eur Heart J* 2003;**24**:883 LP-896.

56. Bristow MR. beta-adrenergic receptor blockade in chronic heart failure. *Circulation* 2000;**101**:558–569.

57. Antos CL, Frey N, Marx SO, Reiken S, Gaburjakova M, Richardson JA, Marks AR, Olson EN. Dilated cardiomyopathy and sudden death resulting from constitutive activation of protein kinase a. *Circ Res* 2001;**89**:997–1004.

58. Wilkins BJ, Molkentin JD. Calcium–calcineurin signaling in the regulation of cardiac hypertrophy. *Biochem Biophys Res Commun* 2004;**322**:1178–1191.

59. Wilkins BJ, Dai Y-S, Bueno OF, Parsons SA, Xu J, Plank DM, Jones F, Kimball TR, Molkentin JD. Calcineurin/NFAT Coupling Participates in Pathological, but not Physiological, Cardiac Hypertrophy. *Circ Res* 2004;**94**:110 LP-118.

60. McKinsey T a. Derepression of pathological cardiac genes by members of the CaM kinase superfamily. *Cardiovasc Res* 2007;**73**:667–677.

61. Backs J, Backs T, Neef S, Kreusser MM, Lehmann LH, Patrick DM, Grueter CE, Qi X, Richardson JA, Hill JA, Katus HA, Bassel-Duby R, Maier LS, Olson EN. The delta isoform of CaM kinase II is required for pathological cardiac hypertrophy and remodeling after pressure overload. *Proc Natl Acad Sci U S A* 2009;**106**:2342–2347.

62. Bueno OF, Windt LJ De, Tymitz KM, Witt S a, Kimball TR, Klevitsky R, Hewett TE, Jones SP, Lefer DJ, Peng CF, Kitsis RN, Molkentin JD. The MEK1-ERK1/2 signaling pathway promotes compensated cardiac hypertrophy in transgenic mice. *EMBO J* 2000;**19**:6341–6350.

63. Nishida K, Yamaguchi O, Hirotani S, Hikoso S, Higuchi Y, Watanabe T, Takeda T, Osuka S, Morita T, Kondoh G, Uno Y, Kashiwase K, Taniike M, Nakai A, Matsumura Y, Miyazaki J, Sudo T, Hongo K, Kusakari Y, Kurihara S, Chien KR, Takeda J, Hori M, Otsu K, Kazuhiko Nishida, Osamu Yamaguchi, Shinichi Hirotani, Shungo Hikoso, Yoshiharu Higuchi, Tetsuya Watanabe, Toshihiro Takeda, Soh Osuka, Takashi Morita, Gen Kondoh, Yoshihiro Uno, Kazunori Kashiwase, Masayuki Taniike, Atsuko Nakai, Yasushi Matsumura, Jun-ic KO. p38α Mitogen-Activated Protein Kinase Plays a Critical Role in Cardiomyocyte Survival but Not in Cardiac Hypertrophic Growth in Response to Pressure Overload. *Mol Cell Biol* 2004;**24**:10611–10620.

64. Zhang S, Weinheimer C, Courtois M, Kovacs A, Zhang CE, Cheng AM, Wang Y, Muslin AJ. The role of the Grb2 – p38 MAPK signaling pathway in cardiac hypertrophy and fibrosis. 2003;**111**:833–841.

65. Erwig L-P, Henson PM. Clearance of apoptotic cells by phagocytes. *Cell Death Differ* Nature Publishing Group; 2007;**15**:243–250

66. Mughal W, Kirshenbaum LA. Cell death signalling mechanisms in heart failure. *Exp Clin Cardiol* 2011;**16**:102–108.

67. Olivetti G, Abbi R, Quaini F, Kajstura J, Cheng W, Nitahara JA, Quaini E, Loreto C Di, Beltrami CA, Krajewski S, Reed JC, Anversa P. Apoptosis in the Failing Human Heart. *N Engl J Med* Massachusetts Medical Society; 1997;**336**:1131–1141.

68. Regula KM, Kirshenbaum LA. Apoptosis of ventricular myocytes: a means to an end. *J Mol Cell Cardiol* Elsevier; 2016;**38**:3–13.

69. Berghe T Vanden, Vanlangenakker N, Parthoens E, Deckers W, Devos M, Festjens N, Guerin CJ, Brunk UT, Declercq W, Vandenabeele P, Berghe T Vanden, Vanlangenakker N, Parthoens E, Deckers W, Devos M, Festjens N, Guerin CJ, Brunk UT, Declercq W, Vandenabeele P. Necroptosis, necrosis and secondary necrosis converge on similar cellular disintegration features. *Cell Death Differ* Nature Publishing Group; 2010;**17**:922–930.

70. Chautan M, Chazal G, Cecconi F, Gruss P, Golstein P. Interdigital cell death can occur through a necrotic and caspase-independent pathway. *Curr Biol* Elsevier; 2016;**9**:967–970.

71. Fliss H, Gattinger D. Apoptosis in Ischemic and Reperfused Rat Myocardium. *Circ Res* 1996;**79**:949 LP-956.

72. Saraste A, Pulkki K, Kallajoki M, Henriksen K, Parvinen M, Voipio-Pulkki L-M. Apoptosis in Human Acute Myocardial Infarction. *Circulation* 1997;**95**:320 LP-323.

73. Narula J, Haider N, Virmani R, DiSalvo TG, Kolodgie FD, Hajjar RJ, Schmidt U, Semigran MJ, Dec GW, Khaw B-A. Apoptosis in Myocytes in End-Stage Heart Failure. *N Engl J Med* Massachusetts Medical Society; 1996;**335**:1182–1189.

74. Condorelli G, Morisco C, Stassi G, Notte A, Farina F, Sgaramella G, Rienzo A de, Roncarati R, Trimarco B, Lembo G. <div xmlns="http://www.w3.org/1999/xhtml">Increased Cardiomyocyte Apoptosis and Changes in Proapoptotic and Antiapoptotic Genes bax and bcl-2 During Left Ventricular Adaptations to Chronic Pressure. *Circulation* 1999;**99**:3071 LP-3078.

75. Ikeda S, Hamada M, Qu P, Hiasa G, Hashida H, Shigematsu Y, Hiwada K. Relationship between cardiomyocyte cell death and cardiac function during hypertensive cardiac remodelling in Dahl rats. *Clin Sci* 2002;**102**:329–335.

76. Fulda S, Debatin K-M. Extrinsic versus intrinsic apoptosis pathways in anticancer chemotherapy. *Oncogene* 2006;**25**:4798–4811.

77. Krijnen PAJ, Nijmeijer R, Meijer CJLM, Visser CA, Hack CE, Niessen HWM. Apoptosis in myocardial ischaemia and infarction. *J Clin Pathol* 2002;**55**:801–811.

78. Degterev A, Boyce M, Yuan J. A decade of caspases. *Oncogene* 2003;**22**:8543–8567.

79. Petronilli V, Penzo D, Scorrano L, Bernardi P, Lisa F Di. The mitochondrial permeability transition, release of cytochrome c and cell death. Correlation with the duration of pore openings in situ. *J Biol Chem* 2001;**276**:12030–12034.

80. Baines CP, Molkentin JD. STRESS signaling pathways that modulate cardiac myocyte apoptosis. *J Mol Cell Cardiol* Elsevier; 2016;**38**:47–62.

81. Mani K. Programmed cell death in cardiac myocytes: Strategies to maximize post-ischemic salvage. *Heart Fail Rev* 2008;**13**:193–209.

82. Kirshenbaum LA, Moissac D de. Gene Product Prevents Programmed Cell Death of Ventricular Myocytes</div> *Circulation* 1997;**96**:1580 LP-1585.

83. Gustafsson ÅB, Gottlieb RA. Bcl-2 family members and apoptosis, taken to heart. *Am J Physiol - Cell Physiol* 2007;**292**:C45 LP-C51.

84. Dhillon AS, Hagan S, Rath O, Kolch W. MAP kinase signalling pathways in cancer. *Oncogene* 2007;**26**:3279–3290.

85. Andreka P, Zang J, Dougherty C, Slepak TI, Webster KA, Bishopric NH. Cytoprotection by Jun Kinase During Nitric Oxide–Induced Cardiac Myocyte Apoptosis. *Circ Res* 2001;**88**:305 LP-312.

86. Hreniuk D, Garay M, Gaarde W, Monia BP, McKay RA, Cioffi CL. Inhibition of C-Jun N-Terminal Kinase 1, but Not c-Jun N-Terminal Kinase 2, Suppresses Apoptosis Induced by Ischemia/Reoxygenation in Rat Cardiac Myocytes. *Mol Pharmacol* 2001;**59**:867 LP-874.

87. Rose BA, Force T, Wang Y. NIH Public Access. 2013;**90**.

88. Párrizas M, Saltiel a R, LeRoith D. Insulin-like growth factor 1 inhibits apoptosis using the phosphatidylinositol 3'-kinase and mitogen-activated protein kinase pathways. *J Biol Chem* 1997;**272**:154–161.

89. Jiang Z-S, Srisakuldee W, Soulet F, Bouche G, Kardami E. Non-angiogenic FGF-2 protects the ischemic heart from injury, in the presence or absence of reperfusion. *Cardiovasc Res* 2004;**62**:154 LP-166.

90. Shizukuda Y, Buttrick PM. Subtype Specific Roles of β-Adrenergic Receptors in Apoptosis of Adult Rat Ventricular Myocytes. *J Mol Cell Cardiol* Elsevier; 2016;**34**:823–831.

91. Aries A, Paradis P, Lefebvre C, Schwartz RJ, Nemer M. Essential role of GATA-4 in cell survival and drug-induced cardiotoxicity. *Proc Natl Acad Sci United States Am* 2004;**101**:6975–6980.

92. Communal C, Colucci WS, Singh K. p38 mitogen-activated protein kinase pathway protects adult rat ventricular myocytes against beta -adrenergic receptor-stimulated apoptosis. Evidence for Gi-dependent activation. *J Biol Chem* 2000;**275**:19395–19400.

93. Schneider S, Chen W, Hou J, Steenbergen C, Murphy E. Inhibition of p38 MAPK α/β reduces ischemic injury and does not block protective effects of preconditioning. *Am J Physiol - Hear Circ Physiol* 2001;**280**:H499 LP-H508.

94. Galluzzi L, Kroemer G. Necroptosis: A Specialized Pathway of Programmed Necrosis. *Cell* 2008;**135**:1161–1163.

95. Hitomi J, Christofferson DE, Ng A, Yao J, Degterev A, Xavier RJ, Yuan J. Identification of a Molecular Signaling Network that Regulates a Cellular Necrotic Cell Death Pathway. *Cell* Elsevier Ltd; 2008;**135**:1311–1323.

96. Lin Q, Lu JR, Yanagisawa H, Webb R, Lyons GE, Richardson JA, Olson EN. Requirement of the MADS-box transcription factor MEF2C for vascular development. *Development* 1998;**125**:4565–4574.

97. Feng S, Yang Y, Mei Y, Ma L, Zhu D e., Hoti N, Castanares M, Wu M. Cleavage of RIP3 inactivates its caspase-independent apoptosis pathway by removal of kinase domain. *Cell Signal* 2007;**19**:2056–2067.

98. Cho Y, Challa S, Moquin D, Genga R, Ray TD, Guildford M, Chan FKM. Phosphorylation-Driven Assembly of the RIP1-RIP3 Complex Regulates Programmed Necrosis and Virus-Induced Inflammation. *Cell* Elsevier Inc.; 2009;**137**:1112–1123.

99. Wang H, Sun L, Su L, Rizo J, Liu L, Wang L-F, Wang F-S, Wang X. Mixed Lineage Kinase Domain-like Protein MLKL Causes Necrotic Membrane Disruption upon Phosphorylation by RIP3. *Mol Cell* Elsevier; 2016;**54**:133–146.

100. Degterev A, Huang Z, Boyce M, Li Y, Jagtap P, Mizushima N, Cuny GD, Mitchison TJ, Moskowitz MA, Yuan J. Chemical inhibitor of nonapoptotic cell death with therapeutic potential for ischemic brain injury. *Nat Chem Biol* Nature Publishing Group; 2005;**1**:112–119.

101. Cho Y, Challa S, Moquin D, Genga R, Ray TD, Guildford M, Chan FKM. Phosphorylation-Driven Assembly of the RIP1-RIP3 Complex Regulates Programmed Necrosis and Virus-Induced Inflammation. *Cell* Elsevier Inc.; 2009;**137**:1112–1123.

102. Lymperopoulos A, Rengo G, Koch WJ. Adrenal adrenoceptors in heart failure: fine-tuning cardiac stimulation. *Trends Mol Med* 2007;**13**:503–511.

103. Siryk-Bathgate A, Dabul S, Lymperopoulos A. Current and future G protein-coupled receptor signaling targets for heart failure therapy. *Drug Des Devel Ther* 2013;**7**:1209–1222.

104. Brodde O-E, Bruck H, Leineweber K. Cardiac Adrenoceptors: Physiological and Pathophysiological Relevance. *J Pharmacol Sci* 2006;**100**:323–337.

105. Brodde OE, Michel MC. Adrenergic and muscarinic receptors in the human heart. *Pharmacol Rev* 1999;**51**:651–690.

106. Brum PC, Rolim NPL, Bacurau AVN, Medeiros A. Neurohumoral activation in heart failure: The role of adrenergic receptors. *An Acad Bras Cienc* 2006;**78**:485–503.

107. Devic E, Xiang Y, Gould D, Kobilka B. Beta-adrenergic receptor subtype-specific signaling in cardiac myocytes from beta(1) and beta(2) adrenoceptor knockout mice. *Mol Pharmacol* 2001;**60**:577–583.

108. Xiao R-P, Zhu W, Zheng M, Cao C, Zhang Y, Lakatta EG, Han Q. Subtype-specific α$_1$- and β-adrenoceptor signaling in the heart. *Trends Pharmacol Sci* Elsevier; 2016;**27**:330–337.

109. Xiao R-P. β-Adrenergic Signaling in the Heart: Dual Coupling of the β2-Adrenergic Receptor to G(s) and G(i) proteins; *Sci STKE* 2001;**2001**:re15 LP-re15.

110. A decade of discoveries in cardiac biology Year. 2004;**10**:467–474.

111. Kamp TJ, Hell JW. Regulation of Cardiac L-Type Calcium Channels by Protein Kinase A and Protein Kinase C. *Circ Res* 2000;**87**:1095 LP-1102.

112. Hulme JT, Westenbroek RE, Scheuer T, Catterall WA. Phosphorylation of serine 1928 in the distal C-terminal domain of cardiac CaV1.2 channels during β1-adrenergic regulation. *Proc Natl Acad Sci* 2006;**103**:16574–16579.

113. Zhou P, Zhao YT, Guo YB, Xu SM, Bai SH, Lakatta EG, Cheng H, Hao XM, Wang SQ. Beta-adrenergic signaling accelerates and synchronizes cardiac ryanodine receptor response to a single L-type Ca2+ channel. *Proc Natl Acad Sci U S A* 2009;**106**:18028–18033.

114. Lohse MJ. What Is the Role of -Adrenergic Signaling in Heart Failure? *Circ Res* 2003;**93**:896–906.

115. Zaugg M, Xu W, Lucchinetti E, Shafiq S a., Jamali NZ, Siddiqui M a. Q. β-Adrenergic Receptor Subtypes Differentially Affect Apoptosis in Adult Rat Ventricular Myocytes. *Circulation* 2000;**102**:344–350.

116. Zhu W, Wang S, Chakir K, Yang D, Zhang T, Brown JH, Devic E, Kobilka BK, Cheng H, Xiao R-P. Linkage of β1-adrenergic stimulation to apoptotic heart cell death through protein kinase A – independent activation of Ca 2 + / calmodulin kinase II. *J Clin …* 2003;**111**:617–625.

117. Zhang X, Szeto C, Gao E, Tang M, Jin J, Fu Q, Makarewich C, Ai X, Li Y, Tang a., Wang J, Gao H, Wang F, Ge XJ, Kunapuli SP, Zhou L, Zeng C, Xiang KY, Chen X. Cardiotoxic and Cardioprotective Features of Chronic -Adrenergic Signaling. *Circ Res* 2013;**112**:498–509.

118. Black JW, Duncan W a. M, Shanks RG. Comparison of Some Properties of Pronethalol and Propanolol. *Surv Anesthesiol* 1966;**10**:423.

119. Black JW, Stephenson JS. PHARMACOLOGY OF A NEW ADRENERGIC BETA-RECEPTOR-BLOCKING COMPOUND (NETHALIDE). *Lancet* 1962;**280**:311–314.

120. Messerli FH, Bangalore S, Yao SS, Steinberg JS. Cardioprotection with beta-blockers: Myths, facts and Pascal's wager. *J Intern Med* 2009;**266**:232–241.

121. Bangalore S, Messerli FH, Kostis JB, Pepine CJ. Cardiovascular protection using beta-blockers: a critical review of the evidence. *J Am Coll Cardiol* 2007;**50**:563–572.

122. Smith C, Teitler M. Beta-Blocker Selectivity at Cloned Human Beta 1 - and Beta 2 -Adrenergic Receptors. *Cardiovasc Drugs Ther* 1999;**13**:123–126.

123. Landesberg G, Beattie WS, Mosseri M, Jaffe AS, Alpert JS. Perioperative myocardial infarction. *Circulation* 2009;**119**:2936–2944.

124. Antman EM, Hand M, Armstrong PW, Bates ER, Green LA, Halasyamani LK, Hochman JS, Krumholz HM, Lamas GA, Mullany CJ, Pearle DL, Sloan MA, Smith SC, Antman EM, Anbe DT, Armstrong PW, Bates ER, Green LA, Hand M, Hochman JS, Krumholz HM, Kushner FG, Lamas GA, Mullany CJ, Ornato JP, Pearle DL, Sloan MA, Smith SC, Smith SC, Jacobs AK, et al. 2007 Focused Update of the ACC/AHA 2004 Guidelines for the Management of Patients With ST-Elevation Myocardial Infarction. *Circulation* 2008;**117**:296 LP-329.

125. Beattie WS, Wijeysundera DN, Karkouti K, McCluskey S, Tait G. Does tight heart rate control improve beta-blocker efficacy? An updated analysis of the noncardiac surgical randomized trials. *Anesth Analg* 2008;**106**:1039–1048.

126. Randomised trial of intravenous streptokinase, oral aspirin, both, or neither among 17,187 cases of suspected acute myocardial infarction: ISIS-2. ISIS-2 (Second International Study of Infarct Survival) Collaborative Group. *Lancet (London, England)* 1988;**2**:349–360.

127. Dorn GW, Molkentin JD. Manipulating cardiac contractility in heart failure - Data from mice and men. *Circulation* 2004;**109**:150–158.

128. Iwai-Kanai E, Hasegawa K, Araki M, Kakita T, Morimoto T, Sasayama S. Alpha- and Beta-Adrenergic Pathways Differentially Regulate Cell Type-Specific Apoptosis in Rat Cardiac Myocytes. *Circulation* 1999;**100**:305–311.

129. Krijnen P a J, Nijmeijer R, Meijer CJLM, Visser C a, Hack CE, Niessen HWM. Apoptosis in myocardial ischaemia and infarction. *J Clin Pathol* 2002;**55**:801–811.

130. DeGeorge BR, Koch WJ. Beta blocker specificity: a building block toward personalized medicine. *J Clin Invest* 2007;**117**:86–89.

131. Zhang X, Szeto C, Gao E, Tang M, Jin J, Fu Q, Makarewich C, Ai X, Li Y, Tang A, Wang J, Gao H, Wang F, Ge XJ, Kunapuli SP, Zhou L, Zeng C, Xiang KY, Chen X. Cardiotoxic and Cardioprotective Features of Chronic beta-Adrenergic Signaling. *Circ Res* 2013;**112**:498–+.

132. Aronow WS. Current role of beta-blockers in the treatment of hypertension. *Expert Opin Pharmacother* 2010;**11**:2599–2607.

133. Zhang H, Xu Q, Krajewski S, Krajewska M, Xie Z, Fuess S, Kitada S, Pawlowski K, Godzik a, Reed JC. BAR: An apoptosis regulator at the intersection of caspases and Bcl-2 family proteins. *Proc Natl Acad Sci U S A* 2000;**97**:2597–2602.

134. Du M, Perry RLS, Nowacki NB, Gordon JW, Salma J, Zhao J, Aziz A, Chan J, Siu KWM, McDermott JC. Protein kinase A represses skeletal myogenesis by targeting myocyte enhancer factor 2D. *Mol Cell Biol* 2008;**28**:2952–2970.

135. Black BL, Olson EN. Transcriptional control of muscle development by myocyte enhancer factor-2 (MEF2) proteins. *Annu Rev Cell Dev Biol* 1998;**14**:167–196.

136. Dodou E, Verzi MP, Anderson JP, Xu S-M, Black BL. Mef2c is a direct transcriptional target of ISL1 and GATA factors in the anterior heart field during mouse embryonic development. *Development* 2004;**131**:3931–3942.

137. Xu J, Gong NL, Bondi I, Aronow BJ, Backx PH, Molkentin JD. Myocyte enhancer factors 2A and 2C induce dilated cardiomyopathy in transgenic mice. *J Biol Chem* 2006;**281**:9152–9162.

138. Papait R, Kunderfranco P, Stirparo GG, Latronico MVG, Condorelli G. Long noncoding RNA: A new player of heart failure? *J Cardiovasc Transl Res* 2013;**6**:876–883.

139. Potthoff MJ, Olson EN. MEF2: a central regulator of diverse developmental programs. *Development* 2007;**134**:4131–4140.

140. Kim Y, Phan D, Rooij E van, Wang D-Z, McAnally J, Qi X, Richardson JA, Hill JA, Bassel-Duby R, Olson EN. The MEF2D transcription factor mediates stress-dependent cardiac remodeling in mice. *J Clin Invest* 2008;**118**:124–132.

141. Mao ZX, Wiedmann M. Calcineurin enhances MEF2 DNA binding activity in calcium-dependent survival of cerebellar granule neurons. *J Biol Chem* 1999;**274**:31102–31107.

142. Ewen EP, Snyder CM, Wilson M, Desjardins D, Naya FJ. The Mef2A transcription factor coordinately regulates a costamere gene program in cardiac muscle. *J Biol Chem* 2011;**286**:29644–29653.

143. Wales S, Hashemi S, Blais A, McDermott JC. Global MEF2 target gene analysis in cardiac and skeletal muscle reveals novel regulation of DUSP6 by p38MAPK-MEF2 signaling. *Nucleic Acids Res* 2014;**42**:11349–11362.

144. Boyle EI, Weng SA, Gollub J, Jin H, Botstein D, Cherry JM, Sherlock G. GO::TermFinder - open source software for accessing Gene Ontology information and finding significantly enriched Gene Ontology terms associated with a list of genes. *Bioinformatics* 2004;**20**:3710–3715.

145. Mostafavi S, Ray D, Warde-Farley D, Grouios C, Morris Q. GeneMANIA: a real-time multiple association network integration algorithm for predicting gene function. *Genome Biol* 2008;**9 Suppl 1**:S4.

146. Miled C, Pontoglio M, Garbay S, Yaniv M, Weitzman JB. A genomic map of p53 binding sites identifies novel p53 targets involved in an apoptotic network. *Cancer Res* 2005;**65**:5096–5104.

147. Diwan A, Krenz M, Syed FM, Wansapura J, Ren X, Koesters AG, Li H, Kirshenbaum LA, Hahn HS, Robbins J, Jones WK, Dorn II GW. Inhibition of ischemic cardiomyocyte apoptosis through targeted ablation of Bnip3 restrains postinfarction remodeling in mice. *J Clin Invest* 2007;**117**:2825–2833.

148. Dorn II GW, Kirshenbaum LA. Cardiac reanimation: targeting cardiomyocyte death by BNIP3 and NIX/BNIP3L. *Oncogene* 2008;**27**:S158–S167.

149. Allen NPC, Donninger H, Vos MD, Eckfeld K, Hesson L, Gordon L, Birrer MJ, Latif F, Clark GJ. RASSF6 is a novel member of the RASSF family of tumor suppressors. *Oncogene* 2007;**26**:6203–6211.

150. Kim M-Y, Seo EJ, Lee DH, Kim EJ, Kim HS, Cho H-Y, Chung EY, Lee SH, Baik EJ, Moon C-H, Jung Y-S. Gadd45 beta is a novel mediator of cardiomyocyte apoptosis induced by ischaemia/hypoxia. *Cardiovasc Res* 2010;**87**:119–126.

151. Naya FJ, Wu CZ, Richardson JA, Overbeek P, Olson EN. Transcriptional activity of MEF2 during mouse embryogenesis monitored with a MEF2-dependent transgene. *Development* 1999;**126**:2045–2052.

152. Angelis L De, Zhao J, Andreucci JJ, Olson EN, Cossu G, McDermott JC. Regulation of vertebrate myotome development by the p38 MAP kinase-MEF2 signaling pathway. *Dev Biol* 2005;**283**:171–179.

153. Dionyssiou MG, Nowacki NB, Hashemi S, Zhao J, Kerr a., Tsushima RG, McDermott JC. Cross-talk between glycogen synthase kinase 3β (GSK3β) and p38MAPK regulates myocyte enhancer factor 2 (MEF2) activity in skeletal and cardiac muscle. *J Mol Cell Cardiol* Elsevier Ltd; 2013;**54**:35–44.

154. McBride K, Nemer M. Regulation of the ANF and BNP promoters by GATA factors: Lessons learned for cardiac transcription. *Can J Physiol Pharmacol* 2001;**79**:673–681.

155. Wittstein IS, Thiemann DR, Lima J a C, Baughman KL, Schulman SP, Gerstenblith G, Wu KC, Rade JJ, Bivalacqua TJ, Champion HC. Neurohumoral features of myocardial stunning due to sudden emotional stress. *N Engl J Med* 2005;**352**:539–548.

156. Reiken S, Gaburjakova M, Guatimosim S, Gomez AM, D'Armiento J, Burkhoff D, Wang J, Vassort G, Lederer WJ, Marks AR. Protein kinase A phosphorylation of the cardiac calcium release channel (ryanodine receptor) in normal and failing hearts - Role of phosphatases and response to isoproterenol. *J Biol Chem* 2003;**278**:444–453.

157. Teerlink JR, Pfeffer JM, Pfeffer MA. Progressive Ventricular Remodeling in Response to Diffuse Isoproterenol-Induced Myocardial Necrosis in Rats. *Circ Res* 1994;**75**:105–113.

158. Shizukuda Y, Buttrick PM, Geenen DL, Borczuk AC, Kitsis RN, Sonnenblick EH. beta-Adrenergic stimulation causes cardiocyte apoptosis: influence of tachycardia and hypertrophy. *Am J Physiol Circ Physiol* 1998;**275**:H961–H968.

159. Marx SO, Reiken S, Hisamatsu Y, Jayaraman T, Burkhoff D, Rosemblit N, Marks AR. PKA phosphorylation dissociates FKBP12.6 from the calcium release channel (ryanodine receptor): defective regulation in failing hearts. *Cell* 2000;**101**:365–376.

160. Yu B, Song B. Notch 1 Signalling Inhibits Cardiomyocyte Apoptosis in ischaemic Postconditioning. *Hear Lung Circ* 2014;**23**:152–158.

161. Li Y, Hiroi Y, Liao JK. Notch Signaling as an Important Mediator of Cardiac Repair and Regeneration After Myocardial Infarction. *Trends Cardiovasc Med* 2010;**20**:228–231.

162. Chatila K, Ren G, Xia Y, Huebener P, Bujak M, Frangogiannis NG. The role of the thrombospondins in healing myocardial infarcts. *Cardiovasc Hematol Agents Med Chem* 2007;**5**:21–27.

163. Xia Y, Dobaczewski M, Gonzalez-Quesada C, Chen W, Biernacka A, Li N, Lee D-W, Frangogiannis NG. Endogenous Thrombospondin 1 Protects the Pressure-Overloaded Myocardium by Modulating Fibroblast Phenotype and Matrix Metabolism. *Hypertension* 2011;**58**:902–911.

164. Massion PB, Dessy C, Desjardins F, Pelat M, Havaux X, Belge C, Moulin P, Guiot Y, Feron O, Janssens S, Balligand JL. Cardiomyocyte-restricted overexpression of endothelial nitric oxide synthase (NOS3) attenuates beta-adrenergic stimulation and reinforces vagal inhibition of cardiac contraction. *Circulation* 2004;**110**:2666–2672.

165. Bristow MR. Beta-Adrenergic Receptor Blockade in Chronic Heart Failure. *Circulation* 2000;**101**:558–569.

166. Lyons GE, Micales BK, Schwarz J, Martin JF, Olson EN. Expression of Mef2 Genes in the Mouse Central-Nervous-System Suggests a Role in Neuronal Maturation. *J Neurosci* 1995;**15**:5727–5738.

167. Im S-S, Kwon S-K, Kim T-H, Kim H-I, Ahn Y-H. Regulation of glucose transporter type 4 isoform gene expression in muscle and adipocytes. *IUBMB Life* 2007;**59**:134–145.

168. Weems J, Olson AL. Class II Histone Deacetylases Limit GLUT4 Gene Expression during Adipocyte Differentiation. *J Biol Chem* 2011;**286**:460–468.

169. Stephens AS, Stephens SR, Hobbs C, Hutmacher DW, Bacic-Welsh D, Woodruff MA, Morrison NA. Myocyte Enhancer Factor 2C, an Osteoblast Transcription Factor Identified by Dimethyl Sulfoxide (DMSO)-enhanced Mineralization. *J Biol Chem* 2011;**286**:30071–30086.

170. Han JH, Molkentin JD. Regulation of MEF2 by p38 MAPK and its implication in cardiomyocyte biology. *Trends Cardiovasc Med* 2000;**10**:19–22.

171. Lazaro JB, Bailey PJ, Lassar AB. Cyclin D-cdk4 activity modulates the subnuclear localization and interaction of MEF2 with SRC-family coactivators during skeletal muscle differentiation. *Genes Dev* 2002;**16**:1792–1805.

172. McKinsey TA, Olson EN. Toward transcriptional therapies for the failing heart: chemical screens to modulate genes. *J Clin Invest* 2005;**115**:538–546.

173. Konno T, Chen D, Wang L, Wakimoto H, Teekakirikul P, Nayor M, Kawana M, Eminaga S, Gorham JM, Pandya K, Smithies O, Naya FJ, Olson EN, Seidman JG, Seidman CE. Heterogeneous myocyte enhancer factor-2 (Mef2) activation in myocytes predicts focal scarring in hypertrophic cardiomyopathy. *Proc Natl Acad Sci U S A* 2010;**107**:18097–18102.

174. Chiong M, Wang Z V, Pedrozo Z, Cao DJ, Troncoso R, Ibacache M, Criollo a, Nemchenko a, Hill J a, Lavandero S. Cardiomyocyte death: mechanisms and translational implications. *Cell Death Dis* Nature Publishing Group; 2011;**2**:e244.

175. Dirkx E, Costa Martins PA da, Windt LJ De. Regulation of fetal gene expression in heart failure. *Biochim Biophys Acta* 2013;**1832**:2414–2424.

176. Antos CL, Frey N, Marx SO, Reiken S, Gaburjakova M, Richardson J a, Marks a R, Olson EN. Dilated cardiomyopathy and sudden death resulting from constitutive activation of protein kinase A. *Circ Res* 2001;**89**:997–1004.

177. Carr AN, Schmidt AG, Suzuki Y, Monte F del, Sato Y, Lanner C, Breeden K, Jing S-L, Allen PB, Greengard P, Yatani A, Hoit BD, Grupp IL, Hajjar RJ, DePaoli-Roach AA, Kranias EG. Type 1 phosphatase, a negative regulator of cardiac function. *Mol Cell Biol* 2002;**22**:4124–4135.

178. Small KM, McGraw DW, Liggett SB. Pharmacology and physiology of human adrenergic receptor polymorphisms. *Annu Rev Pharmacol Toxicol* 2003;**43**:381–411.

179. Spindler M, Engelhardt S, Niebler R, Wagner H, Hein L, Lohse MJ, Neubauer S. Alterations in the myocardial creatine kinase system precede the development of contractile dysfunction in beta(1)-adrenergic receptor transgenic mice. *J Mol Cell Cardiol* 2003;**35**:389–397.

180. Wagoner LE, Craft LL, Singh B, Suresh DP, Zengel PW, McGuire N, Abraham WT, Chenier TC, Dorn GW, Liggett SB. Polymorphisms of the beta(2)-adrenergic receptor determine exercise capacity in patients with heart failure. *Circ Res* 2000;**86**:834–840.

181. Prichard BNC. p ADRENOCEPTORS IN COMMON CARDIAC DISORDERS. 1971;

182. Papait R, Cattaneo P, Kunderfranco P, Greco C, Carullo P, Guffanti A, Vigano V, Stirparo GG, Latronico MVG, Hasenfuss G, Chen J, Condorelli G. Genome-wide analysis of histone marks identifying an epigenetic signature of promoters and enhancers underlying cardiac hypertrophy. *Proc Natl Acad Sci U S A* 2013;**110**:20164–20169.

183. Kim Y, Phan D, Rooij E van, Wang D-Z, McAnally J, Qi X, Richardson J a, Hill J a, Bassel-Duby R, Olson EN. The MEF2D transcription factor mediates stress-dependent cardiac remodeling in mice. *J Clin Invest* 2008;**118**:124–132.

184. Ornatsky OI, Cox DM, Tangirala P, Andreucci JJ, Quinn ZA, Wrana JL, Prywes R, Yu Y-T, McDermott JC. Post-translational control of the {MEF2A} transcriptional regulatory protein. *Nucleic Acids Res* 1999;**27**:2646–2654.

185. Kato Y. BMK1/ERK5 regulates serum-induced early gene expression through transcription factor MEF2C. *EMBO J* 1997;**16**:7054–7066.

186. Backs J, Worst BC, Lehmann LH, Patrick DM, Jebessa Z, Kreusser MM, Sun Q, Chen L, Heft C, Katus HA, Olson EN. Selective repression of MEF2 activity by PKA-dependent proteolysis of HDAC4. *J Cell Biol* 2011;**195**:403–415.

187. Wang X, Tang X, Li M, Marshall J, Mao Z. Regulation of neuroprotective activity of myocyte-enhancer factor 2 by cAMP-protein kinase A signaling pathway in neuronal survival. *J Biol Chem* 2005;**280**:16705–16713.

188. Vanderlaan RD, Hardy WR, Kabir MG, Pasculescu A, Jones N, deTombe PP, Backx PH, Pawson T. The ShcA phosphotyrosine docking protein uses distinct mechanisms to regulate myocyte and global heart function. *Circ Res* 2011;**108**:184–193.

189. Matkovich SJ, Edwards JR, Grossenheider TC, Guzman Strong C de, Dorn GW. Epigenetic coordination of embryonic heart transcription by dynamically regulated long noncoding RNAs. *Proc Natl Acad Sci U S A* 2014;**111**:12264–12269.

190. Robinson MD, McCarthy DJ, Smyth GK. edgeR: a Bioconductor package for differential expression analysis of digital gene expression data. *Bioinformatics* 2010;**26**:139–140.

191. Hu P, Zhang D, Swenson L, Chakrabarti G, Abel ED, Litwin SE. Minimally invasive aortic banding in mice: effects of altered cardiomyocyte insulin signaling during pressure overload. *Am J Physiol Heart Circ Physiol* 2003;**285**:H1261–H1269.

192. Pacca SRMC, Azevedo AP de, Oliveira CF De, Luca IMS De, Nucci G De, Antunes E. Attenuation of hypertension, cardiomyocyte hypertrophy, and myocardial fibrosis by beta-adrenoceptor blockers in rats under long-term blockade of nitric oxide synthesis. *J Cardiovasc Pharmacol* 2002;**39**:201–207.

193. Aronow WS. Current role of beta-blockers in the treatment of hypertension. *Expert Opin Pharmacother* 2010;**11**:2599–2607.

194. Dadson K, Turdi S, Hashemi S, Zhao J, Polidovitch N, Beca S, Backx PH, McDermott JC, Sweeney G. Adiponectin is required for cardiac MEF2 activation during pressure overload induced hypertrophy. *J Mol Cell Cardiol* Elsevier Ltd; 2015;**86**:102–109.

195. Dadson K, Turdi S, Boo S, Hinz B, Sweeney G. Temporal and Molecular Analyses of Cardiac Extracellular Matrix Remodeling following Pressure Overload in Adiponectin Deficient Mice. *PLoS One* 2015;**10**:e0121049.

196. Son GH, Park SH, Kim Y, Kim JY, Kim JW, Chung S, Kim Y-H, Kim H, Hwang J-J, Seo J-S. Postmortem mRNA expression patterns in left ventricular myocardial tissues and their implications for forensic diagnosis of sudden cardiac death. *Mol Cells* 2014;**37**:241–247.

197. Micheli L, Leonardi L, Conti F, Maresca G, Colazingari S, Mattei E, Lira SA, Farioli-Vecchioli S, Caruso M, Tirone F. PC4/Tis7/IFRD1 Stimulates Skeletal Muscle Regeneration and Is Involved in Myoblast Differentiation as a Regulator of MyoD and NF-κB. *J Biol Chem* 2011;**286**:5691–5707.

198. Tyagi SC, Kumar SG, Haas SJ, Reddy HK, Voelker DJ, Hayden MR, Demmy TL, Schmaltz RA, Curtis JJ. Post-transcriptional regulation of extracellular matrix metalloproteinase in human heart end-stage failure secondary to ischemic cardiomyopathy. *J Mol Cell Cardiol* 1996;**28**:1415–1428.

199. Boixel C, Fontaine V, Rücker-Martin C, Milliez P, Louedec L, Michel JB, Jacob MP, Hatem SN. Fibrosis of the left atria during progression of heart failure is associated with increased matrix metalloproteinases in the rat. *J Am Coll Cardiol* 2003;**42**:336–344.

200. Wei Y, Cui C, Lainscak M, Zhang X, Li J, Huang J, Zhang H, Zheng Z, Hu S. Type-specific dysregulation of matrix metalloproteinases and their tissue inhibitors in end-stage heart failure patients: relationship between MMP-10 and LV remodelling. *J Cell Mol Med* 2011;**15**:773–782.

201. Han P, Li W, Lin C-H, Yang J, Shang C, Nurnberg ST, Jin KK, Xu W, Lin C-Y, Lin C-J, Xiong Y, Chien H-C, Zhou B, Ashley E, Bernstein D, Chen P-S, Chen H-SV, Quertermous T, Chang C-P. A long noncoding RNA protects the heart from pathological hypertrophy. *Nature* 2014;**514**:102–106.

202. Chang Y, Stockinger MP, Tashiro H, Lin CG. A novel noncoding RNA rescues mutant SOD1-mediated cell death. *FASEB J* 2008;**22**:691–702.

203. Huang DW, Sherman BT, Lempicki RA. Systematic and integrative analysis of large gene lists using DAVID bioinformatics resources. *Nat Protoc* 2009;**4**:44–57.

204. Huang DW, Sherman BT, Lempicki RA. Bioinformatics enrichment tools: paths toward the comprehensive functional analysis of large gene lists. *Nucleic Acids Res* 2009;**37**:1–13.

205. Chen SN, Czernuszewicz G, Tan Y, Lombardi R, Jin J, Willerson JT, Marian AJ. Human molecular genetic and functional studies identify TRIM63, encoding Muscle RING Finger Protein 1, as a novel gene for human hypertrophic cardiomyopathy. *Circ Res* 2012;**111**:907–919.

206. Lee CS, Yi J-S, Jung S-Y, Kim B-W, Lee N-R, Choo H-J, Jang S-Y, Han J, Chi S-G, Park M, Lee J-H, Ko Y-G. TRIM72 negatively regulates myogenesis via targeting insulin receptor substrate-1. *Cell Death Differ* 2010;**17**:1254–1265.

207. Bonda TA, Kaminski KA, Dziemidowicz M, Litvinovich S, Kozuch M, Hirnle T, Dmitruk I, Chyczewski L, Winnicka MM. Atrial expression of the CCN1 and CCN2 proteins in chronic heart failure. *Folia Histochem Cytobiol* 2012;**50**:99–103.

208. Eklund L, Piuhola J, Komulainen J, Sormunen R, Ongvarrasopone C, Fässler R, Muona a, Ilves M, Ruskoaho H, Takala TE, Pihlajaniemi T. Lack of type XV collagen causes a skeletal myopathy and cardiovascular defects in mice. *Proc Natl Acad Sci U S A* 2001;**98**:1194–1199.

209. Rasi K, Hurskainen M, Kallio M, Stavén S, Sormunen R, Heape AM, Avila RL, Kirschner D, Muona A, Tolonen U, Tanila H, Huhtala P, Soininen R, Pihlajaniemi T. Lack of collagen XV impairs peripheral nerve maturation and, when combined with laminin-411 deficiency, leads to basement membrane abnormalities and sensorimotor dysfunction. *J Neurosci* 2010;**30**:14490–14501.

210. Vázquez F, Hastings G, Ortega M a., Lane TF, Oikemus S, Lombardo M, Iruela-Arispe ML. METH-1, a human ortholog of ADAMTS-1, and METH-2 are members of a new family of proteins with angio-inhibitory activity. *J Biol Chem* 1999;**274**:23349–23357.

211. Stankunas K, Hang CT, Tsun Z-Y, Chen H, Lee N V., Wu JI, Shang C, Bayle JH, Shou W, Iruela-Arispe ML, Chang C-P. Endocardial Brg1 Represses ADAMTS1 to Maintain the Microenvironment for Myocardial Morphogenesis. *Dev Cell* 2008;**14**:298–311.

212. Hashemi S, Salma J, Wales S, McDermott J. Pro-survival function of MEF2 in cardiomyocytes is enhanced by β-blockers. *Cell Death Discov* Nature Publishing Group; 2015;**1**:15019.

213. Rodríguez-Penas D, Feijóo-Bandín S, García-Rúa V, Mosquera-Leal A, Durán D, Varela A, Portolés M, Roselló-Lletí E, Rivera M, Diéguez C, Gualillo O, González-Juanatey JR, Lago F. The adipokine chemerin induces apoptosis in cardiomyocytes. *Cell Physiol Biochem* 2015;**37**:176–192.

214. Chang C-WJ, Lee L, Yu D, Dao K, Bossuyt J, Bers DM. Acute β-adrenergic activation triggers nuclear import of histone deacetylase 5 and delays G(q)-induced transcriptional activation. *J Biol Chem* 2013;**288**:192–204.

215. Estrella NL, Clark AL, Desjardins CA, Nocco SE, Naya FJ. MEF2D Deficiency in Neonatal Cardiomyocytes Triggers Cell Cycle Re-entry and Programmed Cell Death in Vitro. *J Biol Chem* 2015;**290**:24367–24380.

216. Hill JA, Olson EN. Cardiac plasticity. *N Engl J Med* 2008;**358**:1370–1380.

217. Sawicki KT, Shang M, Wu R, Chang H, Khechaduri A, Sato T, Kamide C, Liu T, Naga Prasad S V., Ardehali H. Increased Heme Levels in the Heart Lead to Exacerbated Ischemic Injury. *J Am Heart Assoc* 2015;**4**:e002272.

218. Alfonso-Jaume MA, Bergman MR, Mahimkar R, Cheng S, Jin ZQ, Karliner JS, Lovett DH. Cardiac ischemia-reperfusion injury induces matrix metalloproteinase-2 expression through the AP-1 components FosB and JunB. *Am J Physiol Heart Circ Physiol* 2006;**291**:H1838-46.

219. Lee JS, Yu Q, Shin JT, Sebzda E, Bertozzi C, Chen M, Mericko P, Stadtfeld M, Zhou D, Cheng L, Graf T, MacRae CA, Lepore JJ, Lo CW, Kahn ML. Klf2 Is an Essential Regulator of Vascular Hemodynamic Forces In Vivo. *Dev Cell* 2006;**11**:845–857.

220. Greulich S, Ferreira VM, Dall'Armellina E, Mahrholdt H. Myocardial Inflammation—Are We There Yet? *Curr Cardiovasc Imaging Rep* 2015;**8**:6.

221. Fang L, Moore X-L, Dart AM, Wang L-M. Systemic inflammatory response following acute myocardial infarction. *J Geriatr Cardiol* 2015;**12**:305–312.

222. Mann DL. MicroRNAs and the Failing Heart. *N Engl J Med* 2007;**356**:2644–2645.

223. Hashemi S, Wales S, Miyake T, McDermott JC. Heart disease: recruitment of MEF2 activity by β-blockers wards off cardiomyocyte death. *Cell Death Dis* 2015;**6**:e1916.

224. Smith CCT, Davidson SM, Lim SY, Simpkin JC, Hothersall JS, Yellon DM. Necrostatin: A Potentially Novel Cardioprotective Agent? *Cardiovasc Drugs Ther* 2007;**21**:227–233.

225. Carè A, Catalucci D, Felicetti F, Bonci D, Addario A, Gallo P, Bang M-L, Segnalini P, Gu Y, Dalton ND, Elia L, Latronico MVG, Høydal M, Autore C, Russo MA, Dorn GW, Ellingsen Ø, Ruiz-Lozano P, Peterson KL, Croce CM, Peschle C, Condorelli G. MicroRNA-133 controls cardiac hypertrophy. *Nat Med* 2007;**13**:613–618.

226. Rooij E van, Sutherland LB, Qi X, Richardson J a, Hill J, Olson EN. Control of stress-dependent cardiac growth and gene expression by a microRNA. *Science* 2007;**316**:575–579.

227. Grimm M, Brown JH. Beta-adrenergic receptor signaling in the heart: role of CaMKII. *J Mol Cell Cardiol* 2010;**48**:322–330.

228. Yang Q, She H, Gearing M, Colla E, Lee M, Shacka JJ, Mao Z. Regulation of neuronal survival factor MEF2D by chaperone-mediated autophagy. *Science* 2009;**323**:124–127.

229. Sinert R, Newman DH, Brandler E, Paladino L. Immediate β-blockade in patients with myocardial infarctions: Is there evidence of benefit? *Ann Emerg Med* Elsevier Inc.; 2010;**56**:571–577.e1.

APPENDIX A

Heart disease: recruitment of MEF2 activity by β−blockers wards off cardiomyocyte death [χ]

Morbidity and mortality associated with cardiovascular disease is a predominant global health problem. Death of cardiac muscle cells (cardiomyocytes) through programmed cell death (apoptosis) is one hallmark of the progression to heart failure [174]. Moreover, loss of cardiomyocytes due to myocardial infarction (MI) in patients who survive the initial insult is a major determinant of residual heart function and ultimately their longer term prognosis. The extent of cardiomyocyte death is thus a primary determinant of subsequent left ventricular remodeling and progress to heart failure [129]. Given that the human heart has virtually no innate capacity for regeneration, the mechanisms of cardiomyocyte cell death, and arguably more importantly, the survival of these cells and ultimately the salvage of the myocardium, is of profound clinical importance. An emergent concept in the report by Hashemi et al. [212] is that a protein complex named MEF2, commonly known for its role in the development of the cardiovascular system, is linked to cardiomyocyte survival. In addition, the β adrenergic signaling pathway that fulfills an extensive role in the physiology and pathology of the

---

χ S Hashemi[1,2,3], S Wales[1,2,3], T Miyake[1,2,3] and JC McDermott*,[1,2,3,4]

[1] Department of Biology, [2] Centre for Research in Mass Spectrometry (CRMS), [3] Muscle Health Research Centre (MHRC), [4] Centre for Research in Biomolecular Interactions (CRBI), York University.

adult heart is shown to intersect with MEF2's pro-survival function in cardiomyocytes. The initial cue that led to the inception of these studies was accumulating evidence in the central nervous system indicating that a primary function of MEF2 in neurons is to protect them from apoptosis [17,228] .In view of the fundamental role played by MEF2 in the control of cardiac gene expression, [30] it was a logical next step to address the question as to whether MEF2 might play a parallel role in the heart. Initially, using cultured rodent cardiomyocytes and flow cytometry as a sensitive indicator of apoptotic cell death, Hashemi et al. [212] report that levels of cell death are dramatically enhanced in cardiomyocytes when the expression of MEF2 is suppressed using siRNA technology. Transcriptome analysis of these MEF2 depleted cells correspondingly indicated extensive differential expression in an apoptotic gene network suggesting therefore that MEF2 does indeed play a key role in cardiomyocyte survival. A further clue to the potential importance of these observations came from previous work from the same group in which β adrenergic signaling mechanisms were found to directly converge on and regulate MEF2 activity [134]. Acting through the β adrenergic receptors, catecholamines, such as adrenaline or noradrenaline, activate adenylate cyclase which, through the classical cAMP signaling pathway, result in activation of Protein kinase A (PKA). The striking connection was that the earlier work, in a skeletal muscle system, elucidated that PKA phosphorylates the MEF2 protein complex enhancing its interaction with a co-repressor (HDAC4), thus inactivating MEF2 function [30,134]. Underlying the relevance of these observations is the long known sensitivity of the heart to β adrenergic stimulation that exerts dynamic physiological control over both chronotropic (rate) and inotropic (strength) properties of cardiac contraction. Moreover, high levels of

β adrenergic signaling, especially after MI, have been linked with cardiomyocyte death in the vicinity of the infarct and also in the more gradual loss seen in progressive heart failure [77,174]. What has perhaps not been fully appreciated is the connection of β adrenergic signaling to the acute and chronic control of myocardial gene expression and cell survival. Collectively, these observations framed the next question…Does β adrenergic signaling impact MEF2's pro-survival function in cardiomyocytes?

Experiments addressing this question indicate that treatment with agonists of the β adrenergic system acutely promotes cardiomyocyte apoptosis while concomitantly shutting down MEF2 function. A tantalizing additional layer of proof

is that expression of an engineered form of MEF2 that is resistant to PKA in cardiomyocytes renders the cells less prone to apoptotic cell death in response to strong β adrenergic activation. Further evidence in this report are 'proof of principle' experiments using β adrenergic blockers such as Atenolol, which competitively block the β1 adrenergic receptors from being activated by its natural ligands (Figure S1). To digress momentarily, since the Nobel prize winning development of this class of drugs by Sir James Black, [118] β-blockers have truly proved to be a seminal 'super-drug', used as a front line treatment for progressive heart disease and many other conditions for several decades. Enhanced sympathetic drive due to binding of catecholamines to the β1 and β2-subtypes of cardiac adrenergic receptors in patients with heart failure is inversely correlated with survival indicating one compelling reason why β blockers are efficacious in heart disease. In the studies of Hashemi et al [212], β blockers rescue MEF2 function from β adrenergic repression and, in so doing, promote cardiomyocyte survival (Figure S1). It is also pertinent, but as yet unanswered, to consider whether

other types of cardiomyocyte death apart from apoptosis, such as autophagy-induced cell death and necroptosis, are also impacted by MEF2. Nevertheless, the logical extrapolation is to question whether β blockers can be effectively used to enhance MEF2 function and promote cardiomyocyte survival under conditions in which their survival is compromised, such as during acute and subacute phases after MI. As with any basic discovery science, questions of efficacy and relevance to the human condition remain. A crucial one being, can timely β blocker treatment after MI and in the subacute stages in humans mitigate cardiomyocyte cell death, ventricular remodeling and progression to heart failure? Although there is no direct evidence addressing this question, one randomized trial reviewed by Sinert et al. [229] demonstrated that β blocker treatment within 24 h in patients presenting with elevated ST segment MI did not reduce mortality or re-infarction when compared with placebo, indicating that β blockade post MI is tolerated with no obvious contraindications for most patients. The impact of this treatment modality for longer term cardiomyocyte survival remains to be determined. An alternate therapeutic approach might also be tailored drugs that transiently activate MEF2 through a different mechanism. No doubt there are myriad hurdles and complexities to consider before these observations can be clinically applied. Further experimentation in more physiological models and in human heart cells will examine the efficacy of these ideas. Moreover, detailed consideration of these findings requires further elaboration by clinical colleagues in the context of other treatment modalities and other cardiovascular system parameters.

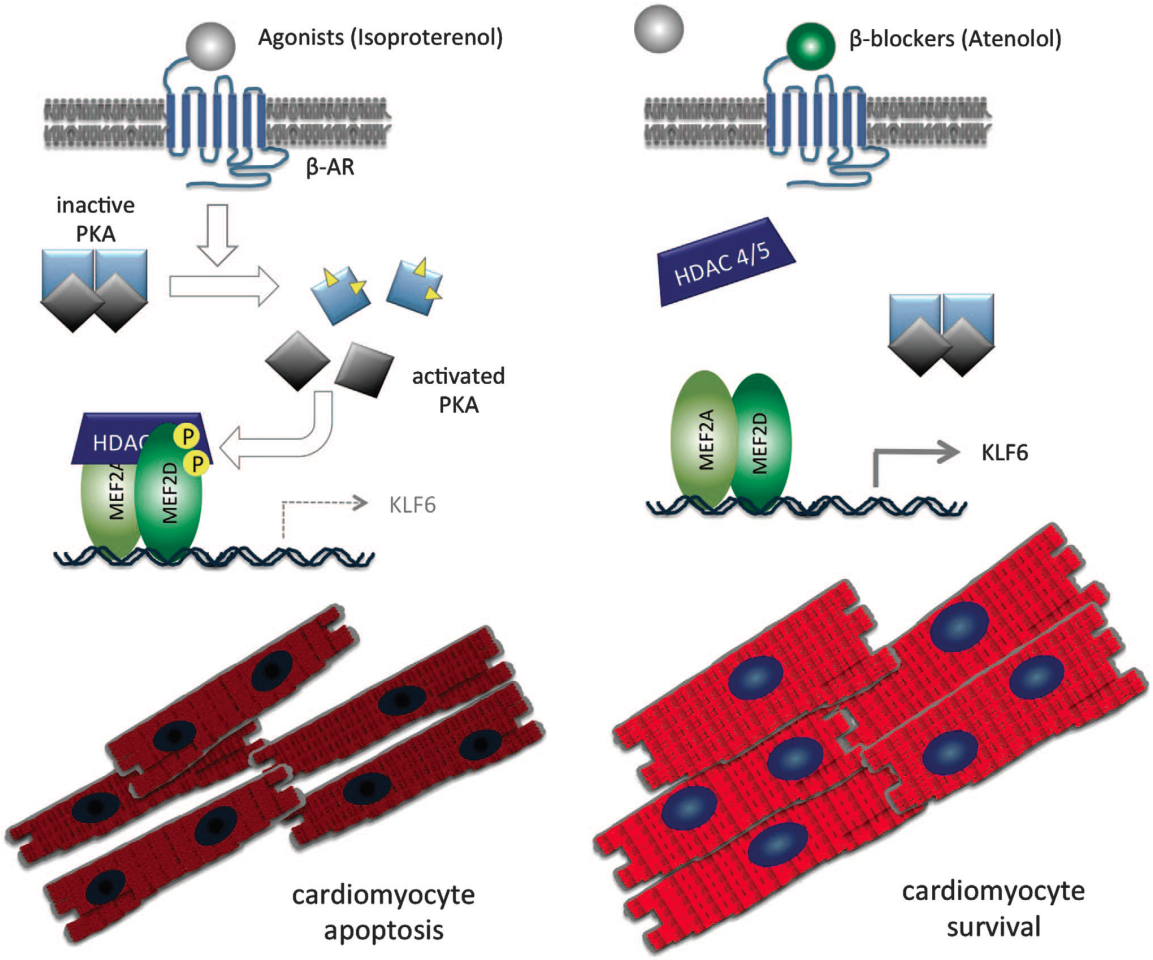
Agonists (Isoproterenol)
β-AR
inactive
PKA
activated
PKA
HDAC
P
P
MEF2A
MEF2D
KLF6
cardiomyocyte
apoptosis
β-blockers (Atenolol)
HDAC 4/5
MEF2A
MEF2D
KLF6
cardiomyocyte
survival

Figure S1

Figure S1. β adrenergic/PKA-mediated inhibition of MEF2 contributes to cardiomyocyte cell death. On the left side, acute activation of β adrenergic receptors invokes cAMP accumulation (yellow triangles) and PKA activation in cardiomyocytes, resulting in suppression of MEF2 transcriptional activity by direct phosphorylation and nuclear interaction with HDAC4/5. Expression of pro-survival genes such as KLF6 is prevented resulting in enhanced cardiomyocyte death. On the right side, β-blockers, such as atenolol, competitively inhibit the activation of the β adrenergic receptors and downstream signaling resulting in enhanced MEF2 activity, thus promoting cardiomyocyte survival.

APPENDIX B

Material and Methods

Transformation

Stock expression plasmids should be diluted to 10ng/µl in a -20 freezer for easy transformation.

- Carrier DNA (has no promoter): Bluescript (pBSK), etc.
- Marker of transfection: ds Red, GFP.
- Backbone: pMT2, pcDNA, etc.
- DNA effectors: Mef2a, mef2d etc.

Obtain competent cells: E. Coli XL1Blue. Once thawed, can't reuse. Thaw on ice. Must be grown at a certain OD prior to freezing.

Add 1 µl (10ng) of expression plasmid to 50 µl of E. Coli. Add plasmid to tube first. Pipette up and down once. Incubate on ice for 30 minutes.

Heat Shock for 1 min at 42oC water bath. Follow up with 2 min on ice. In the meantime take out LB plates and warm them in 37-degree room. Put bacterial waste in a designated waste.

At room temperature add 200 µl of LB+0.1%glucose by open flame to the bacteria. Put in water bath or incubator at 37oC for 30 minutes. Spin at 7000 rpm for 5 minutes. Remove supernatant. Re-suspend in 50 µl LB and plate by an open flame. Place the plates facing down at 37 degrees overnight. Next day put in 4oC or select colony and proceed with maxi-prep. Keep plates for 1 week.

Transfection with Lipofectamine in neonatal cardiomyocytes

For Lipofectamine 2000 (11688, Invitrogen) transfection in primary cardiomyocytes, seed the cells at 80% confluence in 6-well plates 24 hours prior to transfection. For each well, dilute a total of 2.5 µg of DNA in 150 µl in Opti-MEM medium (31985, Invitrogen), and in a separate tube dilute 2.5x of Lipofectamine 2000 reagent in 150 µl Opti-MEM medium. Combine the DNA and Lipofectamine mixtures (300 µl), mix and incubate for a minimum of 5 min. Add the 250 µl of DNA/Lipofectamine mixture to cells in culture medium, incubated at 37°C overnight. Following the incubation, re-feed the media and allow the cells to recover for a minimum 24 hours prior to harvesting, and pharmacological treatments.

For Lipofectamine RNAiMAX (Invitrogen), seed the cells at 80% confluence in 6-well plates 24 hours prior to transfection. For each well, according to the manufacture's instruction, dilute Lipofectamine RNAiMAX reagent into 150 µl in Opti-MEM medium, and in a separate tube, dilute siRNA (100-200nM) in 150 µl Opti-MEM medium, mix and incubate for a minimum 5 min at RT. Add the 250 µl of siRNA/Lipofectamine mixture to cells and incubate at 37°C overnight. Following the incubation, re-feed the media and harvest 48 to 72 hours later for western immunoblotting analysis to determine the efficacy of protein knock down or flow cytometry analysis.

β-galactosidase assay

Per each sample prepare the reaction mixture (500 µl Z buffer, 100 µl ONPG, 2.74 µl β-mercaptoethanol). Mix 600 µl of the reaction mixture with 100 µl of the cell lysate and incubate at RT or for faster result at 37^0C until the reaction is done and a colour changed (yellow) has appeared. To stop the reactions add 300 µl of Na_2CO_3 to each

tube. Measure absorbance of samples at 420 nm using spectrophotometer.

Luciferase assay

Luciferase assays were performed with commercially purchased substrate (Promega). All reporter assays were performed with cells grown in 35 mm dishes. Cells were washed 3X with cold 1X Phosphate buffered saline (PBS). Add 300 µl of luciferase lysis buffer (20 mM Tris, pH 7.4, 0.1% Triton-X 100) in each well per dish. Incubate at RT for 5-10 min. Scrape cells off with rubber policeman and collect into labeled tubes, vortex, spin down cell debris at max speed for 10 min. Collect the supernatant into a new tube and freeze lysate until analysis. When ready to analyze, thaw cells and transfer 50/100 µl to Luciferace assay tubes and use the Berthold Luminometer to detect light units.

Harvesting Cells (Whole cell extracts)

Do everything on ice. Aspirate or dump old media out of dish. Wash 2X PBS; Add 700 µl of PBS onto plate; Scrape into tubes using rubber policeman. Pellet cells: 1.5g for 5 minutes. Aspirate PBS. Add 100 µl of (or 5x the pellet size) NP-40 lysis buffer or β-gal depending on protocol. Pipette up and down to break cells. Vortex for 10 sec, Incubate on ice 5 min. Repeat 3X. Spin at max speed 15 min. Store supernatant at -80^{o}C.

Lysis Buffer Ingredients:

It includes; PMSF, Sodium Othrovanadate, Protease Inhibitor. Then add to NP-40 lysis buffer in 1:100 ratios.

NP-40 Lysis Buffer: Make up to 100 ml, store at 4^{o}C.

Volume	Stock	Take	Final Concentration
250 ml	1 M Tris pH 8.0	5 ml	50 mM
250 ml	5 M NaCl	3 ml	150 mM
50 ml	10% NP-40	5 ml	0.5 %
100 ml	0.5 M EDTA pH 8.0	400 µl	2 mM
100 ml	0.5 M NaF	20 ml	100 mM
100 ml	0.1 M Na Pyrophos.	10 ml	10 mM

Protein extracts

Protein samples were kept on ice during the entire procedure. Cells were washed twice with cold 1x PBS. After aspirating the last PBS wash, 1.0 mL of cold 1xPBS was added to cells. Cells were then gently scraped with a rubber policeman and transferred to a new tube and then centrifuged at 1500xg for 5 min at 4°C. After removing the PBS, the pellet was diluted with five times its volume in NP-40 lysis buffer (supplemented with 1 mM Sodium orthovanadate, 1 mM PMSF and Protease inhibitor cocktail (Sigma, P-8340). Cells were vortexed briefly every 10 minutes for a total of 30-40 min, and centrifuged at high speed (>10 000xg) and supernatant was transferred to a fresh tube. Protein concentrations were determined by Bradford assay (Bio-Rad) with bovine serum albumin (BSA) as a standard. An equal amount of protein was diluted with 4X SDS sample buffer and samples were boiled for 5 min, chill on ice and centrifuge to use for SDS-PAGE.

SDS-PAGE

Prepare resolving gel and then top with stacking gel with appropriate comb inserted in Hoefer gel apparatus. Fill bottom and center well of mini-gel apparatus with 1X Laemmli buffer. Load equal amount of protein samples on the gel. Run the gel at 100 V through stacking and 120 V through running gel.

Western blotting

After SDS PAGE, transfer protein from gel to Immobilon-P (Millipore) membrane by wet transfer at 20 V overnight. Block membrane with odyssey blocking buffer (LI-COR) in (1:2) PBS/TBS for 1 hour at RT. Incubate membrane with primary antibody diluted (1:100-1:1000) in odyssey blocking buffer solution overnight at 4 °C. Wash membrane with 1X PBS/TBST with 0.1% Tween 20 (3 X 5 min). Incubate membrane with secondary antibody IRDye 680RD at 1:5000 in odyssey blocking solution for 2 hours at RT. Wash membrane with 1xPBS/TBST with 0.1% Tween 20 (3 X 10 min) and keep the membrane in 1xPBS at 4 °C. The blots were then imaged using LI-COR odyssey system.

Chromatin immunoprecipitation (ChIP)

ChIP experiments followed the guidelines set by EZ ChIP™ (Upsate) with minor modifications. Cardiomyocyte cells were fixed with 1% formaldehyde (Sigma) for 15 minutes at 37°C. Fixing was quenched by Glycine at a final concentration of 0.125 M. Cells were collected in PBS containing phenylmethylsulfonyl fluoride (PMSF) (Sigma) and protease inhibitor cocktail. Cells were collected at 5000 rpm for 5 minutes at 4°C. Cells were lysed using Wash Buffer I (10 mM HEPES pH 6.5, 0.5 M ethylene glycol tetraacetic acid (EGTA), 10 mM EDTA, 0.25% Triton X-100, protease inhibitor cocktail, PMSF) for 5 minutes on ice. Nuclei were collected and resuspended in Wash Buffer II (10 mM HEPES pH 6.5, 0.5 mM EGTA, 1 mM EDTA, 200 mM NaCl, protease inhibitor cocktail, PMSF) for 10 minutes on ice. Nuclei were again collected and then treated with nuclear lysis buffer (50 mM Tris–HCl pH 8.1, 10 mM EDTA, 1% SDS). Chromatin was sheared using a Misonix sonicator to produce 500 bp fragments. Crosslinked sheared chromatin was collected following a 15-minute spin at maximum speed. Twenty percent

of total chromatin was set aside as input. Sheared crosslinked chromatin was diluted 1:10 with immunoprecipitation (IP) dilution buffer (0.01% SDS, 1.1% Triton-X 100, 1.2 mM EDTA, 16.7 mM Tris–HCl pH 8.1, 167 mM NaCl) and incubated with antibody overnight at 4°C with rocking. Protein G Dynabeads (Invitrogen) were blocked with 20 µg salmon sperm DNA in IP dilution buffer (15 µl of beads + 135 µl IP dilution buffer + 20 µg salmon sperm DNA per IP) overnight at 4°C with rocking. We incubated 152 µl of pre-blocked beads with the IP reaction at 4°C for 1 h. Dynabead-bound antibody-chromatin complexes were washed using IP Wash Buffer I (20 mM Tris pH 8.1, 2 mM EDTA, 150 mM NaCl, 1% Triton-X 100, 0.1% SDS) and II (20 mM Tris pH 8.1, 2 mM EDTA, 500 mM NaCl, 1% Triton X-100, 0.1% SDS), each incubated for 10 minutes at 4°C, and followed with two washes in Tris-EDTA (TE) buffer at 4°C. Protein-DNA complexes were freed from Dynabeads through the addition of elution buffer (0.1 M NaHCO3, 1% SDS) for 30 minutes at RT. To separate protein from DNA, samples were treated with 12 µl of 5 M NaCl (BioShop) at 65°C for 4 h or overnight. Protein was further degraded by the addition of Proteinase K (Sigma), EDTA, Tris pH 6.5 for 1 h at 45°C. DNA samples were then purified using a PCR clean up kit (Qiagen, Mississauga, ON, Canada).

Quantitative PCR.

2.5 µl gDNA or cDNA was combined with SybrGreen (BioRad) and 500 nM primers in a final volume of 20 µl. cDNA was diluted 1:10 prior to use. Each sample was prepared in triplicate and analyzed using Rotor-Gene Q (Qiagen). ChIP-qPCR: 5min 95^{o}C, [5s 95^{o}C, 15s 60^{o}C] x 40 cycles. Fold enrichment (ChIP-qPCR) was quantified using the ΔΔCt method.

APPENDIX C

Supplementary Materials

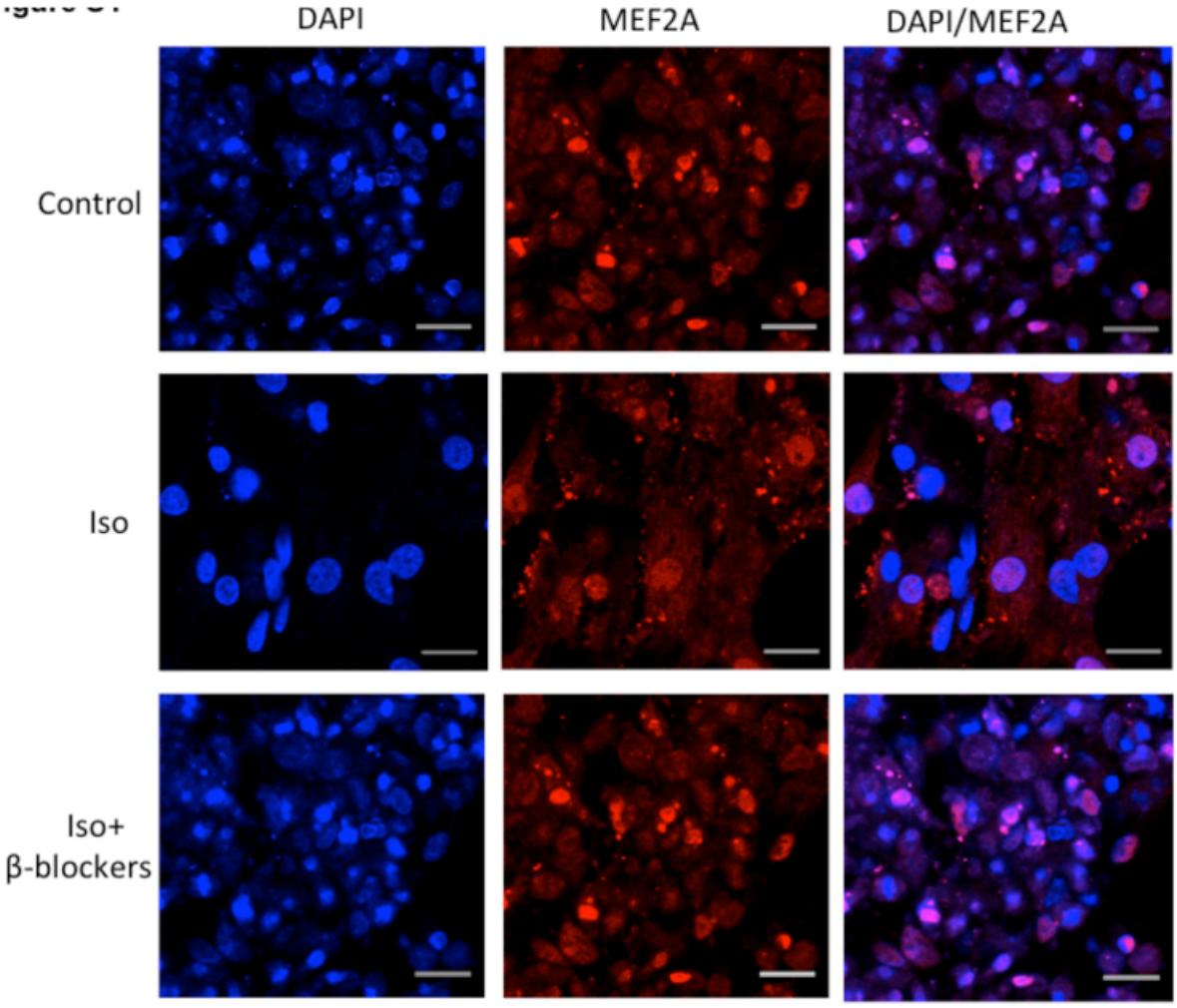

Figure S2

Figure S2. β-AR activation modulates cellular localization of MEF2A in cardiomyocytes. Primary cardiomyocytes were treated with solvent or Isoproterenol (Iso, 10 μM) alone and in combination with β-blockers Atenolol (Ate, 10 μM) and ICI118551 (1 μM). After treatment, cells were fixed with 4% paraformaldehyde and immunofluorescence analysis was performed using a primary antibody to MEF2A (red). DAPI (4,6-diamidino-2-phenylindole) was used to identify nuclei (blue). The merged pictures demonstrate localization of MEF2A (Red) in respect to Isoproterenol (Iso, 10 μM), β-blockers Atenolol (Ate, 10 μM) and ICI118551 (1 μM) treatment, counterstained with DAPI. Scale represents 20 μm.

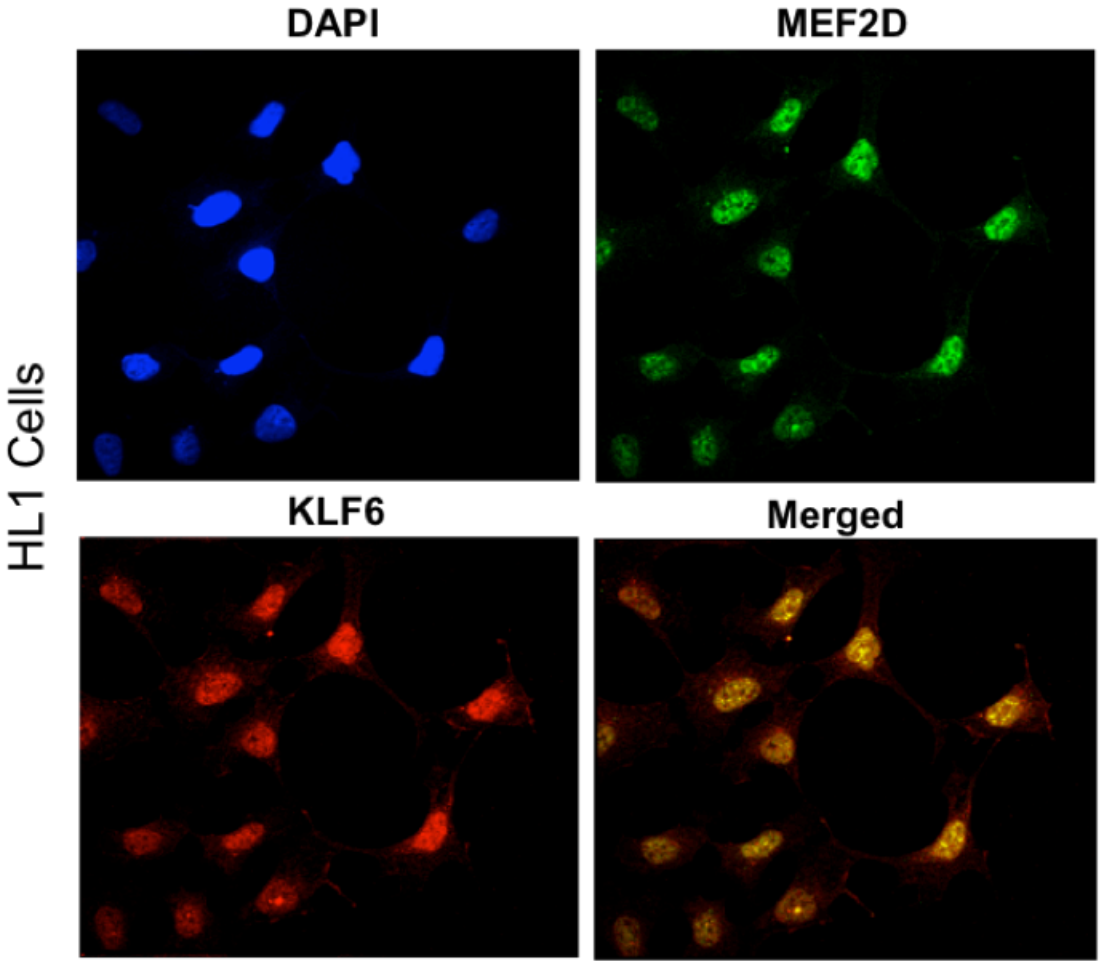

Figure S3

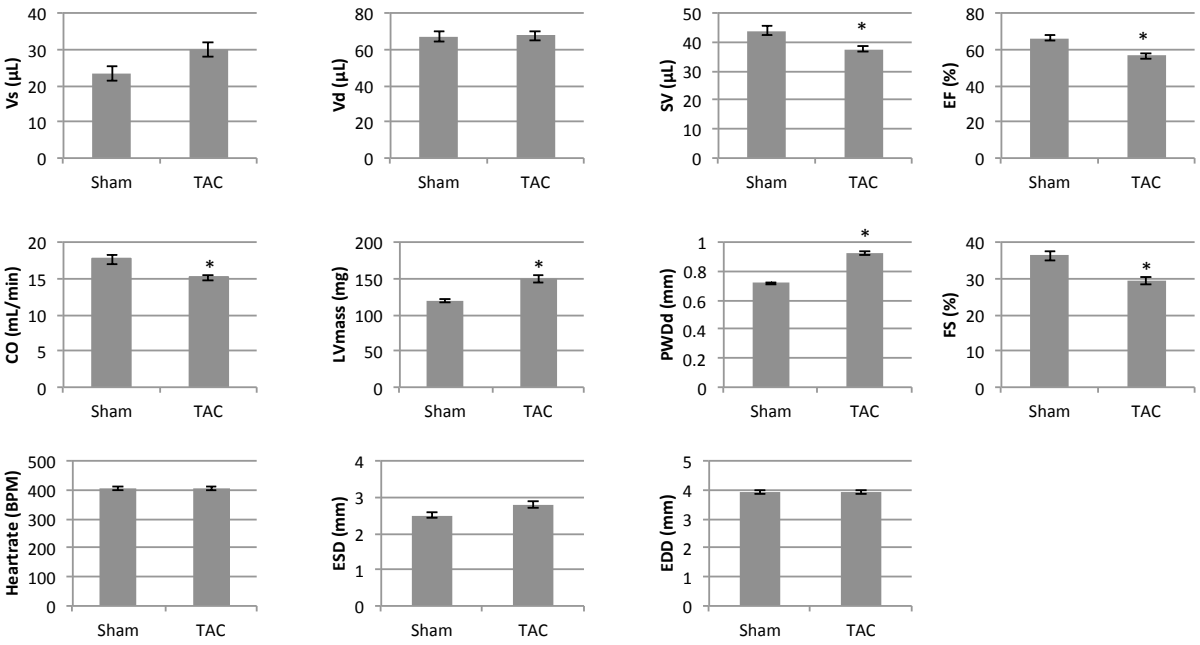

Figure S4. Baseline echocardiography analysis before administration of Atenolol or solvent. Mean ± S.E.M (n=18), t-test was used, *P<0.05 vs. Sham+Sol.

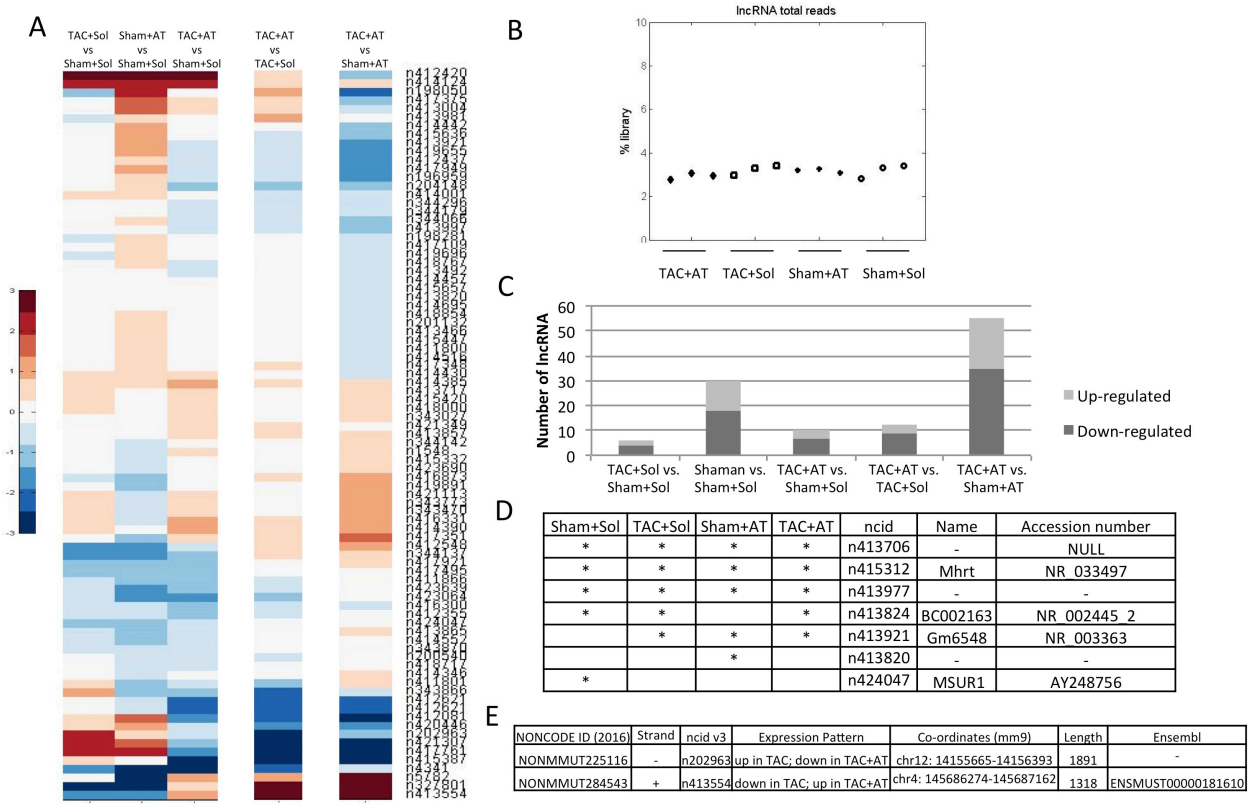

D

Sham+Sol	TAC+Sol	Sham+AT	TAC+AT	ncid	Name	Accession number
*	*	*	*	n413706	-	NULL
*	*	*	*	n415312	Mhrt	NR_033497
*	*	*	*	n413977	-	-
*	*		*	n413824	BC002163	NR_002445_2
	*	*	*	n413921	Gm6548	NR_003363
		*		n413820	-	-
*				n424047	MSUR1	AY248756

E

NONCODE ID (2016)	Strand	ncid v3	Expression Pattern	Co-ordinates (mm9)	Length	Ensembl
NONMMUT225116	-	n202963	up in TAC; down in TAC+AT	chr12: 14155665-14156393	1891	-
NONMMUT284543	+	n413554	down in TAC; up in TAC+AT	chr4: 145686274-145687162	1318	ENSMUST00000181610

Figure S5. Heart failure associated changes in lncRNA expression. A mouse lncRNA database containing 2073 lncRNA genomic positions was obtained from Matkovich et al. [189]. Short paired-end reads from 12 in vivo samples were mapped with RSEM/ Bowtie to the reference index which was built for the 2073 mouse lncRNAs (mm9). All uniquely mappable short reads are included by using the bowtie-m 1 option in the rsem-

calculate-expression command. A) Significant fold changes for 84 lncRNA (FDR<0.2; red upregulated; blue downregulated). lncRNA are sorted by p-value based on the left-most column. The three columns in the left part of the figure show fold changes with respect to reference condition Sham+Sol. The next two columns show the significance of fold changes in TAC+AT with respect to reference conditions TAC+Sol and Sham+AT, respectively. B) The percentages of reads which mapped to lncRNAs varied in a narrow range from 2.8% to 3.4% C) The number of differentially expressed lncRNAs per condition. D) The five most abundant lncRNAs in each treatment. E) DE lncRNAs targeted in both TAC+Sol vs Sham+Sol and TAC+AT vs TAC+Sol.

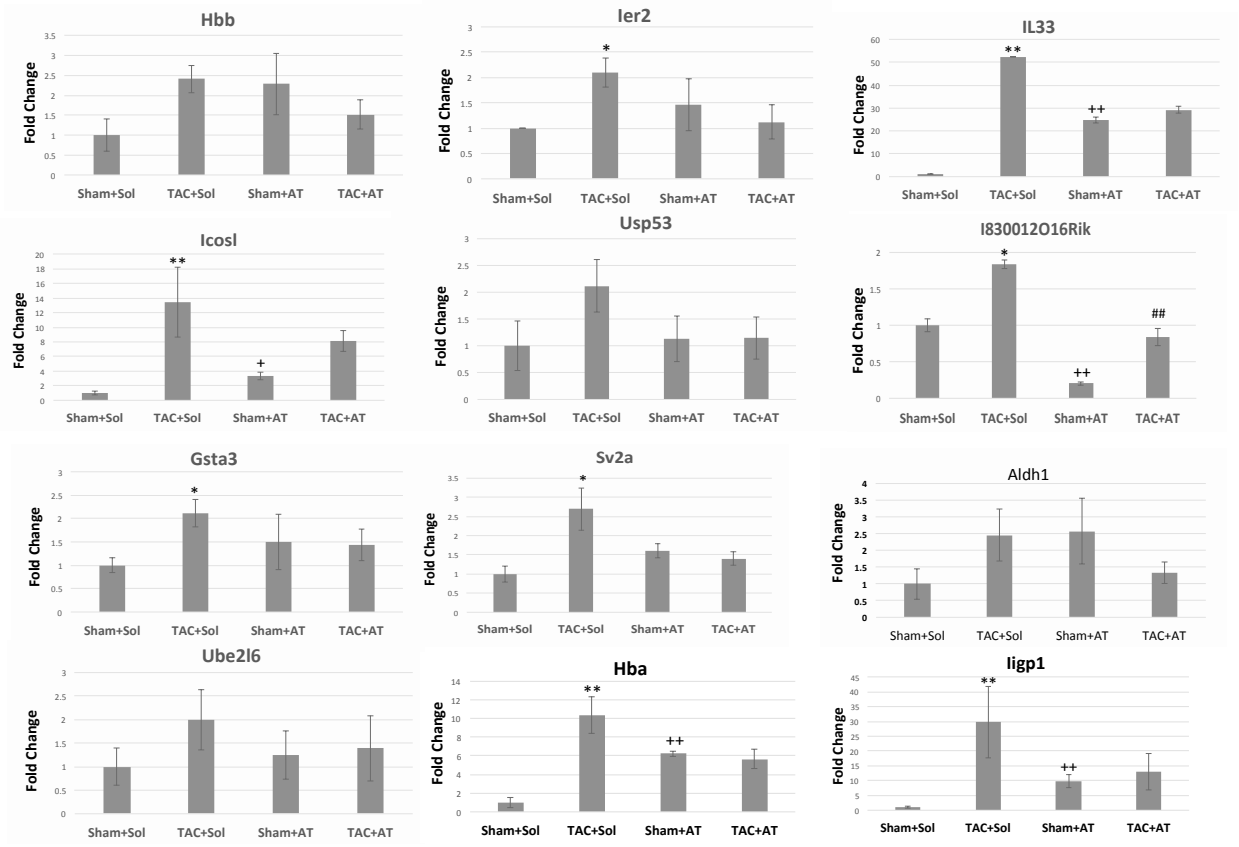

Figure S6. Expression of genes upregulated in TAC and down regulated with Atenolol treatment (Figure 19C), was confirmed using qRT-PCR. Data were normalized to Gapdh and are presented as fold change using the delta delta Ct method (n=3, *P<0.05 **P<0.01 Sham+Sol vs TAC+Sol, +P<0.05 ++P<0.01 Sham+Sol vs Sham+AT, ##P<0.01 TAC+Sol vs TAC+AT).

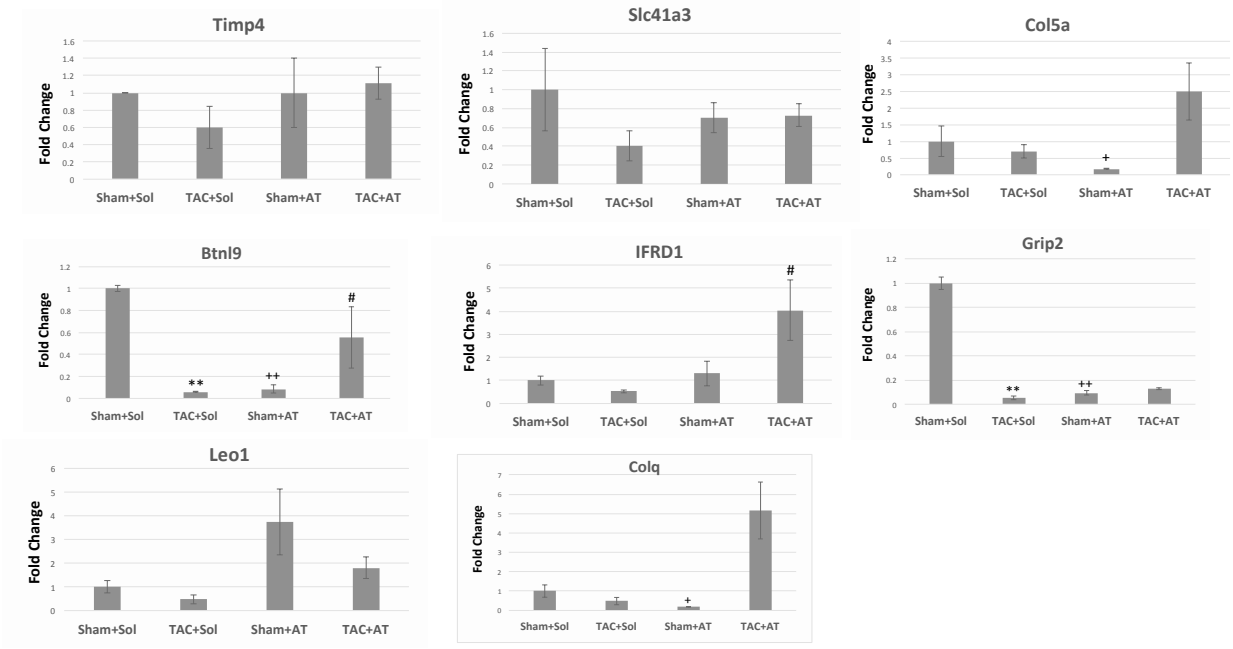

Figure S7. Expression of genes down-regulated in TAC and upregulated with Atenolol treatment (Figure 16C), was confirmed using qRT-PCR. Data were normalized to Gapdh and are presented as fold change using the delta delta Ct method (n=3, **P<0.01 Sham+Sol vs TAC+Sol, +P<0.05 ++P<0.01 Sham+Sol vs Sham+AT, #P<0.05 TAC+Sol vs TAC+AT).

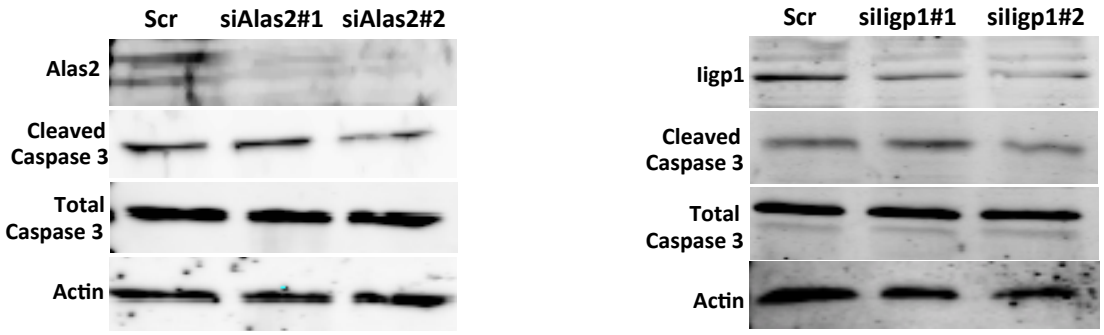

Figure S8. Primary cardiomyocytes were transfected with two independent siRNAs, Alas2 siRNA and ligp1 siRNA or with scramble siRNA control and treated with isoproterenol (10μM) for 48 hours. Equal amounts of total protein were used for western blot analysis and the levels of the indicated proteins were assessed by a standard immunoblotting technique using specific primary antibodies for each as indicated.

Gene ID	Gene Name	Ensembl ID(s)	Chr	Start	End	Strand	TFBS Rel. Start	TFBS Rel. End	Abs. Score	Rel. Score	TFBS Sequence	RNA level
ALDH1A2	aldehyde dehydrogenase family 1, subfamily A2	ENSMUSG00000013584	9	71063596	71144050	+	-4191	-4182	12.569	90.70%	CTATTTTTAT	+
							-4175	-4166	10.009	85.30%	CTCTTTATAA	
							-4	6	9.917	85.10%	CTATATACAG	
ifrd1	interferon-related developmental regulator 1	ENSMUSG00000001627	12	40928154	40975091	-	4593	4602	12.3	90.10%	TTATATATAG	+
junb	Jun-B oncogene	ENSMUSG00000052837	8	87500811	87502617	-	-3601	-3592	14.351	94.40%	CTATTTATAA	++
klf2	Kruppel-like factor 2 (lung)	ENSMUSG00000055148	8	74842932	74845555	+	-89	-80	10.213	85.80%	CTAAATTTAG	+
LEO1	Leo1, Paf1/RNA polymerase II complex component, homolog (S. cerevisiae)	ENSMUSG00000042487	9	75289331	75314239	+	-229	-220	13.587	92.80%	CTATTTTTAA	+
ligp1b/iigp1	interferon inducible GTPase 1; interferon-inducible GTPase-like	ENSMUSG00000054072	18	60535683	60552281	+	-389	-380	12.436	90.40%	CTAATTTTAG	-
RARRES2	retinoic acid receptor responder (tazarotene induced) 2	ENSMUSG00000009281	6	48519697	48522669	-	-1031	-1022	11.561	88.60%	CTATCTTTAG	++
SLC41A3	solute carrier family 41, member 3	ENSMUSG00000030089	6	90554719	90596406	+	-2853	-2844	11.561	88.60%	CTATCTTTAG	++
SV2A	synaptic vesicle glycoprotein 2 a	ENSMUSG00000038486	3	95985074	95999444	+	1503	1512	14.079	93.80%	CTATATTTAG	-
MEF2A	Myocyte Enhancer Factor 2A											+++

RNA Levels (FPKM)
No expression (-)
Less than 10 (+)
Less than 20 (++)
More than 20 (+++)

Figure S9. Predicted MEF2 consensus sequences from 32 overlapping genes in Figure 16D. RNA expression (FPKM) of these genes in heart muscle (Female, age 40-50) were analyzed in Human Protein Atlas program.